超臨界熱水溶液中における金属クロロ錯体の安定性に関する実験

（課題番号 07640647）

平成 7 年度～平成 8 年度科学研究費補助金（基盤研究 (C) (2)）
研究成果報告書

平成 8 年 3 月

研究代表者 内田悦生
（早稲田大学理工学部教授）

はしがき

　超臨界熱水条件下における各種金属の溶存状態に関する情報は、熱水性鉱床の生成機構を考える上で重要である。しかしながら、実験が難かしく、また、時間がかかることから、今までにそれ程多くの研究は成されていない。本研究では、従来とは異なった比較的簡便な実験方法を考案し、塩濃度２Ｎにおける Mg^{2+}、Sr^{2+}、Fe^{2+}、Mn^{2+}、Ni^{2+}、Co^{2+}の超臨界条件下における溶存状態に関する実験を行った。その結果、Mg^{2+}および Sr^{2+}は主として中性溶存種として存在するが、Fe^{2+}、Mn^{2+}、Co^{2+}、Ni^{2+}は NaCl 濃度が低いときには中性溶存種として、NaCl 濃度が高いときにはトリクロロ錯体として存在することが分かった。また、これら遷移金属イオンのトリクロロ錯体の生成定数の順序から超臨界条件下ではこれら遷移金属イオンのトリクロロ錯体は、四面体配位の形をとり、かつ、低スピン状態にあることがわかった。

　また、遷移金属イオンのトリクロロ錯体の生成定数がわかったことにより、従来行われていた鉱物固溶体と塩化物水溶液間におけるイオン交換実験をより正確に解析することができるようになった。

　本報告書では、平成７年度から平成８年度にかけて行われたこれらの研究成果についてまとめる。

研究組織

　　　研究代表者：　　内田悦生（早稲田大学理工学部教授）

研究経費

　　　　　　平成７年度　　　　　　１，５００千円
　　　　　　平成８年度　　　　　　　７００千円

　　　　　　　計　　　　　　　　２，２００千円

研究発表

(1)学会誌等

1. Uchida, E., Goryozono, Y., Naito, M. and Yamagami, M. : Aqueous speciation of iron and manganese chlorides in supercritical hydrothermal solutions. Geochem. J., 29(3), 1995.8.

2. Uchida, E., Goryozono, Y., Naito, M. : Aqueous speciation of magnesium, nickel and cobalt chlorides in hydrothermal solutions at 600℃ and 1kbar. Geochem. J., 30(2), 1996.8.

3. 内田悦生・山上順民 : イルメナイト固溶体－塩化物水溶液間イオン交換平衡実験の再解析. 鉱物学雑誌, 25(3), 1996.8.

4. Uchida, E., Gima, M. and Imai, N. : Experimental study on ion exchange of Ca^{2+}, Fe^{2+} and Mn^{2+} between garnet solid solution and 2N aqueous chloride solution at 600℃ and 1kb. J. Min. Pet. Econ. Geol., 91(8), 1996.9.

(2)口頭発表

1. 内田悦生・御領園裕一・内藤真弘 : 600℃, 1kb における 2N 塩化物水溶液中のマグネシウム、ストロンチウム、ニッケル、コバルトの溶存形態. 資源地質学会. 1995.5.

2. 内田悦生・上田俊之介・小松宏之・内藤真弘 : 超臨界熱水溶液中における亜鉛の溶存状態に関する実験. 三鉱学会. 1995.10.

3. 内田悦生・内藤真弘・上田俊之介 : 超臨界熱水条件下におけるトリクロロ亜鉛錯体の生成定数の温度・圧力依存性. 三鉱学会. 1996.9.

Aqueous speciation of iron and manganese chlorides in supercritical hydrothermal solutions

ETSUO UCHIDA, YUICHI GORYOZONO, MASAHIRO NAITO and MASAHITO YAMAGAMI

Department of Mineral Resources Engineering, Waseda University, Ohkubo 3-4-1, Shinjuku, Tokyo 169, Japan

Aqueous speciation of iron and manganese chlorides in supercritical hydrothermal solutions was determined by monitoring the effects of NaCl and KCl on the Ca/(Ca + Fe) and Ca/(Ca + Mn) ratios of aqueous chloride solutions in equilibrium with scheelite and ferberite and with scheelite and huebnerite, respectively. The experiments were carried out under supercritical conditions of 400 and 600°C, and 1 kbar. The ratios decrease significantly with increasing NaCl and KCl concentrations at both 400°C and 600°C. This is attributable to the formation of higher-order aqueous chloride complexes of Fe and Mn, presumably $FeCl_3^-{}_{aq}$ and $MnCl_3^-{}_{aq}$. Based on the thermodynamic analysis of the experimental results using published dissociation constants for $NaCl_{aq}$, KCl_{aq} and $CaCl_{2aq}$, logarithms of the formation constants for $FeCl_3^-{}_{aq}$ were obtained to be 0.2(NaCl) and 1.2(KCl) for 400°C, and 1.9(NaCl) and 1.9(KCl) for 600°C, and those for $MnCl_3^-{}_{aq}$ to be 0.4(NaCl) and 1.1(KCl) for 400°C and 2.3(NaCl) and 2.3(KCl) for 600°C. This means that the supposition of $m(MeCl_{2aq}) = \Sigma m_{Me}$ for supercritical hydrothermal solutions is invalid.

INTRODUCTION

A considerable number of experiments of ion exchange equilibria between minerals and aqueous chloride solutions under supercritical conditions has been performed previously. However, most of them have treated Na-K exchange (e.g., Orville, 1963; Iiyama, 1964; Roux, 1974). Studies using transition elements are limited (e.g., Schulien *et al.*, 1970; Schulien, 1980; Lehmann and Roux, 1986; Ilton and Eugster, 1989). The ion exchange experiments using transition elements are useful in order to estimate the chemical compositions of hydrothermal solutions related to the formation of ore deposits based on the chemical compositions of constituting minerals. Thus we have carried out ion exchange experiments using transition elements (Uchida *et al.*, 1989; Kakuda *et al.*, 1991; Ogino *et al.*, 1992; Kubo *et al.*, 1992a, b; Uchida, 1993; Miyamoto and Uchida, 1994). Fluid inclusion studies revealed that NaCl and KCl are the most dominant solutes in natural hydrothermal solutions.

Therefore, the effect of their presence on ion exchange equilibria should be taken into consideration when the experimental results are applied to natural systems. This means that we need knowledge of thermodynamic properties of aqueous chloride solutions.

In this study, the effects of NaCl and KCl on ion exchange equilibria in the systems $CaWO_4$(scheelite)-$FeWO_4$(ferberite)-$CaCl_2$-$FeCl_2$-H_2O and $CaWO_4$ (scheelite)-$MnWO_4$(huebnerite)-$CaCl_2$-$MnCl_2$-H_2O were investigated experimentally in order to reveal the aqueous speciation and thermodynamic behavior of aqueous chloride solutions under supercritical conditions of 400 and 600°C, 1 kbar. Ion exchange experiments in the NaCl-free and KCl-free systems were previously performed by Uchida *et al.* (1989) at the same experimental conditions. The ion exchange reactions in these systems can be expressed as:

$$CaWO_4(\text{scheelite}) + FeCl_{2aq}$$
$$= FeWO_4(\text{ferberite}) + CaCl_{2aq}, \qquad (1)$$

and

$$CaWO_4(\text{scheelite}) + MnCl_{2aq}$$
$$= MnWO_4(\text{huebnerite}) + CaCl_{2aq}. \quad (2)$$
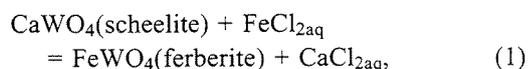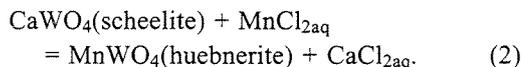
As scheelite is almost immiscible to ferberite and huebnerite under the experimental conditions, the effects of NaCl and KCl can be easily monitored by using the Ca/(Ca + Fe) and Ca/(Ca + Mn) ratios of the hydrothermal solution in equilibrium with both scheelite and ferberite and with both scheelite and huebnerite, respectively. The thermodynamic analysis of the experimental results will give us the information of aqueous speciation under supercritical conditions. These experimental systems have a potential to be applied to those containing metals other than Fe and Mn.

Previously it was shown experimentally that $NaCl_{aq}$, KCl_{aq}, $CaCl_{2aq}$, $FeCl_{2aq}$ and $MnCl_{2aq}$ are dominant aqueous chloride species in NaCl, KCl, $CaCl_2$, $FeCl_2$ and $MnCl_2$ aqueous solutions, respectively, under the supercritical conditions (Quist and Marshall, 1968; Franck, 1956; Popp and Frantz, 1979; Boctor *et al.*, 1980; Boctor, 1985). Based on the experiments of metal partitioning between granitic melt and aqueous chloride solution, Holland (1972) also suggested that neutral species are dominant at the supercritical conditions of 770 to 880°C and 1.4 to 2.4 kbar.

However, there is a possibility that $FeCl_{2aq}$ and $MnCl_{2aq}$ react with Cl^- released from $NaCl_{aq}$ and KCl_{aq}, which have relatively large dissociation constants, and then form higher-order iron and manganese chloride complexes such as $FeCl_3^-{}_{aq}$, $FeCl_4^{2-}{}_{aq}$, $MnCl_3^-{}_{aq}$ and $MnCl_4^{2-}{}_{aq}$. The effect of NaCl on mineral-solution equilibria has been investigated since the late 1980's (Fahlquist and Popp, 1989; Fein and Walther, 1989; Grabman and Popp, 1991). Fahlquist and Popp (1989) measured the solubility of bunsenite in $NiCl_2$-NaCl-H_2O solution. They confirmed the presence of $NiCl_3^-{}_{aq}$ complex at temperatures in the range 550–750°C at 1 kbar, and found that the formation constant of $NiCl_3^-{}_{aq}$ increases with increasing temperature. At present, we have no sufficient knowledge of the aqueous speciation of chlorides of transition

metals under supercritical conditions. In this paper, we will show through the experiments that $FeCl_3^-{}_{aq}$ and $MnCl_3^-{}_{aq}$ are dominant aqueous species of Fe and Mn, respectively, in natural supercritical hydrothermal solutions.

EXPERIMENTAL PROCEDURES

Scheelite as a starting material was synthesized hydrothermally from the equimolar mixture of CaO and WO_3 enclosed in a gold capsule with 2 N $CaCl_2$ aqueous chloride solution using a standard cold-seal pressure vessel at temperatures in the range 600–700°C at 1 kbar during 2 to 3 days. The starting material for ferberite was also prepared from the equimolar mixture of Fe and WO_3 under the presence of 2 N $FeCl_2$ aqueous chloride solution in the same conditions. A small amount of anthracene was added as a reducing agent. The starting meterial for huebnerite was prepared from Mn and WO_3 in the same method as that for ferberite. The solid products were checked for any other phases by a powder X-ray diffractometer. Scheelite, ferberite and huebnerite synthesized in this manner were ground with an agate mortar, and then used as starting materials. As reactant solutions, we prepared mixed solutions of 2 N $CaCl_2$, $FeCl_2$ or $MnCl_2$ aqueous solution with 2 N NaCl or KCl aqueous solution, respectively, in the proportions of 10, 20, 30, 40, 60, and 80 vol%. Thus, the prepared solutions contain 2 molal Cl. Scheelite was reacted with $FeCl_2$-bearing or $MnCl_2$-bearing aqueous chloride solutions, and ferberite and huebnerite were reacted with $CaCl_2$-bearing aqueous chloride solutions. Ten to 20 mg of solid starting material was sealed into gold capsules (30 to 35 mm in length, 3.0 mm o.d. and 2.7 mm i.d.) with 15 to 40 μl of 2 N aqueous chloride solutions and approximately 1 mg of anthracene. The charge was reacted using a standard cold-seal pressure vessel at temperatures of 400 and 600°C and a pressure of 1 kbar. Run durations were 10 to 11 days for the 400°C experiments and 5 days for the 600°C experiments. The pressure vessel was heated with an electric furnace settled horizontally. Temperature was monitored

with a chromel-alumel thermocouple attached to the outside wall of the pressure vessel. A steel rod was inserted in the pressure vessel in order to minimize a temperature gradient (Boettcher and Kerrick, 1971). Temperature during runs was controlled within ±5°C. Water was used as a pressure medium. Pressure was measured using a Heise gauge. The runs were equilibrated from different directions, that is, scheelite was reacted with $FeCl_2$-bearing or $MnCl_2$-bearing aqueous solution, whereas ferberite and huebnerite with $CaCl_2$-bearing aqueous solution.

After the run, the pressure vessel was cooled rapidly with cold water in order to prevent any back reaction during the quench, and then the gold capsule was removed from the pressure vessel. After the check for any leakage, the run product was washed out into a beaker with distilled water. The solid product was separated from the aqueous chloride solution with a millipore filter of 0.45 μm pore size. The coexistence of the two phases, scheelite and ferberite or huebnerite, was confirmed optically with a petrographic microscope

and by an X-ray diffractometer (Rigaku RAD-IB). The chemical compositions of the solid phases were determined on the crystal surfaces by an energy dispersive X-ray microanalyser (JSM-5400 with Link QX-200JI system). The cations, Na, K, Ca, Fe and Mn in the aqueous chloride solutions were analysed using an atomic absorption/flame spectrophotometer (Shimadzu AA-610S).

EXPERIMENTAL RESULTS

Experimental results are summarized in Tables 1 to 8. The coexistence of the two phases, scheelite and ferberite or huebnerite was confirmed for all run products. The EPMA analysis revealed that $FeWO_4$ and $MnWO_4$ contents in scheelite and $CaWO_4$ content in ferberite and huebnerite are negligible (less than a few mol%). Figure 1 shows the equilibrium compositions of aqueous chloride solutions in equilibrium with both scheelite and ferberite as a function of Σm_{Na} or Σm_K, and Fig. 2 shows those for the assemblage of scheelite and huebnerite. Data for Na-free and K-free systems

Table 1. Experimental results for mineral-solution equilibria in the system $CaWO_4$-$FeWO_4$-$CaCl_2$-$FeCl_2$-$NaCl$-H_2O at 600°C, 1 kbar

Run No.	Duration	Starting materials						Run products (solution)		
		Solid		Solution				Σm_{Fe}	Σm_{Ca}	Σm_{Na}
	days	mg			μl		μl			
A013	5	sch*	16.6	$FeCl_2$	32	NaCl	8	0.659	0.150	0.382
A018	5	fer**	12.1	$CaCl_2$	36	NaCl	4	0.673	0.201	0.252
A026	5	fer	12.8	$CaCl_2$	36	NaCl	4	0.651	0.240	0.218
A028	5	fer	13.5	$CaCl_2$	32	NaCl	8	0.651	0.141	0.416
A029	5	fer	11.2	$CaCl_2$	28	NaCl	12	0.567	0.107	0.652
A030	5	sch	8.8	$FeCl_2$	28	NaCl	12	0.552	0.109	0.678
A031	5	fer	13.2	$CaCl_2$	24	NaCl	16	0.515	0.071	0.828
A033	5	fer	10.4	$CaCl_2$	16	NaCl	24	0.371	0.031	1.196
A035	5	fer	11.8	$CaCl_2$	8	NaCl	32	0.185	0.022	1.586
A037	5	fer	10.2	$CaCl_2$	36	NaCl	4	0.658	0.216	0.252
A038	5	sch	12.6	$FeCl_2$	36	NaCl	4	0.653	0.214	0.266
A039	5	fer	10.5	$CaCl_2$	32	NaCl	8	0.630	0.155	0.430
A040	5	sch	10.4	$FeCl_2$	32	NaCl	8	0.598	0.174	0.456
A041	5	fer	11.7	$CaCl_2$	24	NaCl	16	0.521	0.051	0.856
A042	5	sch	10.0	$FeCl_2$	24	NaCl	16	0.491	0.060	0.898
A043	5	fer	11.6	$CaCl_2$	16	NaCl	24	0.410	0.027	1.126
A044	5	sch	10.4	$FeCl_2$	16	NaCl	24	0.325	0.039	1.272
A045	5	fer	11.9	$CaCl_2$	8	NaCl	32	0.182	0.010	1.616
A046	5	sch	10.1	$FeCl_2$	8	NaCl	32	0.156	0.019	1.650

*sch: scheelite.
**fer: ferberite.

5

Table 2. *Experimental results for mineral-solution equilibria in the system $CaWO_4$-$FeWO_4$-$CaCl_2$-$FeCl_2$-$NaCl$-H_2O at 400°C, 1 kbar*

Run No.	Duration	Starting materials					Run products (solution)		
		Solid		Solution			$\sum m_{Fe}$	$\sum m_{Ca}$	$\sum m_{Na}$
	days		mg		μl		μl		
B035	10	fer*	10.0	$CaCl_2$	36	NaCl	4	0.271	0.619	0.220
B036	10	sch**	13.1	$FeCl_2$	36	NaCl	4	0.288	0.600	0.224
B037	10	fer	12.1	$CaCl_2$	32	NaCl	8	0.269	0.507	0.448
B038	10	sch	16.5	$FeCl_2$	32	NaCl	8	0.283	0.512	0.410
B039	10	fer	11.7	$CaCl_2$	28	NaCl	12	0.252	0.431	0.634
B042	10	sch	13.7	$FeCl_2$	24	NaCl	16	0.245	0.332	0.846
B043	10	fer	11.0	$CaCl_2$	16	NaCl	24	0.179	0.237	1.168
B044	10	sch	11.9	$FeCl_2$	16	NaCl	24	0.183	0.230	1.174
B045	10	fer	10.3	$CaCl_2$	8	NaCl	32	0.108	0.113	1.558
B046	10	sch	13.9	$FeCl_2$	8	NaCl	32	0.099	0.113	1.576
B047	10	fer	11.9	$CaCl_2$	28	NaCl	12	0.259	0.415	0.652
B048	10	sch	10.7	$FeCl_2$	28	NaCl	12	0.265	0.407	0.656
B049	10	fer	10.4	$CaCl_2$	24	NaCl	16	0.228	0.348	0.848
B050	10	sch	13.3	$FeCl_2$	24	NaCl	16	0.234	0.342	0.848

*fer: ferberite.
**sch: scheelite.

Table 3. *Experimental results for mineral-solution equilibria in the system $CaWO_4$-$FeWO_4$-$CaCl_2$-$FeCl_2$-KCl-H_2O at 600°C, 1 kbar*

Run No.	Duration	Starting materials					Run products (solution)		
		Solid		Solution			$\sum m_{Fe}$	$\sum m_{Ca}$	$\sum m_{K}$
	days		mg		μl		μl		
C003	5	sch*	10.8	$FeCl_2$	36	KCl	4	0.702	0.208	0.180
C004	5	fer**	10.1	$CaCl_2$	36	KCl	4	0.667	0.248	0.170
C005	5	sch	17.8	$FeCl_2$	32	KCl	8	0.606	0.196	0.396
C006	5	fer	10.0	$CaCl_2$	32	KCl	8	0.574	0.263	0.328
C007	5	sch	18.3	$FeCl_2$	28	KCl	12	0.590	0.111	0.598
C008	5	sch	13.7	$FeCl_2$	24	KCl	16	0.559	0.054	0.774
C017	5	fer	14.8	$CaCl_2$	28	KCl	12	0.588	0.095	0.634
C018	5	sch	10.8	$FeCl_2$	28	KCl	12	0.545	0.114	0.684
C019	5	fer	10.0	$CaCl_2$	24	KCl	16	0.533	0.042	0.850
C020	5	sch	12.9	$FeCl_2$	24	KCl	16	0.472	0.073	0.910
C021	5	fer	13.8	$CaCl_2$	36	KCl	4	0.617	0.278	0.210
C022	5	sch	10.7	$FeCl_2$	36	KCl	4	0.612	0.266	0.224
C023	5	fer	11.3	$CaCl_2$	32	KCl	8	0.611	0.174	0.430
C024	5	sch	11.1	$FeCl_2$	32	KCl	8	0.595	0.177	0.456
C025	5	fer	10.1	$CaCl_2$	16	KCl	24	0.347	0.025	1.256
C026	5	sch	13.7	$FeCl_2$	16	KCl	24	0.360	0.025	1.230
C027	5	fer	13.0	$CaCl_2$	8	KCl	32	0.183	0.013	1.608
C028	5	sch	15.1	$FeCl_2$	8	KCl	32	0.183	0.013	1.608
C029	5	fer	15.3	$CaCl_2$	24	KCl	16	0.524	0.056	0.840
C030	5	sch	10.3	$FeCl_2$	24	KCl	16	0.488	0.066	0.892
C031	5	fer	12.5	$CaCl_2$	16	KCl	24	0.326	0.044	1.260
C032	5	sch	10.0	$FeCl_2$	16	KCl	24	0.320	0.053	1.254
C033	5	fer	15.0	$CaCl_2$	8	KCl	32	0.170	0.026	1.608

*sch: scheelite.
**fer: ferberite.

Table 4. Experimental results for mineral-solution equilibria in the system $CaWO_4$-$FeWO_4$-$CaCl_2$-$FeCl_2$-KCl-H_2O at 400°C, 1 kbar

Run No.	Duration	Starting materials				Run products (solution)		
		Solid		Solution				
	days	mg		μl		μl	Σm_{Fe}	Σm_{Ca}	Σm_K
D003	10	sch*	16.2	$FeCl_2$	36	KCl	4	0.332	0.561	0.214
D004	10	fer**	11.0	$CaCl_2$	36	KCl	4	0.328	0.563	0.218
D007	10	sch	11.8	$FeCl_2$	28	KCl	12	0.278	0.417	0.610
D008	10	fer	15.3	$CaCl_2$	28	KCl	12	0.280	0.417	0.606
D009	10	fer	11.0	$CaCl_2$	32	KCl	8	0.282	0.501	0.434
D010	10	sch	15.0	$FeCl_2$	32	KCl	8	0.290	0.489	0.442
D011	10	fer	11.2	$CaCl_2$	24	KCl	16	0.258	0.337	0.810
D012	10	sch	16.3	$FeCl_2$	24	KCl	16	0.262	0.318	0.840
D015	10	fer	10.6	$CaCl_2$	8	KCl	32	0.091	0.064	1.690
D016	10	sch	19.8	$FeCl_2$	8	KCl	32	0.116	0.090	1.588
D019	10	fer	13.4	$CaCl_2$	32	KCl	8	0.248	0.549	0.406
D020	10	sch	11.1	$FeCl_2$	32	KCl	8	0.246	0.548	0.412
D021	10	fer	11.9	$CaCl_2$	16	KCl	24	0.208	0.189	1.206
D022	10	sch	19.1	$FeCl_2$	16	KCl	24	0.190	0.194	1.232
D023	10	fer	13.6	$CaCl_2$	36	KCl	4	0.297	0.608	0.190
D024	10	sch	15.6	$FeCl_2$	36	KCl	4	0.323	0.566	0.222
D025	10	fer	16.5	$CaCl_2$	24	KCl	16	0.247	0.360	0.786
D026	10	sch	16.5	$FeCl_2$	24	KCl	16	0.261	0.344	0.790
D027	10	fer	11.0	$CaCl_2$	16	KCl	24	0.227	0.185	1.178
D028	10	sch	10.0	$FeCl_2$	16	KCl	24	0.238	0.160	1.204
D029	10	fer	11.0	$CaCl_2$	8	KCl	32	0.117	0.087	1.592
D030	10	sch	11.9	$FeCl_2$	8	KCl	32	0.110	0.092	1.596
D031	10	fer	11.0	$CaCl_2$	8	KCl	32	0.122	0.079	1.598
D032	10	sch	13.0	$FeCl_2$	8	KCl	32	0.113	0.081	1.612
D033	11	fer	15.0	$CaCl_2$	24	KCl	16	0.262	0.329	0.818
D034	11	sch	10.9	$FeCl_2$	24	KCl	16	0.238	0.359	0.806
D035	11	fer	10.9	$CaCl_2$	16	KCl	24	0.209	0.202	1.178
D036	11	sch	12.4	$FeCl_2$	16	KCl	24	0.202	0.200	1.196
D037	12	fer	12.4	$CaCl_2$	36	KCl	4	0.355	0.544	0.202
D038	12	sch	10.8	$FeCl_2$	36	KCl	4	0.378	0.516	0.212

*sch: scheelite.
**fer: ferberite.

are taken from Uchida et al. (1989). The attainment of equilibrium was confirmed by the experiments using different starting materials, which gave identical results. The direction of approach to equilibrium of the aqueous solution compositions is indicated with that of triangles in the figures. The Ca/(Ca + Fe) and Ca/(Ca + Mn) ratios of the aqueous chloride solution in equilibrium with both scheelite and ferberite and with both scheelite and huebnerite, respectively, decrease significantly with the addition of NaCl and KCl at both 400 and 600°C. This is attributable to the formation of higher-order aqueous chloride complexes of Fe and Mn. The experimental results may suggest that NaCl and KCl behave as donors of Cl⁻ to $FeCl_{2aq}$ and $MnCl_{2aq}$ to form higher-order aqueous chloride complexes of Fe and Mn such as $FeCl_3^-{}_{aq}$ and $MnCl_3^-{}_{aq}$ respectively, under the supercritical conditions. For 400°C experiments, the effect of KCl is larger than that of NaCl, whereas for 600°C experiments, NaCl and KCl have similar effects on the equilibrium compositions of the aqueous chloride solutions. This indicates that dissociation constant of KCl_{aq} is larger than that of $NaCl_{aq}$ at 400°C, whereas $NaCl_{aq}$ and KCl_{aq} have similar dissociation constants at 600°C.

THERMODYNAMIC CONSIDERATION

Here we analyze thermodynamically the present experimental results. In this consideration,

Table 5. Experimental results for mineral-solution equilibria in the system $CaWO_4$-$MnWO_4$-$CaCl_2$-$MnCl_2$-$NaCl$-H_2O at 600°C, 1 kbar

Run No.	Duration	Starting materials					Run products (solution)		
		Solid		Solution			Σm_{Mn}	Σm_{Ca}	Σm_{Na}
	days		mg		μl		μl			
E033	5	hue*	14.4	$CaCl_2$	32	NaCl	8	0.684	0.124	0.384
E034	5	hue	14.4	$CaCl_2$	32	NaCl	8	0.680	0.134	0.372
E035	5	sch**	13.5	$MnCl_2$	32	NaCl	8	0.668	0.122	0.420
E036	5	sch	10.6	$MnCl_2$	32	NaCl	8	0.671	0.122	0.414
E037	5	sch	12.6	$MnCl_2$	24	NaCl	16	0.549	0.043	0.816
E038	5	sch	12.6	$MnCl_2$	24	NaCl	16	0.548	0.042	0.820
E039	5	hue	15.1	$CaCl_2$	24	NaCl	16	0.554	0.048	0.796
E040	5	hue	10.5	$CaCl_2$	24	NaCl	16	0.544	0.045	0.822
E041	5	sch	12.6	$MnCl_2$	16	NaCl	24	0.376	0.014	1.220
E042	5	sch	9.3	$MnCl_2$	16	NaCl	24	0.395	0.015	1.180
E043	5	hue	10.2	$CaCl_2$	16	NaCl	24	0.372	0.012	1.232
E044	5	hue	12.9	$CaCl_2$	16	NaCl	24	0.385	0.014	1.202
E045	5	sch	19.8	$MnCl_2$	8	NaCl	32	0.189	0.002	1.618
E046	5	sch	15.0	$MnCl_2$	8	NaCl	32	0.195	0.001	1.608
E047	5	hue	10.0	$CaCl_2$	8	NaCl	32	0.186	0.002	1.624
E048	5	hue	15.3	$CaCl_2$	8	NaCl	32	0.173	0.002	1.650
E083	5	sch	16.9	$MnCl_2$	36	NaCl	4	0.724	0.157	0.238
E084	5	hue	10.5	$CaCl_2$	36	NaCl	4	0.728	0.171	0.202
E087	5	sch	13.3	$MnCl_2$	28	NaCl	12	0.634	0.060	0.612
E088	5	hue	10.5	$CaCl_2$	28	NaCl	12	0.634	0.060	0.612

*hue: huebnerite.
**sch: scheelite.

Table 6. Experimental results for mineral-solution equilibria in the system $CaWO_4$-$MnWO_4$-$CaCl_2$-$MnCl_2$-$NaCl$-H_2O at 400°C, 1 kbar

Run No.	Duration	Starting materials					Run products (solution)		
		Solid		Solution			Σm_{Mn}	Σm_{Ca}	Σm_{Na}
	days		mg		μl		μl			
F102	11	sch*	14.7	$MnCl_2$	36	NaCl	4	0.347	0.530	0.246
F104	11	sch	15.0	$MnCl_2$	24	NaCl	16	0.319	0.250	0.862
F105	11	sch	10.6	$MnCl_2$	16	NaCl	24	0.214	0.171	1.230
F106	11	sch	13.8	$MnCl_2$	8	NaCl	32	0.121	0.083	1.592
F108	11	hue**	11.7	$CaCl_2$	36	NaCl	4	0.363	0.484	0.306
F109	11	hue	16.7	$CaCl_2$	32	NaCl	8	0.380	0.400	0.440
F111	11	hue	10.4	$CaCl_2$	16	NaCl	24	0.212	0.160	1.256
F112	11	hue	12.8	$CaCl_2$	8	NaCl	32	0.120	0.067	1.626
F114	12	sch	11.3	$MnCl_2$	32	NaCl	8	0.410	0.384	0.412
F115	12	sch	12.6	$MnCl_2$	28	NaCl	12	0.359	0.332	0.618
F121	12	hue	10.4	$CaCl_2$	28	NaCl	12	0.342	0.316	0.684
F122	12	hue	11.5	$CaCl_2$	24	NaCl	16	0.325	0.235	0.874
F123	12	hue	12.2	$CaCl_2$	16	NaCl	24	0.213	0.142	1.290
F125	11	sch	13.2	$MnCl_2$	36	NaCl	4	0.410	0.472	0.236
F126	11	hue	15.6	$CaCl_2$	36	NaCl	4	0.353	0.535	0.224
F127	11	sch	10.6	$MnCl_2$	28	NaCl	12	0.358	0.355	0.574
F128	11	hue	10.8	$CaCl_2$	28	NaCl	12	0.303	0.399	0.596
F129	10	sch	10.3	$MnCl_2$	32	NaCl	8	0.356	0.427	0.434
F132	10	sch	13.2	$MnCl_2$	8	NaCl	32	0.115	0.078	1.614
F133	12	hue	15.7	$CaCl_2$	32	NaCl	8	0.393	0.384	0.446
F134	12	hue	13.0	$CaCl_2$	24	NaCl	16	0.326	0.257	0.835
F135	12	hue	13.0	$CaCl_2$	16	NaCl	24	0.245	0.149	1.212
F136	12	hue	10.5	$CaCl_2$	8	NaCl	32	0.101	0.084	1.630

*sch: scheelite.
**hue: huebnerite.

Table 7. Experimental results for mineral-solution equilibria in the system $CaWO_4$-$MnWO_4$-$CaCl_2$-$MnCl_2$-KCl-H_2O at 600°C, 1 kbar

Run No.	Duration	Starting materials						Run products (solution)		
		Solid		Solution				Σm_{Mn}	Σm_{Ca}	Σm_K
	days		mg		μl		μl			
G059	5	sch*	14.6	$MnCl_2$	32	KCl	8	0.702	0.109	0.378
G060	5	hue**	13.1	$CaCl_2$	32	KCl	8	0.686	0.124	0.380
G061	5	sch	16.9	$MnCl_2$	24	KCl	16	0.578	0.038	0.768
G062	5	hue	13.2	$CaCl_2$	24	KCl	16	0.567	0.025	0.816
G063	5	sch	12.0	$MnCl_2$	16	KCl	24	0.375	0.008	1.234
G064	5	hue	7.8	$CaCl_2$	16	KCl	24	0.397	0.004	1.198
G065	5	sch	9.9	$MnCl_2$	8	KCl	32	0.191	0.003	1.612
G066	5	hue	10.8	$CaCl_2$	8	KCl	32	0.191	0.000	1.618
G085	5	sch	15.1	$MnCl_2$	36	KCl	4	0.720	0.169	0.222
G086	5	hue	13.3	$CaCl_2$	36	KCl	4	0.741	0.161	0.196
G089	5	sch	10.9	$MnCl_2$	28	KCl	12	0.675	0.060	0.530
G090	5	hue	11.5	$CaCl_2$	28	KCl	12	0.649	0.062	0.578

*sch: scheelite.
**hue: huebnerite.

Table 8. Experimental results for mineral-solution equilibria in the system $CaWO_4$-$MnWO_4$-$CaCl_2$-$MnCl_2$-KCl-H_2O at 400°C, 1 kbar

Run No.	Duration	Starting materials						Run products (solution)		
		Solid		Solution				Σm_{Mn}	Σm_{Ca}	Σm_K
	days		mg		μl		μl			
H069	10	sch*	17.2	$MnCl_2$	24	KCl	16	0.289	0.315	0.792
H070	10	hue**	10.7	$CaCl_2$	24	KCl	16	0.272	0.284	0.888
H071	10	sch	19.7	$MnCl_2$	16	KCl	24	0.236	0.140	1.248
H072	10	hue	11.8	$CaCl_2$	16	KCl	24	0.238	0.162	1.200
H073	10	sch	16.3	$MnCl_2$	8	KCl	32	0.153	0.050	1.594
H074	10	hue	12.1	$CaCl_2$	8	KCl	32	0.139	0.064	1.594
H079	10	sch	13.1	$MnCl_2$	36	KCl	4	0.320	0.568	0.224
H080	10	hue	10.7	$CaCl_2$	36	KCl	4	0.318	0.574	0.216
H081	10	sch	10.8	$MnCl_2$	28	KCl	12	0.295	0.408	0.594
H082	10	hue	32.3	$CaCl_2$	28	KCl	12	0.293	0.403	0.608
H093	10	sch	7.8	$MnCl_2$	36	KCl	4	0.341	0.563	0.192
H094	10	hue	12.4	$CaCl_2$	36	KCl	4	0.314	0.576	0.220
H095	10	sch	12.3	$MnCl_2$	32	KCl	8	0.296	0.517	0.374
H096	10	hue	12.3	$CaCl_2$	32	KCl	8	0.341	0.452	0.414
H097	10	sch	11.3	$MnCl_2$	32	KCl	8	0.345	0.441	0.428
H098	10	hue	10.9	$CaCl_2$	32	KCl	8	0.345	0.431	0.448
H099	10	sch	14.2	$MnCl_2$	8	KCl	32	0.137	0.074	1.578
H100	10	hue	7.9	$CaCl_2$	8	KCl	32	0.140	0.056	1.608

*sch: scheelite.
**hue: huebnerite.

higher-order aqueous chloride complexes other than $NaCl_{aq}$, KCl_{aq} and $CaCl_{2aq}$ were neglected due to the ionic property of NaCl, KCl and $CaCl_2$. Experimental results for calcite and wollasonite solubilities in supercritical NaCl-HCl aqueous solutions by Fein and Walther (1989) and Xie and Walther (1993), respectively, did not support the presence of higher-order aqueous chloride complexes of Ca than $CaCl_{2aq}$. On the other hand, $FeCl_2$ and $MnCl_2$ are compounds of coordination bond. Therefore, higher-order charged chloride complexes of Fe and Mn such as $FeCl_3{}^-_{aq}$,
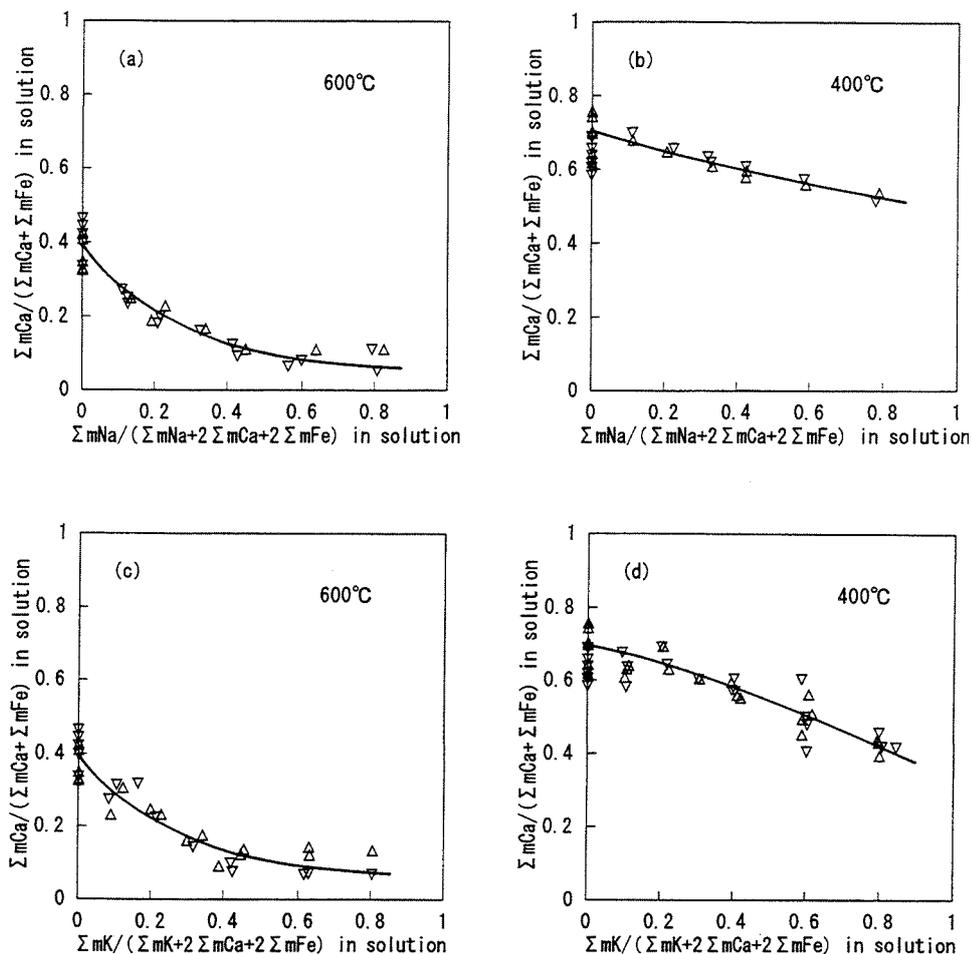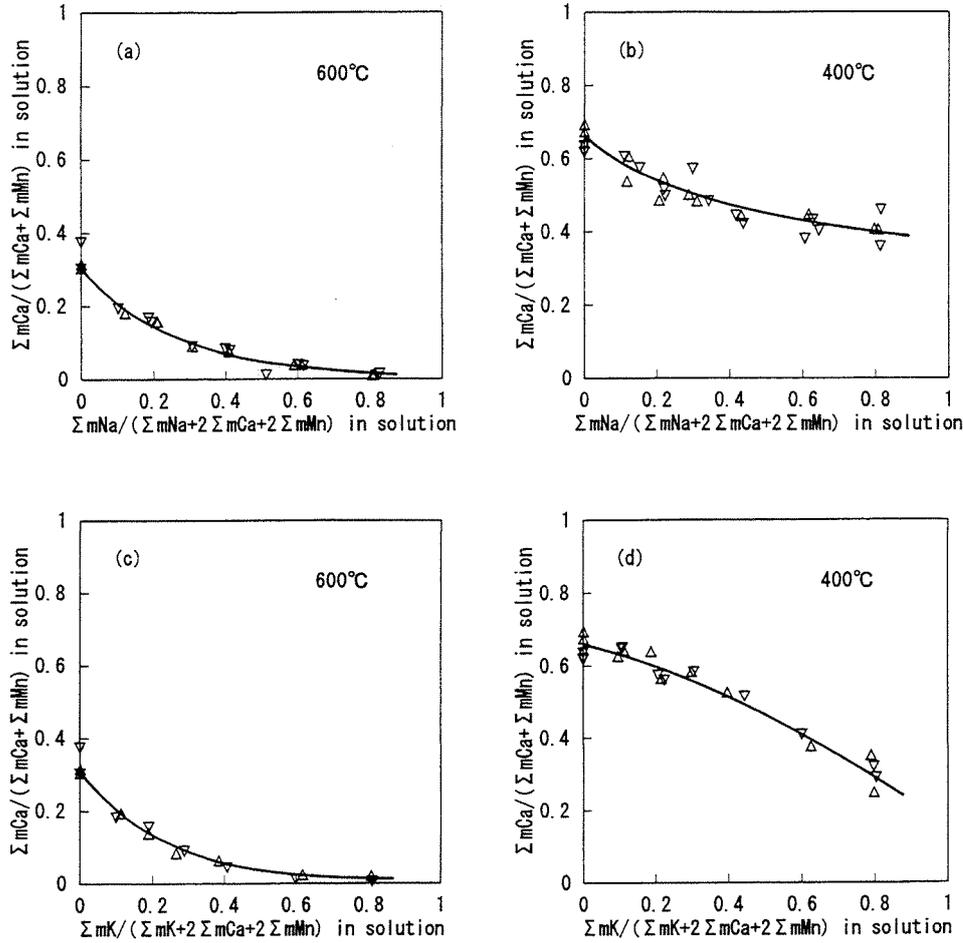
Fig. 1. Plots of $\Sigma m_{Ca}/(\Sigma m_{ca} + \Sigma m_{Fe})$ vs. $\Sigma m_{Na}/(2\Sigma m_{Ca} + 2\Sigma m_{Fe} + \Sigma m_{Na})$ or $\Sigma m_K/(2\Sigma m_{Ca} + 2\Sigma m_{Fe} + \Sigma m_K)$ for the aqueous chloride solutions in equilibrium with scheelite and ferberite at 400°C and 600°C, and 1 kbar. The direction of triangles in the figure indicates that of attainment to equilibrium. Data for Na-free and K-free systems are from Uchida et al. (1989). (a) Effect of NaCl at 600°C, (b) effect of NaCl at 400°C, (c) effect of KCl at 600°C and (d) effect of KCl at 400°C.

$FeCl_4^{2-}{}_{aq}$, $MnCl_3^-{}_{aq}$ and $MnCl_4^{2-}{}_{aq}$ may be preferred under supercritical conditions. Here we assume $FeCl_3^-{}_{aq}$ and $MnCl_3^-{}_{aq}$ as representative species of higher-order aqueous chloride complexes of Fe and Mn, respectively. On the other hand, $Fe^{2+}{}_{aq}$, $FeCl^+{}_{aq}$, $Mn^{2+}{}_{aq}$ and $MnCl^+{}_{aq}$ were neglected in the present calculation. This is supported by the experiments of Boctor et al. (1980), Fein et al. (1992) and Boctor (1985). Therefore, the decrease of the Ca/(Ca + Fe) and Ca/(Ca + Mn) ratios of the aqueous chloride solutions in equilibrium with scheelite and ferberite and with scheelite and huebnerite, respectively, with increasing NaCl and KCl concentrations is attributable mainly to the formation of higher-order aqueous chloride complexes, $FeCl_3^-{}_{aq}$ and $MnCl_3^-{}_{aq}$. Aqueous hydroxide complexes were also deleted from consideration. This assumption may be valid for the aqueous solutions with high chlorine contents used in the present study. Based on these assumptions we estimate the dissociation constants of $FeCl_3^-{}_{aq}$ and $MnCl_3^-{}_{aq}$ from the experimental results using the published dissociation constants for KCl_{aq}, $NaCl_{aq}$, $CaCl_{2aq}$ and $CaCl^+{}_{aq}$.

Fig. 2. Plots of $\Sigma m_{Ca}/(\Sigma m_{Ca} + \Sigma m_{Mn})$ vs. $\Sigma m_{Na}/(2\Sigma m_{Ca} + 2\Sigma m_{Mn} + \Sigma m_{Na})$ or $\Sigma m_{K}/(2\Sigma m_{Ca} + 2\Sigma m_{Mn} + \Sigma m_{K})$ for the aqueous chloride solutions in equilibrium with scheelite and huebnerite at 400°C and 600°C, and 1 kbar. The direction of triangles in the figure indicates that of attainment of equilibrium. Data for Na-free and K-free systems are from Uchida et al. (1989). (a) Effect of NaCl at 600°C, (b) effect of NaCl at 400°C, (c) effect of KCl at 600°C and (d) effect of KCl at 400°C.

Oelkers and Helgeson (1990) recently have suggested that the presence of aqueous triple chloride complexes such as Na_2Cl^+ and $NaCl_2^-$ for 1:1 electrolytes is not negligible in supercritical aqueous solutions. Moreover, Oelkers and Helgeson (1991) have demonstrated that the activity coefficients for aqueous neutral species of 1:1 electrolytes deviate significantly from unity under supercritical temperatures and pressures. However, in this study we neglect the presence of aqueous triple chloride complexes, and also assume the activity coefficients for the neutral spe-

cies to be unity because we have not sufficient thermodynamic data for all the aqueous species at present. The following calculation, therefore, will have to be reconsidered in the near future.

The following twelve aqueous species were included in the calculations; Cl^-_{aq}, Na^+_{aq}, $NaCl_{aq}$, K^+_{aq}, KCl_{aq}, Ca^{2+}_{aq}, $CaCl^+_{aq}$, $CaCl_{2aq}$, $FeCl_{2aq}$, $FeCl_3^-_{aq}$, $MnCl_{2aq}$ and $MnCl_3^-_{aq}$. The calculations can be carried out by solving simultaneously the following mass-balance and mass-action equations:

$$\Sigma m_{Na} = m(Na^+_{aq}) + m(NaCl_{aq}) \qquad (3)$$

$$\sum m_{\text{K}} = m(\text{K}^+_{\text{aq}}) + m(\text{KCl}_{\text{aq}}) \qquad (4)$$

$$\sum m_{\text{Ca}} = m(\text{Ca}^{2+}_{\text{aq}}) + m(\text{CaCl}^+_{\text{aq}}) + m(\text{CaCl}_{2\text{aq}}) \quad (5)$$

$$\sum m_{\text{Fe}} = m(\text{FeCl}_{2\text{aq}}) + m(\text{FeCl}_3^-{}_{\text{aq}}) \qquad (6)$$

$$\sum m_{\text{Mn}} = m(\text{MnCl}_{2\text{aq}}) + m(\text{MnCl}_3^-{}_{\text{aq}}) \qquad (7)$$

$$\begin{aligned}\sum m_{\text{Cl}} &= m(\text{Cl}^-_{\text{aq}}) + m(\text{NaCl}_{\text{aq}}) + m(\text{KCl}_{\text{aq}}) \\ &+ m(\text{CaCl}^-_{\text{aq}}) + 2m(\text{CaCl}_{2\text{aq}}) + 2m(\text{FeCl}_{2\text{aq}}) \\ &+ 3m(\text{FeCl}_3^-{}_{\text{aq}}) + 2m(\text{MnCl}_{2\text{aq}}) \\ &+ 3m(\text{MnCl}_3^-{}_{\text{aq}}) = 2\end{aligned} \qquad (8)$$

$$K(\text{NaCl}) = a(\text{Na}^+_{\text{aq}}){\cdot}a(\text{Cl}^-_{\text{aq}})/a(\text{NaCl}_{\text{aq}}) \quad (9)$$

$$K(\text{KCl}) = a(\text{K}^+_{\text{aq}}){\cdot}a(\text{Cl}^-_{\text{aq}})/a(\text{KCl}_{\text{aq}}) \quad (10)$$

$$K(\text{CaCl}^-) = a(\text{Ca}_{\text{aq}}){\cdot}a(\text{Cl}^-_{\text{aq}})/a(\text{CaCl}^+_{\text{aq}}) \quad (11)$$

$$K(\text{CaCl}_2) = a(\text{CaCl}^-_{\text{aq}}){\cdot}a(\text{Cl}^-_{\text{aq}})/a(\text{CaCl}_{2\text{aq}}) \quad (12)$$

$$\begin{aligned}&K(\text{FeCl}_3^-) \\ &= a(\text{FeCl}_3^-{}_{\text{aq}})/\{a(\text{FeCl}_{2\text{aq}}){\cdot}a(\text{Cl}^-_{\text{aq}})\}\end{aligned} \qquad (13)$$

$$\begin{aligned}&K(\text{MnCl}_3^-) \\ &= a(\text{MnCl}_3^-{}_{\text{aq}})/\{a(\text{MnCl}_{2\text{aq}}){\cdot}a(\text{Cl}^-_{\text{aq}})\},\end{aligned} \qquad (14)$$

where $m(i)$ refers to the molality of i aqueous species, $\sum m_i$ denotes the sum of the molalities of i-bearing aqueous species, $a(i)$ designates the activity of i aqueous species, and K is the dissociation or formation constant. The activity coefficients for the neutral aqueous species were assumed to be unity in this study, whereas those for the charged aqueous species were computed from the Debye-Huckel equation:

$$\log \gamma_i = -Z_i A I^{1/2} / \left(1 + a_i B I^{1/2}\right), \qquad (15)$$

where Z_i donotes the ionic charge and I is the true ionic strength which is defined by

$$I = 1 / 2 \sum m_i Z_i^2. \qquad (16)$$

A and B represent the Debye-Huckel coefficients

and are taken from Helgeson and Kirkham (1974b). a_i signifies the ion size parameter for i species and is taken from Kharaka and Barnes (1973). The ion size parameters for $\text{CaCl}^+_{\text{aq}}$, $\text{FeCl}_3^-{}_{\text{aq}}$ and $\text{MnCl}_3^-{}_{\text{aq}}$ are assumed to be 4 as done for $\text{PbCl}^+_{\text{aq}}$ and $\text{PbCl}_3^-{}_{\text{aq}}$ by Seward (1984). In this study, we adopted the dissociation constant of Quist and Marshall (1968) for NaCl_{aq}, that of Franck (1956) for KCl_{aq}, and that of Frantz and Marshall (1982) for $\text{CaCl}^+_{\text{aq}}$ and $\text{CaCl}_{2\text{aq}}$. The dissociation constant of Ritzert and Franck (1968) for KCl_{aq} seems to be too small compared to that for NaCl_{aq} at 400°C and 1 kbar. As described above, we can deduce from the experimental results that the dissociation constant of KCl_{aq} should be larger than that of NaCl_{aq}. Therefore, we prefer the dissociation constant of Franck (1956) for KCl_{aq}, which shows a similar value to that for NaCl_{aq}. The dissociation constants for $\text{FeCl}_3^-{}_{\text{aq}}$ and $\text{MnCl}_3^-{}_{\text{aq}}$ were calculated from the experimental results so as to find adequate values which make the calculated ratios of $m(\text{CaCl}_{2\text{aq}})/m(\text{FeCl}_{2\text{aq}})$ and $m(\text{CaCl}_{2\text{aq}})/m(\text{MnCl}_{2\text{aq}})$ to be constant as required by the reactions (1) and (2):

$$\begin{aligned}&K(1) \\ &= a(\text{ferberite}){\cdot}m(\text{CaCl}_{2\text{aq}})/(a(\text{scheelite}){\cdot}m(\text{FeCl}_{2\text{aq}})) \\ &= m(\text{CaCl}_{2\text{aq}})/m(\text{FeCl}_{2\text{aq}})\end{aligned} \qquad (17)$$

$$\begin{aligned}&K(2) \\ &= a(\text{huebnerite}){\cdot}m(\text{CaCl}_{2\text{aq}})/(a(\text{scheelite}){\cdot}m(\text{MnCl}_{2\text{aq}})) \\ &= m(\text{CaCl}_{2\text{aq}})/m(\text{MnCl}_{2\text{aq}}),\end{aligned} \qquad (18)$$

where activities for scheelite, ferberite and huebnerite were assumed to be unity, respectively, because of limited solubilities between scheelite and ferberite or huebnerite. The obtained values for $\log K(\text{FeCl}_3^-)$ are 0.2(NaCl) and 1.2(KCl) for 400°C, and 1.9(NaCl) and 1.9(KCl) for 600°C, and those for $\log K(\text{MnCl}_3^-)$ are 0.4(NaCl) and 1.1(KCl) for 400°C, and 2.3(NaCl) and 2.3(KCl) for 600°C. There is a consistency between formation constants obtained using NaCl and those obtained using KCl for 600°C, but this is not the case for 400°C. This may be attributable to the unreliable dissociation constant of KCl_{aq} at 400°C.

12

Figures 3(a) and (b) depict the relations of $\Sigma m_{Ca}/(\Sigma m_{Ca} + \Sigma m_{Me})$ (Me: Fe or Mn) vs. Σm_{Na} concentration in the aqueous chloride solutions at 600°C and 1 kbar, as a function of $\log K(\text{MeCl}_3^-{}_{aq})$ and $\log K(\text{MeCl}_4^{2-}{}_{aq})$, respectively, where

$$K(\text{MnCl}_4{}^{2-})$$
$$= a(\text{MnCl}_4{}^{2-}{}_{aq})/\{a(\text{MnCl}_{2aq}) \cdot a(\text{Cl}^-{}_{aq})^2\}. \quad (19)$$

In Fig. 3(b), aqueous species $\text{MnCl}_3^-{}_{aq}$ was neglected. The observed curves agree well with those for $\log K(\text{MeCl}_3^-{}_{aq})$ rather than those for $\log K(\text{MeCl}_4^{2-}{}_{aq})$. This means that $\text{FeCl}_3^-{}_{aq}$ and $\text{MnCl}_3^-{}_{aq}$ are predominant among the higher-order aqueous chloride complexes of Fe and Mn, respectively. This may be the case for 400°C due to relatively small formation constants for $\text{FeCl}_3^-{}_{aq}$

and $\text{MnCl}_3^-{}_{aq}$. Therefore, our assumption made for the calculation is justified. Figure 4 gives the aqueous species concentrations calculated for the aqueous chloride solutions in equilibrium with scheelite and huebnerite using the dissociation constants for $\text{MnCl}_3^-{}_{aq}$ obtained in this study. Concentrations of aqueous species are plotted in the figure as a function of $\Sigma m_{Na}/(2\Sigma m_{Ca} + 2\Sigma m_{Mn} + \Sigma m_{Na})$. At 400°C, concentrations of $\text{Na}^+{}_{aq}$, $\text{Cl}^-{}_{aq}$ and NaCl_{aq} increase monotonously with the increase of Σm_{Na}, whereas those of other species except for $\text{MnCl}_3^-{}_{aq}$ decrease. $\text{Na}^+{}_{aq}$ is a dominant Na species, and CaCl_{2aq} and CaCl^+ are dominant Ca species. MnCl_{2aq} is dominant at lower $\Sigma m_{Na}/(2\Sigma m_{Ca} + 2\Sigma m_{Mn} + \Sigma m_{Na})$ value (<0.3), but $\text{MnCl}_3^-{}_{aq}$ becomes dominant at higher $\Sigma m_{Na}/(2\Sigma m_{Ca} + 2\Sigma m_{Mn} + \Sigma m_{Na})$ value. At 600°C,
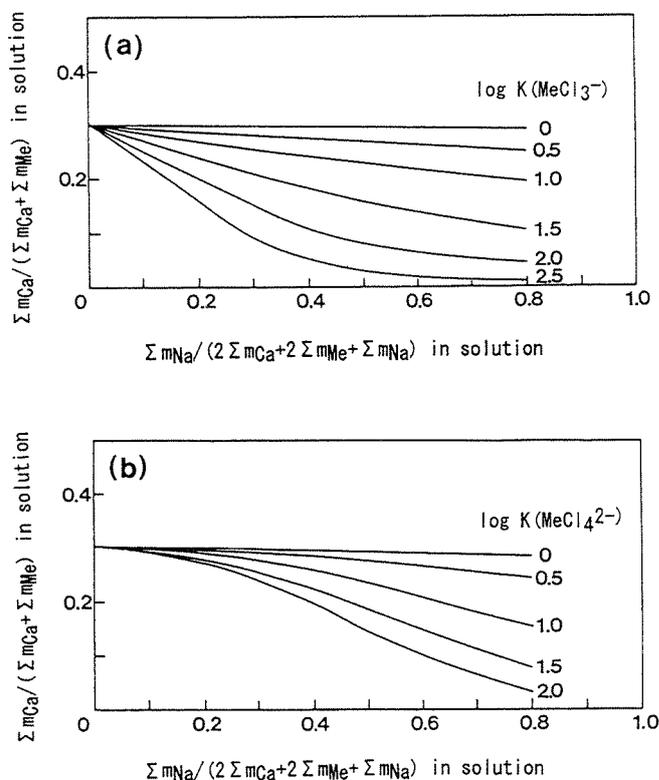
Fig. 3. Relation between $\Sigma m_{Ca}/(\Sigma m_{Ca} + \Sigma m_{Me})$ and $\Sigma m_{Na}/(2\Sigma m_{Ca} + 2\Sigma m_{Me} + \Sigma m_{Na})$ (Me: divalent ion) at 600°C, and 1 kbar for the 2 N aqueous chloride solution in equilibrium with scheelite and ferberite or huebnerite, (a) as a function of $\log K(\text{MeCl}_3^-{}_{aq})$ and (b) as a function of $\log K(\text{MeCl}_4^{2-}{}_{aq})$, calculated using published dissociation constants for NaCl_{aq}, CaCl_{2aq} and $\text{CaCl}^+{}_{aq}$. In Fig. 3(b), aqueous species $\text{MeCl}_3^-{}_{aq}$ was neglected.

concentrations of $NaCl_{aq}$ and Cl^-_{aq} increase with the increase of Σm_{Na}, whereas those of $MnCl_{2aq}$, $CaCl_{2aq}$, $CaCl^+_{aq}$ and Ca^{2+}_{aq} decrease. Concentrations of $MnCl_3^-_{aq}$ and Na^+_{aq} increase with the increase of Σm_{Na}, but show maxima, and then decrease. $CaCl_{2aq}$ is a dominant Ca species. Na^+_{aq} and $MnCl_{2aq}$ are dominant at lower Σm_{Na} value, but $NaCl_{aq}$ and $MnCl_3^-_{aq}$ become dominant at higher Σm_{Na} value. A similar behavior can be observed for the Fe-bearing system. Experimental results show that $FeCl_3^-_{aq}$ and $MnCl_3^-_{aq}$ are dominant aqueous species in natural hydrothermal

Fig. 4. Concentrations of aqueous species vs. $\Sigma m_{Na}/$ $(2\Sigma m_{Ca} + 2\Sigma m_{Mn} + \Sigma m_{Na})$ *for the 2 N aqueous chloride solutions in equilibrium with scheelite and huebnerite at (a) 400°C and (b) 600°C, and 1 kbar. The calculations were carried out using dissociation constants for* $MnCl_3^-_{aq}$ *obtained in this study.*

solutions at both 400°C and 600°C, and probably this may be the case at higher temperatures. The predominance of the higher-order aqueous chloride complexes at higher temperatures have been demonstrated experimentally for Ni by Fahlquist and Popp (1989) and for Mg by Grabman and Popp (1991). This seems to be a consequence of the decrease of the dielectric constant of H_2O at higher temperatures (e.g., Helgeson and Kirkham, 1974a).

Thus large formation constants (the reciprocal of dissociation constant) for $FeCl_3^-_{aq}$ and $MnCl_3^-_{aq}$ were obtained from the present experiments under the supercritical conditions. This means that the supposition of $m(MeCl_{2aq}) = \Sigma m_{Me}$ for supercritical hydrothermal solutions made in most previous studies (e.g., Kubo *et al.*, 1992b) is invalid. Therefore, when thermodynamic properties of solid solutions are calculated from ion exchange experiments with aqueous chloride solutions, we have to take it into consideration as Pascal and Roux (1985) have done for $KCl-NaCl-H_2O$ solutions.

REFERENCES

Boctor, N. Z. (1985) Rhodonite solubility and thermodynamic properties of aqueous $MnCl_2$ in the system $MnO-SiO_2-HCl-H_2O$. *Geochim. Cosmochim. Acta* **49**, 565–575.

Boctor, N. Z., Popp, R. K. and Frantz, J. D. (1980) Mineral-solution equilibria IV. Solubilities and the thermodynamic properties of $FeCl_2^0$ in the system $Fe_2O_3-H_2-H_2O-HCl$. *Geochim. Cosmochim. Acta* **44**, 1509–1518.

Boettcher, A. L. and Kerrick, D. M. (1971) Temperature calibration in cold-seal pressure vessels. *Research Techniques for High Pressure and High Temperature* (Ulmer, G. C., ed.), 179–193, Springer-Verlag, New York.

Fahlquist, L. S. and Popp, R. K. (1989) The effect of NaCl on bunsenite solubility and Ni-complexing in supercritical aqueous fluids. *Geochim. Cosmochim. Acta* **53**, 989–995.

Fein, J. B., Hemley, J. J., D'Angelo, W. M., Komninou, A. K. and Sverjensky, D. A. (1992) Experimental study of iron-chloride complexing in hydrothermal fluids. *Geochim. Cosmochim. Acta* **56**, 3179–3190.

Fein, J. B. and Walther, J. V. (1989) Calcite solubility and speciation in supercritical NaCl-HCl aqueous fluids. *Contrib. Mineral. Petrol.* **103**, 317–324.

Franck, E. U. (1956) Hochverdichteter wasserdamph— I. Elektolytishe leifahigkeit in KCl-H2O-losungen bis 750°C. *Z. Phys. Chem.* **8**, 92–106.

Frantz, J. D. and Marshall, W. L. (1982) Electrical conductances and ionization constants of calcium chloride and magnesium chloride in aqueous solutions at temperatures to 600°C and pressures to 4000 bars. *Am. J. Sci.* **282**, 1666–1693.

Grabman, K. B. and Popp, R. K. (1991) Experimental investigation of talc solubility in H2O-MgCl2-NaCl-HCl fluids in the range 500–700°C, 2 kb. *Geochim. Cosmochim. Acta* **55**, 2819–2829.

Helgeson, H. C. and Kirkham, D. H. (1974a) Theoretical prediction of the thermodynamic behavior of aqueous electrolytes at high pressures and temperatures: I. Summary of the thermodynamic/electrostatic properties of the solvent. *Am. J. Sci.* **274**, 1089–1198.

Helgeson, H. C. and Kirkham, D. H. (1974b) Theoretical prediction of the thermodynamic behavior of aqueous electrolytes at high pressures and temperatures: II. Debye-Huckel parameters for activity coefficients and relative partial molal properties. *Am. J. Sci.* **274**, 1199–1261.

Holland, H. D. (1972) Granites, solutions, and base metal deposits. *Econ. Geol.* **67**, 281–301.

Iiyama, J. T. (1964) Etude des reactions d'echange d'ions Na-K dans la serie muscovite-paragonite. *Bull. Soc. Franc. Miner. Crist.* **87**, 532–541.

Ilton, E. S. and Eugster, H. P. (1989) Base metal exchange between magnetite and a chloride-rich hydrothermal fluid. *Geochim. Cosmochim. Acta* **53**, 291–301.

Kakuda, Y., Uchida, E. and Imai, N. (1991) Experimental study on phase equilibria in the system CaSiO3-MnSiO3-(Ca,Mn)Cl2-H2O by means of ion exchange. *Mining Geology* **41**, 339–349.

Kharaka, Y. K. and Barnes, I. (1973) SOLMNEQ; solution-mineral equilibrium computations. *NTIS Tech. Rept.* **PB215-899**, 82 pp.

Kubo, T., Nakato, T. and Uchida, E. (1992a) An experimental study on partitioning of Zn, Fe, Mn and Cd between sphalerite and aqueous chloride solution. *Mining Geology* **42**, 301–309.

Kubo, T., Uchida, E., Furukawa, Y. and Imai, N. (1992b) Experimental study on ion exchange equilibria between ilmenite solid solution $(Fe^{2+},Mn^{2+},Mg)TiO_3$ and aqueous $(Fe^{2+},Mn^{2+}$

$Mg)Cl_2$ solution. *J. Min. Soc. Jpn.* **21**, 59–67 (in Japanese).

Lenmann, J. and Roux, J. (1986) Experimental and theoretical study of $(Fe^{2+},Mg)(Al,Fe^{3+})_2O_4$ spinels: Activity-composition relationships, miscibility gaps, vacancy contents. *Geochim. Cosmochim. Acta* **50**, 1765–1783.

Miyamoto, Y. and Uchida, E. (1994) Experiments for the partitioning of Mg^{2+}, Fe^{2+} and Mn^{2+} ions between spinel group minerals and aqueous chloride solution at 600°C and 1 kb. *J. Mineral. Petrol. Econ. Geol.* **89**, 177–188 (in Japanese).

Oelkers, E. H. and Helgeson, H. C. (1990) Triple-ion anions and polynuclear complexing in supercritical electrolyte solutions. *Geochim. Cosmochim. Acta* **54**, 727–738.

Oelkers, E. H. and Helgeson, H. C. (1991) Calculation of activity coefficients and degrees of formation of neutral ion pairs in supercritical electrolyte solutions. *Geochim. Cosmochim. Acta* **55**, 1235–1251.

Ogino, A., Uchida, E., Kakuda, Y. and Imai, N. (1992) Experimental study on phase equilibria in the system $CaSiO_3$-$FeSiO_3$-$MnSiO_3$-$(Ca,Fe,Mn)Cl_2$-H_2O by means of ion exchange at 600°C and 1 kbar. *Min. Geol.* **42**, 119–129.

Orville, P. M. (1963) Alkali ion exchange between vapor and feldspar phases. *Am. J. Sci.* **261**, 201–237.

Pascal, M. L. and Roux, J. (1985) K-Na exchange equilibria between muscovite-paragonite solid solution and hydrothermal chloride solutions. *Mineral. Mag.* **49**, 515–521.

Popp, R. K. and Frantz, J. D. (1979) Mineral-solution equilibria II. An experimental study of mineral solubilities and the thermodynamic properties of aqueous $CaCl_2$ in the system CaO-SiO_2-H_2O-HCl. *Geochim. Cosmochim. Acta* **43**, 1777–1790.

Quist, A. and Marshall, W. L. (1968) Electrical conductances of aqueous sodium chloride solutions from 0 to 800° and at pressures to 4000 bars. *J. Phys. Chem.* **72**, 684–703.

Ritzert, G. and Franck, E. U. (1968) Elektrische Leitfahigkeit wassriger Losungen bei hohen Temperaturen und Drucken. I. KCl, $BaCl_2$, $Ba(OH)_2$ und $MgSO_4$ bis 750°C und 6 kbar. *Ber. Bunsengesell. fur Physik Chemie* **72**, 798–808.

Roux, J. (1974) Etude des solutions solids des nephelines $(Na,K)AlSiO_4$. *Geochim. Cosmochim. Acta* **38**, 1213–1244.

Schulien, S. (1980) Mg-Fe partitioning between biotite and a supercritical chloride solution. *Contrib. Mineral. Petrol.* **74**, 85–93.

Schulien, S., Friedrischen, H. and Hellner, E. (1970) Das Mischkristallverhalten des Olivins zwishen 450°C und 650°C bei 1 kb Druck. *Neues Jahrb.*

Miner. Monatsh. **4**, 141–147.

Seward, T. M. (1984) The formation of lead (II) chloride complexes to 300°C: Spectrophotometric study. *Geochim. Cosmochim. Acta* **48**, 121–134.

Uchida, E. (1993) Estimation of relative concentrations of cations in the skarn-forming solutions based on experimental data of ion exchange equilibria. *Min. Geol.* **43**, 301–310 (in Japanese).

Uchida, E., Gima, M. and Imai, N. (1989) Experimental studies on ion exchange equilibria between minerals and aqueous chloride solution in the system $CaWO_4$-$FeWO_4$-$MnWO_4$ under supercritical condition. *Geochem. J.* **23**, 339–347.

Xie, Z. and Walther, J. V. (1993) Wollastonite + Quartz solubility in supercritical NaCl aqueous solutions. *Am. J. Sci.* **293**, 235–255.

Aqueous speciation of magnesium, strontium, nickel and cobalt chlorides in hydrothermal solutions at 600°C and 1 kbar

ETSUO UCHIDA, YUICHI GORYOZONO and MASAHIRO NAITO

Department of Mineral Resources Engineering, Waseda University,
Ohkubo 3-4-1, Shinjuku, Tokyo 169, Japan

The effect of NaCl on ion exchange equilibria in the system $CaWO_4$-$MeWO_4$-$CaCl_2$-$MeCl_2$-H_2O (Me: Mg, Sr, Ni and Co) was experimentally monitored at 600°C and 1 kbar. The Ca/(Ca + Me) ratio of the aqueous chloride solution in equilibrium with both $CaWO_4$ and $MeWO_4$ was constant for Mg and Sr in spite of the addition of NaCl, whereas the ratio decreased significantly for Ni and Co with the increase of NaCl. The experimental results indicate that both Ni^{2+} and Co^{2+} do form higher-order chloro-complexes such as $NiCl_3^-{}_{aq}$ and $CoCl_3^-{}_{aq}$, whereas both Mg^{2+} and Sr^{2+} may not. The thermodynamic analysis of the experimental results gives 1.5 and 2.1 in logarithm units for the formation constants for $NiCl_3^-{}_{aq}$ and $CoCl_3^-{}_{aq}$, respectively. By combining the results of Uchida et al. (1995), $MeCl_{2aq}$ tends to forms $MeCl_3^-{}_{aq}$ in the order of $SrCl_{2aq}$= $CaCl_{2aq}$ = $MgCl_{2aq}$ << $NiCl_{2aq}$ < $FeCl_{2aq}$ < $CoCl_{2aq}$ < $MnCl_{2aq}$ at 600°C and 1 kbar. Based on ligand field theory, the above order may suggest that the transition metal cations exist as tetrahedral chloro-complexes with low-spin state in the supercritical hydrothermal solutions.

INTRODUCTION

Based on fluid inclusion studies, ore-forming solutions can be considered as aqueous chloride solutions, and NaCl is the most important solute. Accordingly, information on aqueous speciation of metal chlorides in NaCl-bearing hydrothermal solutions is indispensable for a thorough understanding of the hydrothermal ore-forming process. Previously, many experiments on aqueous speciation of metal chlorides were conducted using Ag-AgCl buffer technique in NaCl-free systems under supercritical conditions (e.g., Chou and Eugster, 1977; Frantz and Popp, 1979; Popp and Frantz, 1979, 1980; Boctor et al., 1980; Boctor, 1985; Lin and Popp, 1984). On the other hand, little is known about aqueous speciation of metal chlorides in supercritical NaCl-bearing hydrothermal solutions. This study aims to obtain the information on aqueous speciation of $MgCl_2$, $SrCl_2$, $NiCl_2$ and $CoCl_2$ in NaCl-bearing hydrothermal solutions at 600°C and 1 kbar.

Uchida et al. (1995) have carried out experiments on the effects of NaCl and KCl on ion exchange equilibria in the system $CaWO_4$-$FeWO_4$-$CaCl_2$-$FeCl_2$-H_2O and $CaWO_4$-$MnWO_4$-$CaCl_2$-$MnCl_2$-H_2O at 400 and 600°C, 1 kbar. They showed that $FeCl_3^-{}_{aq}$ and $MnCl_3^-{}_{aq}$ are dominant aqueous species of $FeCl_2$ and $MnCl_2$, respectively, in natural supercritical hydrothermal solutions, and obtained large formation constants for $FeCl_3^-{}_{aq}$ and $MnCl_3^-{}_{aq}$. In this study, the same experimental technique was applied to $MgCl_2$, $SrCl_2$, $NiCl_2$ and $CoCl_2$ instead of $FeCl_2$ and $MnCl_2$, in order to obtain the information on aqueous speciation of these chlorides at 600°C and 1 kbar.

Fahlquist and Popp (1989) have performed experiments on the effect of NaCl on bunsenite solubility in the temperature range 550 to 750°C at 2 kbar, and revealed that the addition of NaCl enhanced the formation of higher-order nickel complexes than $NiCl_{2aq}$. Experimental investigation of the effect of NaCl on talc solubility by

17

Grabman and Popp (1991) also showed that higher-order magnesium complexes may be required to explain the increased solubility at 600 and 700°C, 2 kbar. Unfortunately, there are no experiments on aqueous speciation for $SrCl_2$ and $CoCl_2$ under supercritical hydrothermal conditions.

EXPERIMENTAL PROCEDURES

A starting material of $CaWO_4$ was synthesized from a 1:1 mixture of CaO and WO_3 by heating at 800°C in air for one day using an electric furnace. Starting materials of $MgWO_4$, $SrWO_4$, $NiWO_4$ and $CoWO_4$ were hydrothermally synthesized. A 1:1 mixture of MeO (Me:Mg, Sr, Ni and Co) and WO_3 was sealed into a gold capsule (3.0 mm o.d., 2.7 mm i.d. and about 35 mm in length) with 2N $MeCl_2$ solution and a few milligrams of anthracene (only for Ni and Co) as a reducing agent, and was reacted using a standard cold seal type pressure vessel at 600 or 700°C, 1 kbar during 2 or 3 days. Thus synthesized starting materials were checked for impurity by the X-ray diffractometer (Rigaku RAD I-B).

Ten to 20 mg of ground starting material $CaWO_4$ or $MeWO_4$ was sealed into gold capsule (3.0 mm o.d., 2.7 mm i.d. and about 35 mm in length) with 40 μl of 2N aqueous chloride solution and a few milligrams of anthracene (only for Ni and Co). For the confirmation of the attainment to equilibrium, $CaWO_4$ was reacted with 2N $MeCl_2$-NaCl aqueous solution, and reversely $MeWO_4$ with 2N $CaCl_2$-NaCl aqueous solution. NaCl concentration in the aqueous chloride solutions was varied from 0 to 1.6 mol/l (0, 0.2, 0.4, 0.6, 0.8, 1.2 and 1.6 mol/l). The experiments were carried out using a standard cold seal type pressure vessel at 600°C, 1 kbar during 5 to 7 days. In order to minimize a temperature gradient, the pressure vessel was settled horizontally in an electric furnace and a filler rod was inserted into the pressure vessel. Two charged gold capsules were settled in parallel in the bottom of the pressure vessel. Water was used as a pressure medium, and pressure was measured by a Heise gauge. Temperature was measured by a chromel-alumel

thermocouple attached on the outer wall of the pressure vessel, and was controlled within ±2°C.

After the run, the pressure vessel was quenched with cold water and reached to the room temperature within a minute. The gold capsule was checked for a leakage by measuring the weight. Then the run product was washed away into a beaker with distilled water. The solid product was separated from the solution with a millipore filter with a pore size of 0.45 μm.

In order to confirm the coexistence of the two phases $CaWO_4$ and $MeWO_4$, the solid product was observed under the polarizing microscope and was also examined by the X-ray diffractometer. Chemical analysis was carried out for some run products using an energy dispersive X-ray microanalyzer (JEOL JSM-5400 equipped with Link QX-200JI). Cations in the separated solution were analyzed by an atomic absorption/flame spectrophotometer (Shimadzu AA-610S). The concentrations of the cations were normalized so that the total concentration of the cations is 2N.

EXPERIMENTAL RESULTS

$CaWO_4$-$MgWO_4$-$CaCl_2$-$MgCl_2$-NaCl-H_2O system

The experimental results in the system $CaWO_4$-$MgWO_4$-$CaCl_2$-$MgCl_2$-NaCl-H_2O are summarized in Table 1. The coexistence of the two phases $CaWO_4$ (tetragonal) and $MgWO_4$ (monoclinic) were confirmed for all run products. Both phases are white in color. The $CaWO_4$ (tetragonal) phase dissolved the $MgWO_4$ component in solid solution only up to 1.0 mol%, and the $MgWO_4$ (monoclinic) phase dissolved the $CaWO_4$ component only up to 0.9 mol%. The Ca/(Ca + Mg) molar ratio in the aqueous solution in equilibrium with both phases is nearly constant (about 0.5) against NaCl concentration (Fig. 1(a)).

$CaWO_4$-$SrWO_4$-$CaCl_2$-$SrCl_2$-NaCl-H_2O system

The experimental results in the system $CaWO_4$-$SrWO_4$-$CaCl_2$-$SrCl_2$-NaCl-H_2O are given in Table 2. There is considerable solid solution of $SrWO_4$ and $CaWO_4$ components. The chemical compositions of the coexisting phases can be written as

Table 1. Experimental results for the effect of NaCl on mineral-solution equilibria in the system $CaWO_4$-$MgWO_4$-$CaCl_2$-$MgCl_2$-H_2O at 600°C and 1 kbar

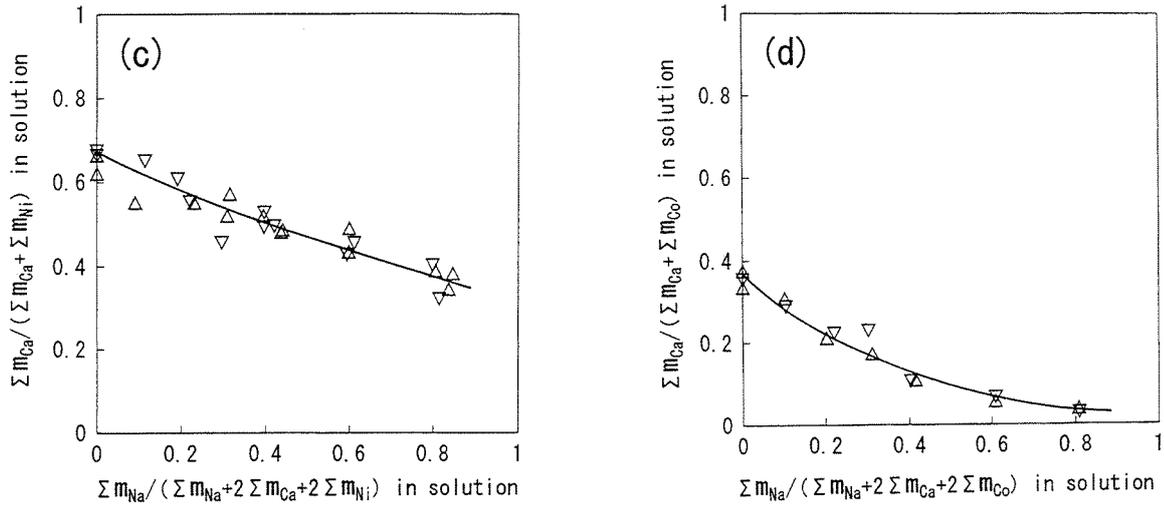| Run No.	Duration	Starting materials						Run products (solution)		
		solid			solution			Σm_{Mg}	Σm_{Ca}	Σm_{Na}
	days	mg			μl		μl			
001	6	$CaWO_4$	13.7	$MgCl_2$	40	NaCl	0	0.491	0.509	0.000
002	6	$CaWO_4$	13.0	$MgCl_2$	40	NaCl	0	0.505	0.495	0.000
003	6	$MgWO_4$	11.7	$CaCl_2$	40	NaCl	0	0.546	0.454	0.000
004	6	$MgWO_4$	10.5	$CaCl_2$	40	NaCl	0	0.553	0.447	0.000
005	6	$CaWO_4$	11.3	$MgCl_2$	36	NaCl	4	0.459	0.450	0.182
006	6	$CaWO_4$	13.6	$MgCl_2$	32	NaCl	8	0.402	0.412	0.372
007	6	$MgWO_4$	10.4	$CaCl_2$	36	NaCl	4	0.464	0.444	0.184
008	6	$MgWO_4$	15.2	$CaCl_2$	32	NaCl	8	0.408	0.391	0.402
009	5	$CaWO_4$	12.2	$MgCl_2$	28	NaCl	12	0.385	0.325	0.580
010	7	$MgWO_4$	14.0	$CaCl_2$	28	NaCl	12	0.318	0.360	0.644
011	7	$CaWO_4$	14.4	$MgCl_2$	24	NaCl	16	0.327	0.278	0.790
012	7	$MgWO_4$	15.3	$CaCl_2$	24	NaCl	16	0.275	0.316	0.818
013	7	$CaWO_4$	12.3	$MgCl_2$	16	NaCl	24	0.198	0.212	1.180
014	5	$MgWO_4$	10.6	$CaCl_2$	16	NaCl	24	0.193	0.218	1.178
015	5	$CaWO_4$	13.2	$MgCl_2$	8	NaCl	32	0.083	0.105	1.624
016	5	$MgWO_4$	11.1	$CaCl_2$	8	NaCl	32	0.093	0.127	1.560
017	5	$CaWO_4$	14.3	$MgCl_2$	36	NaCl	4	0.428	0.474	0.196
018	5	$MgWO_4$	13.0	$CaCl_2$	36	NaCl	4	0.418	0.481	0.202
019	5	$CaWO_4$	18.2	$MgCl_2$	32	NaCl	8	0.393	0.420	0.374
020	5	$MgWO_4$	14.0	$CaCl_2$	32	NaCl	8	0.382	0.423	0.390
021	5	$CaWO_4$	11.5	$MgCl_2$	28	NaCl	12	0.327	0.395	0.556
022	5	$MgWO_4$	13.1	$CaCl_2$	28	NaCl	12	0.348	0.369	0.566
023	5	$CaWO_4$	13.2	$MgCl_2$	8	NaCl	32	0.298	0.304	0.796
024	5	$MgWO_4$	10.5	$CaCl_2$	24	NaCl	16	0.298	0.308	0.788
025	5	$CaWO_4$	12.3	$MgCl_2$	16	NaCl	24	0.213	0.190	1.194
026	5	$MgWO_4$	11.4	$CaCl_2$	16	NaCl	24	0.202	0.202	1.192
027	5	$CaWO_4$	13.7	$MgCl_2$	8	NaCl	32	0.099	0.104	1.594
028	5	$MgWO_4$	14.2	$CaCl_2$	8	NaCl	32	0.091	0.101	1.616
029	5	$MgWO_4$	11.6	$CaCl_2$	40	NaCl	0	0.477	0.523	0.000
030	5	$MgWO_4$	11.1	$CaCl_2$	40	NaCl	0	0.464	0.536	0.000
031	5	$CaWO_4$	15.0	$MgCl_2$	8	NaCl	32	0.084	0.103	1.626

$(Ca_{0.73},Sr_{0.27})WO_4$ and $(Ca_{0.30},Sr_{0.70})WO_4$. Both phases show white color. The Ca/(Ca + Sr) molar ratio in the aqueous chloride solution in equilibrium with both phases does not depend on NaCl concentration and is about 0.35 at 600°C and 1 kbar (Fig. 1(b)).

CaWO4-NiWO4-CaCl2-NiCl2-NaCl-H2O system

The experimental results in the system $CaWO_4$-$NiWO_4$-$CaCl_2$-$NiCl_2$-$NaCl$-H_2O are listed in Table 3 and shown in Fig. 1(c). Both $CaWO_4$ (tetragonal) and $NiWO_4$ (monoclinic) were produced in all runs. $NiWO_4$ (monoclinic) shows ol-

ive color. Coexisting $CaWO_4$ (tetragonal) and $NiWO_4$ (monoclinic) phases dissolve 0.9 mol% of $NiWO_4$ and $CaWO_4$ components, respectively. The Ca/(Ca + Ni) molar ratio in the aqueous chloride solution in equilibrium with both phases decreases from 0.67 to 0.37 with the increase of Na/(Na + 2Ca + 2Ni) molar ratio from 0 to 0.8.

CaWO4-CoWO4-CaCl2-CoCl2-NaCl-H2O system

The experimental results in the system $CaWO_4$-$CoWO_4$-$CaCl_2$-$CoCl_2$-$NaCl$-H_2O are compiled in Table 4 and shown in Fig. 1(d). The coexistence of $CaWO_4$ (tetragonal) and $CoWO_4$ (monoclinic)

Table 2. Experimental results for the effect of NaCl on mineral-solution equilibria in the system $CaWO_4$-$SrWO_4$-$CaCl_2$-$SrCl_2$-H_2O at 600°C and 1 kbar

Run No.	Duration	Starting materials					Run products (solution)		
		solid		solution			Σm_{Sr}	Σm_{Ca}	Σm_{Na}
	days	mg		μl		μl			
201	6	$CaWO_4$	11.3	$SrCl_2$	40	NaCl 0	0.671	0.329	0.000
202	6	$CaWO_4$	11.6	$SrCl_2$	32	NaCl 8	0.504	0.280	0.432
203	6	$CaWO_4$	12.7	$SrCl_2$	24	NaCl 16	0.341	0.222	0.874
205	7	$SrWO_4$	12.6	$CaCl_2$	36	NaCl 4	0.571	0.315	0.228
206	7	$CaWO_4$	11.7	$SrCl_2$	36	NaCl 4	0.582	0.307	0.222
207	7	$CaWO_4$	15.4	$SrCl_2$	28	NaCl 12	0.423	0.270	0.614
209	6	$SrWO_4$	11.0	$CaCl_2$	40	NaCl 0	0.642	0.358	0.000
210	6	$SrWO_4$	10.2	$CaCl_2$	32	NaCl 8	0.512	0.268	0.440
211	6	$SrWO_4$	10.2	$CaCl_2$	24	NaCl 16	0.390	0.204	0.812
218	6	$SrWO_4$	11.3	$CaCl_2$	28	NaCl 12	0.484	0.214	0.604
N26	5	$CaWO_4$	11.8	$SrCl_2$	40	NaCl 0	0.659	0.341	0.000
N27	5	$SrWO_4$	5.7	$CaCl_2$	20	NaCl 30	0.595	0.405	1.216
N28	5	$CaWO_4$	4.6	$SrCl_2$	20	NaCl 30	0.666	0.334	1.278
N29	5	$SrWO_4$	4.7	$CaCl_2$	10	NaCl 40	0.700	0.300	1.564
N30	5	$CaWO_4$	5.3	$SrCl_2$	10	NaCl 40	0.602	0.398	1.663
N31	5	$SrWO_4$	8.7	$CaCl_2$	20	NaCl 30	0.573	0.427	1.124
N32	5	$CaWO_4$	8.7	$SrCl_2$	20	NaCl 30	0.604	0.396	1.248
N45	5	$SrWO_4$	3.9	$CaCl_2$	10	NaCl 40	0.660	0.340	1.575
N46	5	$CaWO_4$	4.1	$SrCl_2$	10	NaCl 40	0.640	0.360	1.622
N47	5	$SrWO_4$	4.1	$CaCl_2$	10	NaCl 40	0.666	0.334	1.563
N48	5	$CaWO_4$	4.5	$SrCl_2$	10	NaCl 40	0.618	0.382	1.636
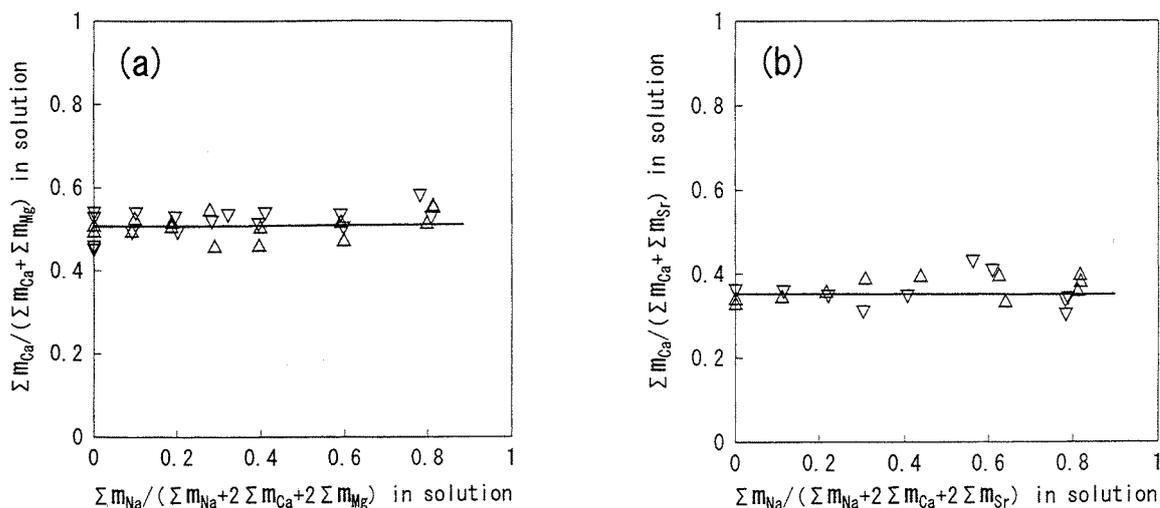
Fig. 1. Effect of NaCl on the chemical composition of the 2N aqueous chloride solution in equilibrium with $CaWO_4$ and $MeWO_4$ (Me:Mg, Sr, Ni and Co) at 600°C and 1 kbar. The direction of triangles in the figures indicates the direction of change in chemical composition of aqueous chloride solution from the initial composition. (a) $CaWO_4$-$MgWO_4$-$CaCl_2$-$MgCl_2$-H_2O system, (b) $CaWO_4$-$SrWO_4$-$CaCl_2$-$SrCl_2$-H_2O system, (c) $CaWO_4$-$NiWO_4$-$CaCl_2$-$NiCl_2$-H_2O system and (d) $CaWO_4$-$CoWO_4$-$CaCl_2$-$CoCl_2$-H_2O system.

Fig. 1. (continued).

Table 3. Experimental results for the effect of NaCl on mineral-solution equilibria in the system CaWO$_4$-NiWO$_4$-CaCl$_2$-NiCl$_2$-H$_2$O at 600°C and 1 kbar

Run No.	Duration	Starting materials						Run products (solution)		
		solid		solution				Σm_{Ni}	Σm_{Ca}	Σm_{Na}
	days	mg		μl		μl				
032	5	CaWO$_4$	15.6	NiCl$_2$	40	NaCl	0	0.382	0.618	0.000
033	5	NiWO$_4$	12.8	CaCl$_2$	40	NaCl	0	0.328	0.672	0.000
034	5	CaWO$_4$	14.5	NiCl$_2$	36	NaCl	4	0.409	0.499	0.184
037	6	NiWO$_4$	14.5	CaCl$_2$	32	NaCl	8	0.320	0.489	0.382
038	6	CaWO$_4$	15.0	NiCl$_2$	28	NaCl	12	0.334	0.359	0.614
039	5	NiWO$_4$	10.9	CaCl$_2$	28	NaCl	12	0.385	0.321	0.588
040	6	CaWO$_4$	14.3	NiCl$_2$	32	NaCl	8	0.347	0.423	0.460
041	6	NiWO$_4$	12.7	CaCl$_2$	32	NaCl	8	0.350	0.430	0.440
042	6	CaWO$_4$	10.3	NiCl$_2$	24	NaCl	16	0.289	0.271	0.880
043	6	NiWO$_4$	11.0	CaCl$_2$	24	NaCl	16	0.294	0.286	0.840
044	6	CaWO$_4$	13.8	NiCl$_2$	16	NaCl	24	0.229	0.174	1.194
045	6	NiWO$_4$	11.9	CaCl$_2$	16	NaCl	24	0.234	0.173	1.186
046	6	CaWO$_4$	10.7	NiCl$_2$	8	NaCl	32	0.120	0.075	1.610
047	6	NiWO$_4$	10.8	CaCl$_2$	8	NaCl	32	0.121	0.081	1.596
048	6	CaWO$_4$	12.5	NiCl$_2$	40	NaCl	0	0.339	0.661	0.000
049	6	NiWO$_4$	12.8	CaCl$_2$	40	NaCl	0	0.339	0.661	0.000
050	6	CaWO$_4$	11.4	NiCl$_2$	24	NaCl	16	0.292	0.314	0.788
051	6	NiWO$_4$	11.1	CaCl$_2$	24	NaCl	16	0.287	0.317	0.792
053	7	NiWO$_4$	11.6	CaCl$_2$	36	NaCl	4	0.312	0.573	0.230
054	7	CaWO$_4$	10.4	NiCl$_2$	28	NaCl	12	0.295	0.392	0.626
056	7	CaWO$_4$	11.0	NiCl$_2$	16	NaCl	24	0.206	0.196	1.196
057	7	NiWO$_4$	12.0	CaCl$_2$	16	NaCl	24	0.214	0.176	1.120
N13	5	NiWO$_4$	12.3	CaCl$_2$	24	NaCl	16	0.509	0.491	0.790
N14	5	CaWO$_4$	11.1	NiCl$_2$	24	NaCl	16	0.521	0.479	0.872
N18	5	CaWO$_4$	11.2	NiCl$_2$	8	NaCl	32	0.657	0.343	1.673
N19	5	NiWO$_4$	10.8	CaCl$_2$	8	NaCl	32	0.682	0.318	1.628
N20	5	CaWO$_4$	10.8	NiCl$_2$	8	NaCl	32	0.620	0.380	1.693

Table 4. Experimental results for the effect of NaCl on mineral-solution equilibria in the system CaWO₄-CoWO₄-CaCl₂-CoCl₂-H₂O at 600°C and 1 kbar

Run No.	Duration	Starting materials						Run products (solution)		
		solid		solution				Σm_{Co}	Σm_{Ca}	Σm_{Na}
	days	mg		μl		μl				
181	5	CaWO₄	11.9	CoCl₂	40	NaCl	0	0.666	0.334	0.000
182	7	CoWO₄	12.6	CaCl₂	28	NaCl	12	0.540	0.159	0.602
183	7	CoWO₄	11.2	CaCl₂	8	NaCl	32	0.186	0.005	1.618
185	5	CaWO₄	13.5	CoCl₂	40	NaCl	0	0.626	0.374	0.000
186	5	CaWO₄	13.0	CoCl₂	32	NaCl	8	0.631	0.167	0.404
187	5	CaWO₄	11.6	CoCl₂	24	NaCl	16	0.523	0.062	0.830
188	5	CaWO₄	11.5	CoCl₂	16	NaCl	24	0.370	0.021	1.218
189	7	CaWO₄	11.0	CoCl₂	36	NaCl	4	0.622	0.275	0.206
190	7	CoWO₄	11.9	CaCl₂	36	NaCl	4	0.637	0.257	0.212
191	7	CaWO₄	10.8	CoCl₂	28	NaCl	16	0.572	0.118	0.620
192	7	CaWO₄	12.7	CoCl₂	8	NaCl	32	0.185	0.007	1.616
193	5	CoWO₄	10.9	CaCl₂	40	NaCl	0·	0.647	0.353	0.000
194	5	CoWO₄	11.0	CaCl₂	32	NaCl	8	0.608	0.172	0.440
195	5	CoWO₄	10.9	CaCl₂	24	NaCl	16	0.535	0.062	0.806
196	5	CoWO₄	13.0	CaCl₂	16	NaCl	24	0.366	0.025	1.218

was confirmed for all run products. CoWO₄ (monoclinic) is blue in color. The CoWO₄ and CaWO₄ contents in the coexisting CaWO₄ (tetragonal) and CoWO₄ (monoclinic) phases are extremely small, and are 0.7 mol% and 0.9 mol%, respectively. The Ca/(Ca + Co) molar ratio in the aqueous chloride solution in equilibrium with the two phases decreases significantly from 0.37 to 0.03 with the increase of Na/(Na + 2Ca + 2Co) molar ratio from 0 to 0.8.

DISCUSSION

Previous studies on solubility of minerals in NaCl-free systems using Ag-AgCl buffer technique revealed that neutral species, $CaCl_{2aq}$, $MgCl_{2aq}$, $FeCl_{2aq}$, $MnCl_{2aq}$ and $NiCl_{2aq}$ are dominant at 600°C and 1 kbar (Popp and Frantz, 1979, 1980; Frantz and Popp, 1979; Boctor *et al.*, 1980; Boctor, 1985; Lin and Popp, 1984). Presumably, this is the case for SrCl₂ and CoCl₂. However, the addition of NaCl to the systems changes the situation. The dissociation constant of $NaCl_{aq}$ is still high even at 600°C and 1 kbar. Accordingly, the addition of NaCl results in the supply of Cl^-_{aq} to the

systems. The increase in Cl^-_{aq} of the aqueous solutions will enhance the formation of higher-order chloro-complexes. Reversely, solubility measurements in the system with various NaCl concentrations will give the information of aqueous speciation (e.g., Fahlquist and Popp, 1989; Fein and Walther, 1989; Grabman and Popp, 1991; Xie and Walther, 1993, and Cygan *et al.*, 1994).

Uchida *et al.* (1995) have examined experimentally the effect of NaCl and KCl on the ion exchange equilibria in the systems CaWO₄-FeWO₄-CaCl₂-FeCl₂-NaCl-H₂O and CaWO₄-MnWO₄-CaCl₂-MnCl₂-NaCl-H₂O at both 400 and 600°C, 1 kbar. They explained the decrease of Ca/(Ca + Fe) and Ca/(Ca + Mn) molar ratio in the aqueous chloride solutions with the addition of NaCl by considering the formation of $FeCl_3^-_{aq}$ and $MnCl_3^-_{aq}$. On the assumption that CaCl₂ does not form higher-order chloro-complexes other than $CaCl_{2aq}$, they estimated the formation constants of $FeCl_3^-_{aq}$ and $MnCl_3^-_{aq}$ from the experimental results.

In the present experimental systems CaWO₄-MgWO₄-CaCl₂-MgCl₂-NaCl-H₂O and CaWO₄-SrWO₄-CaCl₂-SrCl₂-NaCl-H₂O, Ca/(Ca + Mg) and

Ca/(Ca + Sr) ratios do not depend on NaCl concentration. This may indicate that $CaCl_2$, $MgCl_2$ and $SrCl_2$ do not form higher-order chloro-complexes due to their ionic property, and that they exist almost entirely as neutral species in the hydrothermal solution under the present experimental condition. On the other hand, based on the effect of NaCl on talc solubility, Grabman and Popp (1991) suggested the formation of higher-order Mg chloro-complexes. Therefore, it is also possible to interpret that the present experimental results may indicate that the formation constant of $CaCl_3^-aq$ is accidentally the same as that of $MgCl_3^-aq$ and $SrCl_3^-aq$. However, we can not find the reason why the ion size effect was not observed among them. Therefore, we consider that $CaCl_2$, $MgCl_2$ and $SrCl_2$ do not form higher-order chloro-complexes.

In the systems $CaWO_4$-$NiWO_4$-$CaCl_2$-$NiCl_2$-NaCl-H_2O and $CaWO_4$-$CoWO_4$-$CaCl_2$-$CoCl_2$-NaCl-H_2O, the Ca/(Ca + Ni) and Ca/(Ca + Co) ratios in the aqueous solutions decreased with the increase of NaCl. According to Uchida et al. (1995), this will be explained by the formation of higher-order chloro-complexes, probably $NiCl_3^-aq$ and $CoCl_3^-aq$. Their formation constants will be obtained by the same method as Uchida et al. (1995), as follows.

In the calculation, higher-order complexes other than $NaCl_{aq}$ and $CaCl_{2aq}$ were neglected due to their ionic property. Also, Ni^{2+}_{aq} and $NiCl^+_{aq}$ were neglected in the calculation. This is supported by the experiments by Lin and Popp (1984). The similar assumption was made for $CoCl_2$ by the analogy to $FeCl_2$, $MnCl_2$ and $NiCl_2$. Thus the following eight aqueous species were taken into consideration in the calculation; Cl^-_{aq}, Na^+_{aq}, $NaCl_{aq}$, Ca^{2+}_{aq}, $CaCl^+_{aq}$, $CaCl_{2aq}$, $MeCl_{2aq}$ and $MeCl_3^-aq$ (Me:Ni or Co). The following four mass balance equations can be written among these aqueous species:

$$\Sigma m_{Na} = m(Na^+_{aq}) + m(NaCl_{aq}), \tag{1}$$

$$\Sigma m_{Ca} = m(Ca^{2+}_{aq}) + m(CaCl^+_{aq}) + m(CaCl_{2aq}), \tag{2}$$

$$\Sigma m_{Me} = m(MeCl_{2aq}) + m(MeCl_3^-aq), \tag{3}$$

and

$$\Sigma m_{Cl} = m(Cl^-_{aq}) + m(NaCl_{aq}) + m(CaCl^+_{aq})$$
$$+ 2m(CaCl_{2aq}) + 2m(MeCl_{2aq})$$
$$+ 3m(MeCl_3^-aq) = 2, \tag{4}$$

where m(i) signifies the molarity of aqueous species i, and Σm_i the total molarity of i-bearing species. Corresponding to the following four reactions:
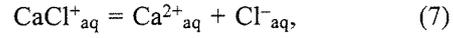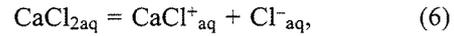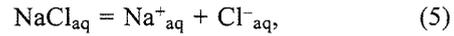
$$NaCl_{aq} = Na^+_{aq} + Cl^-_{aq}, \tag{5}$$

$$CaCl_{2aq} = CaCl^+_{aq} + Cl^-_{aq}, \tag{6}$$

$$CaCl^+_{aq} = Ca^{2+}_{aq} + Cl^-_{aq}, \tag{7}$$

and

$$MeCl_{2aq} + Cl^-_{aq} = MeCl_3^-aq, \tag{8}$$
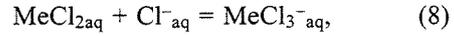
the following four mass action equations can be written:

$$K(NaCl_{aq}) = a(Na^+_{aq}) \cdot a(Cl^-_{aq})/a(NaCl_{aq}), \tag{9}$$

$$K(CaCl_{2aq}) = a(CaCl^+_{aq}) \cdot a(Cl^-_{aq})/a(CaCl_{2aq}), \tag{10}$$

$$K(CaCl^+_{aq}) = a(Ca^{2+}_{aq}) \cdot a(Cl^-_{aq})/a(CaCl^+_{aq}), \tag{11}$$

and

$$K(MeCl_3^-aq) = a(MeCl_3^-aq)/\{a(MeCl_{2aq}) \cdot a(Cl^-_{aq})\}, \tag{12}$$

where a(i) is the activity of aqueous species i, and K(i) the dissociation or formation constant of aqueous species i. The activity coefficient of neutral aqueous species was assumed to be unity. On the other hand, the activity coefficient of charged aqueous species γ_i was calculated from the Debye-Huckel equation:

$$\log\gamma_i = -Z_iAI^{1/2}/(1 + a_iBI^{1/2}), \tag{13}$$

where Z_i is the ionic charge and I the true ionic

E. Uchida *et al.*

strength defined as

$$I = 1/2\sum m_i Z_i^2. \qquad (14)$$

The Debye-Huckel coefficients A and B were taken from Helgeson and Kirkham (1974), and the ion size parameter a_i from Kharaka and Barnes (1973). The ion size parameters for $CaCl^+_{aq}$, $NiCl_3^-{}_{aq}$ and $CoCl_3^-{}_{aq}$ were assumed to be 4 (Seward, 1984). The dissociation constant for $NaCl_{aq}$ was taken from Quist and Marshall (1968), and that of $CaCl^+_{aq}$ and $CaCl_{2aq}$ from Frantz and Marshall (1982).

The ion exchange reaction in the systems can be written using neutral species as

$$CaWO_4 \text{ (tetragonal)} + MeCl_{2aq}$$
$$= MeWO_4 \text{ (monoclinic)} + CaCl_{2aq}. \qquad (15)$$
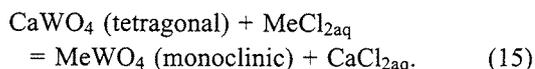
The equilibrium constant K(Ca-Me) for the reaction is

$$K(Ca\text{-}Me) = a(MeWO_4)\cdot a(CaCl_{2aq})$$
$$/\{a(CaWO_4)\cdot a(MeCl_2)\}. \qquad (16)$$

The activity coefficient for neutral aqueous species is assumed to be unity in the present study. Moreover, activities for $CaWO_4$ and $MeWO_4$ can be considered as unity due to limited solubility between $CaWO_4$ and $MeWO_4$. Therefore, the equilibrium constant K (Ca-Me) can be rewritten as follows:

$$K(Ca\text{-}Me) = m(CaCl_{2aq})/m(MeCl_{2aq}) = const.(17)$$

The formation constant for $NiCl_3^-{}_{aq}$ and $CoCl_3^-{}_{aq}$ can be found out so as to satisfy the above constraint (17) using Eqs. (1) to (4) and (9) to (12). As a result, logarithm of the formation constant for $NiCl_3^-{}_{aq}$ was estimated to be 1.5, and that for $CoCl_3^-{}_{aq}$ to be 2.1 at 600°C and 1 kbar. According to Fahlquist and Popp (1989) (Eq. (14)), the formation constant for $NiCl_3^-{}_{aq}$ can be obtained to be 0.69 in logarithm at 600°C and 2 kbars. The two sets of experimental data indicate that the formation constant for $NiCl_3^-{}_{aq}$ decreases with

increasing pressure. This is concordant with the general trend for ion complexing, that is, ion complexing increases with increasing temperature, but decreases with increasing pressure (e.g., Eugster and Baumgartner, 1987).

Figures 2(a) and (b) show the concentration of each aqueous species in the aqueous chloride solutions in equilibrium with both $CaWO_4$ and $NiWO_4$ and with both $CaWO_4$ and $CoWO_4$ calculated using the obtained formation constants for $NiCl_3^-{}_{aq}$ and $CoCl_3^-{}_{aq}$, respectively. $CaCl_{2aq}$ is a dominant Ca species in both systems with any Na concentrations. At lower Na concentrations, Na^+_{aq}, $NiCl_{2aq}$ and $CoCl_{2aq}$ are dominant Na, Ni and Co species, respectively, whereas $NaCl_{aq}$, $NiCl_3^-{}_{aq}$ and $CoCl_3^-{}_{aq}$ become dominant at higher Na concentrations.

Uchida *et al.* (1995) have already obtained the formation constants for $FeCl_3^-{}_{aq}$ and $MnCl_3^-{}_{aq}$ as 1.9 and 2.3 in logarithm at 600°C and 1 kb, respectively, using the same experimental method. As a result, $MeCl_{2aq}$ tends to form $MeCl_3^-{}_{aq}$ in the following order:

$$SrCl_{2aq} = CaCl_{2aq} = MgCl_{2aq}$$
$$\ll NiCl_{2aq} < FeCl_{2aq} < CoCl_{2aq} < MnCl_{2aq}.$$
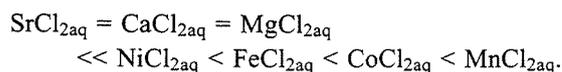
As mentioned above, it seems that Sr, Mg and Ca do not form higher-order chloro-complexes. On the contrary, the formation constants for $MeCl_3^-{}_{aq}$ of the transition elements are large. Therefore, the transition metal cations seem to exist as higher-order chloro-complexes in natural supercritical hydrothermal solutions. As a consequence, solubility of transition elements in hydrothermal solutions seems to increase significantly under supercritical conditions.

Here, we consider the above order of the formation constants of chloro-complexes of transition metal cations. The followings is a so-called Irving-Williams series:

$$Mn^{2+} < Fe^{2+} < Co^{2+} < Ni^{2+} < Cu^{2+} > Zn^{2+}.$$
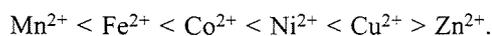
The series shows the relative stability of the divalent metal complexes under room conditions.

24
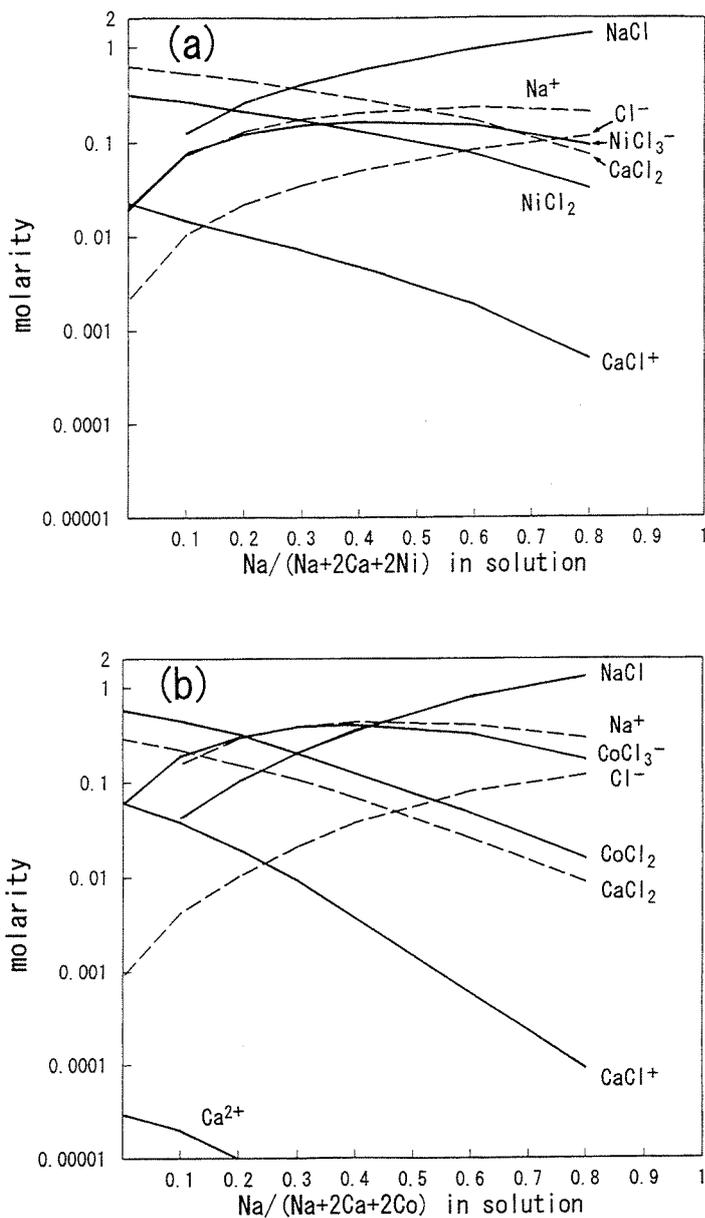
Fig. 2. Concentrations of aqueous species vs. NaCl concentration for the 2N aqueous chloride solution in equilibrium with $CaWO_4$ and $MeWO_4$ (Me:Ni and Co) at 600°C and 1 kbar, calculated using the formation constants for $NiCl_3^-{}_{aq}$ and $CoCl_3^-{}_{aq}$ obtained in the present study. (a) $CaWO_4$-$NiWO_4$-$CaCl_2$-$NiCl_2$-H_2O system and (b) $CaWO_4$-$CoWO_4$-$CaCl_2$-$CoCl_2$-H_2O system.

Table 5 shows ligand field stabilization energy for octahedral and tetrahedral complexes. The ligand field theory suggests that the transition metal cations form octahedral complex with high-spin state under room conditions. On the other hand, though

there is a reverse between Fe^{2+} and Co^{2+}, the order obtained in the present study may indicate that the transition metal cations form tetrahedral chlorocomplexes with low-spin state under the experimental conditions. This is supported by the stud-

Table 5. Ligand field stabilization energy of transition metal cations in octahedral and tetrahedral complexes (Burns, 1970)

Transition metal cation	Number of d electrons	Ligand field stabilization energy			
		Octahedral complex		Tetrahedral complex	
		High-spin	Low-spin	High-spin	Low-spin
Mn^{2+}	5	0	$10/5\,\Delta_0$	0	$10/5\,\Delta_t$
Fe^{2+}	6	$2/5\,\Delta_0$	$12/5\,\Delta_0$	$3/5\,\Delta_t$	$8/5\,\Delta_t$
Co^{2+}	7	$4/5\,\Delta_0$	$9/5\,\Delta_0$	$6/5\,\Delta_t$	$6/5\,\Delta_t$
Ni^{2+}	8	$6/5\,\Delta_0$	$6/5\,\Delta_0$	$4/5\,\Delta_t$	$4/5\,\Delta_t$
Cu^{2+}	9	$3/5\,\Delta_0$	$3/5\,\Delta_0$	$2/5\,\Delta_t$	$2/5\,\Delta_t$
Zn^{2+}	10	0	0	0	0

ies of Susak and Crerar (1985) and Ewald *et al.* (1964). Based on a spectroscopic study, Susak and Crerar (1985) elucidated that Co^{2+} and Ni^{2+} chloro-complexes change from octahedral to tetrahedral with increasing temperature from 25 to 300°C under water-saturated vapor pressures. The experiments on the pressure effect by Ewald *et al.* (1964) demonstrated that the Fe(III) chloro-complex with high-spin state changes into that with low-spin state at higher pressures. As a conclusion, it is considered that the chloro-complexes of the transition metal cations exist as tetrahedral chloro-complexes such as $Co(H_2O)_2Cl_{2aq}$ and $Co(H_2O)Cl_3^-{}_{aq}$ with low-spin state under the present experimental condition.

REFERENCES

Boctor, N. Z. (1985) Rhodonite solubility and thermodynamic properties of aqueous $MnCl_2$ in the system MnO-SiO_2-HCl-H_2O. *Geochim. Cosmochim. Acta* **49**, 565–575.

Boctor, N. Z., Popp, R. K. and Frantz, J. D. (1980) Mineral-solution equilibria IV. Solubilities and the thermodynamic properties of $FeCl_2°$ in the system Fe_2O_3-H_2-H_2O-HCl. *Geochim. Cosmochim. Acta* **44**, 1509–1518.

Burns, R. G. (1970) *Mineralogical Applications of Crystal Field Theory.* Cambridge University Press, England, 224 pp.

Chou, I-M. and Eugster, H. P. (1977) Solubility of magnetite in supercritical chloride solutions. *Am. J. Sci.* **277**, 1296–1314.

Cygan, G. L., Hemley, J. J. and D'Angelo, W. M. (1994) An experimental study of zinc chloride speciation from 300 to 600°C and 0.5 to 2.0 kbar in buffered hydrothermal solutions. *Geochim. Cosmochim. Acta* **58**, 4841–4855.

Eugster, H. P. and Baumgartner, L. (1987) Mineral solubilities and speciation in supercritical metamorphic fluids. *Rev. Mineral.* **17**, 367–403.

Ewald, A. H., Martin, R. L., Ross, I. G. and White, A. H. (1964) Anomalous behaviour at the $^6A_1$-$^2T_2$ crossover in iron (III) complexes. *Proc. Roy. Soc., London (A)* **280**, 235–257.

Fahlquist, L. S. and Popp, R. K. (1989) The effect of NaCl on bunsenite solubility and Ni-complexing in supercritical aqueous fluids. *Geochim. Cosmochim. Acta* **53**, 989–995.

Fein, J. B. and Walther, J. V. (1989) Calcite solubility and speciation in supercritical NaCl-HCl aqueous fluids. *Contrib. Mineral. Petrol.* **103**, 317–324.

Frantz, J. D. and Marshall, W. L. (1982) Electrical conductances and ionization constants of calcium chloride and magnesium chloride in aqueous solutions at temperatures to 600°C and pressures to 4000 bars. *Am. J. Sci.* **282**, 1666–1693.

Frantz, J. D. and Popp, R. K. (1979) Mineral-solution equilibria I. An experimental study of complexing and thermodynamic properties of aqueous $MgCl_2$ in the system MgO-SiO_2-H_2O-HCl. *Geochim. Cosmochim. Acta* **43**, 1223–1239.

Grabman, K. B. and Popp, R. K. (1991) Experimental investigation of talc solubility in H_2O-$MgCl_2$-NaCl-HCl fluids in the range 500–700°C, 2 kb. *Geochim. Cosmochim. Acta* **55**, 2819–2829.

Helgeson, H. C. and Kirkham, D. H. (1974) Theoretical prediction of the thermodynamic behavior of aqueous electrolytes at high pressures and temperatures: II. Debye-Huckel parameters for activity coefficients and relative partial molal properties. *Am. J. Sci.* **274**, 1199–1261.

Kharaka, Y. K. and Barnes, I. (1973) SOLMNEQ; solution-mineral equilibrium computations. *NTIS Tech. Rept.* **PB215-899**, 82 pp.

Lin, S. and Popp, R. K. (1984) Solubility and complexing of Ni in the system NiO-H_2O-HCl. *Geochim. Cosmochim. Acta* **48**, 2713–2722.

Popp, R. K. and Frantz, J. D. (1979) Mineral-solution equilibria II. An experimental study of mineral solubilities and the thermodynamic properties of aqueous $CaCl_2$ in the system CaO-SiO_2-H_2O-HCl. *Geochim. Cosmochim. Acta* **43**, 1777–1790.

Popp, R. K. and Frantz, J. D. (1980) Mineral-solution equilibria III. The system Na_2O-Al_2O_3-SiO_2-H_2O-HCl. *Geochim. Cosmochim. Acta* **44**, 1029–1037.

Quist, A. and Marshall, W. L. (1968) Electrical conductances of aqueous sodium chloride solutions from 0 to 800° and at pressures to 4000 bars. *J. Phys. Chem.* **72**, 684–703.

Seward, T. M. (1984) The formation of lead (II) chloride complexes to 300°C: Spectrophotometric study. *Geochim. Cosmochim. Acta* **48**, 121–134.

Susak, N. J. and Crerar, D. A. (1985) Spectra and coordination changes of transition metals in hydrothermal solutions: Implications for ore genesis. *Geochim. Cosmochim. Acta* **49**, 555–564.

Uchida, E., Goryozono, Y., Naito, M. and Yamagami, M. (1995) Aqueous speciation of iron and manganese chlorides in supercritical hydrothermal solutions. *Geochim. J.* **29**, 175–188.

Xie, Z. and Walther, J. V. (1993) Wollastonite + quartz solubility in supercritical NaCl aqueous solutions. *Am. J. Sci.* **293**, 235–255.

27

Experimental study on ion exchange of Ca^{2+}, Fe^{2+} and Mn^{2+} between garnet solid solution and 2N aqueous chloride solution at 600°C and 1 kb

Etsuo UCHIDA, Masataka GIMA and Naoya IMAI

Department of Mineral Resources Engineering, School of Science and
Engineering, Waseda University, Shinjuku, Tokyo 169, Japan

Experiments on ion exchange of Ca^{2+}, Fe^{2+} and Mn^{2+} between grossular-almandine-spessartine garnet solid solution and 2N aqueous chloride solution were conducted at 600°C and 1kb under relatively reducing conditions in order to determine the stability relation and mixing property of the garnet solid solution. The experimental results revealed that calcium ion is slightly preferentially partitioned into aqueous chloride solution compared with ferrous and manganese ions. Grossular, almandine and spessartine form an almost continuous solid solution except for the semicircular region along the grossular-almandine join, where mineral assemblages of fayalite + anorthite and hedenbergite+anorthite+wustite appear instead of the garnet solid solution. Mixing properties of the garnet solid solution were evaluated from the experimental results by considering the formation of $FeCl_3^-{}_{aq}$ and $MnCl_3^-{}_{aq}$ in the aqueous phase. Almandine-spessartine solid solution shows slightly negative deviation from ideality. On the other hand, grossular-spessartine solid solution shows slightly positive deviation. Mixing property of grossular-almandine solid solution was not well determined due to the large unstable region.

Keywords: Garnet, Aqueous chloride solution, Ion exchange, Mixing property, Stability relation

I. Introduction

Two series of garnet solid solutions, pyralspite and grandite, are common in metamorphic, metasomatic and igneous rocks. It is well known that pyrope, almandine and spessartine, and grossular and andradite form complete solid solutions in nature, respectively. The pyralspite and grandite series garnet solid solutions were originally defined based on their miscibility relations. However, garnet solid solutions with intermediate compositions between pyralspite and grandite have been reported from metamorphic rocks and skarns (Frondel and Ito, 1965 ; Nemec, 1967 ; Brown, 1969 ; Ackermand *et al.*, 1972 ; Shimazaki, 1977 ; Hsu, 1980). Experimental studies have

also revealed that grossular and spessartine (Ito and Frondel, 1968 ; Shoji *et al.*, 1995), and grossular and almandine (Hariya and Nakano, 1972) form continuous solid solutions, respectively.

Although the extensive solid solution of garnet is widely known, its mixing properties are less well constrained. Therefore, we have conducted ion exchange experiments of Ca^{2+}, Fe^{2+} and Mn^{2+} between garnet solid solution and 2N aqueous chloride solution in order to clarify the stability relation and mixing property of the garnet solid solution, and to obtain the chemical composition of the aqueous chloride solution in equilibrium with the garnet solid solution of variable composition. Experiments were carried out for the following binary and ternary systems :

Table 1. Experimental data for the ion exchange in the system $Fe_3Al_2Si_3O_{12}$-$Mn_3Al_2Si_3O_{12}$-(Fe, Mn)Cl_2-H_2O at 600°C and 1 kb

Run	Duration	Starting Materials				Run Products					
		Solid		Solution		Garnet		Solution			
No.	days	Solid	mg	Solution	μl	Alm	Spe	Σm_{Fe}	Σm_{Mn}	$mFeCl_2^*$	$mMnCl_2^*$
202	7	Spe	28.5	FeCl$_2$	30	0.131	0.869	0.132	0.868	0.132	0.868
203	7	Spe	24.3	FeCl$_2$	40	0.186	0.814	0.150	0.850	0.150	0.850
204	7	Spe	19.4	FeCl$_2$	50	0.382	0.618	0.435	0.565	0.435	0.565
211	7	Alm	15.4	MnCl$_2$	50	0.728	0.272	0.776	0.224	0.776	0.224
212	7	Alm	18.2	MnCl$_2$	30	0.868	0.132	0.911	0.089	0.911	0.089
214	7	Alm	30.3	MnCl$_2$	30	0.951	0.049	0.969	0.031	0.969	0.031
215	7	Alm$_{50}$Spe$_{50}$	31.1	FeCl$_2$	20	0.756	0.244	0.816	0.184	0.816	0.184
216	7	Alm$_{50}$Spe$_{50}$	20.7	FeCl$_2$	40	0.712	0.288	0.768	0.232	0.768	0.232
217	7	Alm$_{50}$Spe$_{50}$	31.9	MnCl$_2$	20	0.720	0.280	0.789	0.211	0.789	0.211
218	7	Alm$_{50}$Spe$_{50}$	20.4	MnCl$_2$	40	0.517	0.483	0.603	0.397	0.603	0.397
243	7	Alm$_{50}$Spe$_{50}$	20.2	MnCl$_2$	30	0.501	0.499	0.550	0.450	0.550	0.450
244	7	Alm$_{40}$Spe$_{60}$	27.0	MnCl$_2$	20	0.412	0.588	0.435	0.565	0.435	0.565
245	7	Alm$_{40}$Spe$_{60}$	19.1	MnCl$_2$	30	0.342	0.658	0.390	0.610	0.390	0.610
246	7	Alm$_{40}$Spe$_{60}$	14.2	MnCl$_2$	40	0.365	0.635	0.398	0.602	0.398	0.602

* Calculated values.

(1) $Fe_3Al_2Si_3O_{12}$-$Mn_3Al_2Si_3O_{12}$-(Fe, Mn)Cl_2-H_2O ;

(2) $Ca_3Al_2Si_3O_{12}$-$Mn_3Al_2Si_3O_{12}$-(Ca, Mn)Cl_2-H_2O;

(3) $Ca_3Al_2Si_3O_{12}$-$Fe_3Al_2Si_3O_{12}$-(Ca, Fe)Cl_2-H_2O and

(4) $Ca_3Al_2Si_3O_{12}$-$Fe_3Al_2Si_3O_{12}$-$Mn_3Al_2Si_3O_{12}$-(Ca, Fe, Mn)Cl_2-H_2O.

II. Experimental method

A stoichiometric mixture of reagent-grade CaO, Al_2O_3 and SiO_2 was used as a starting material for a grossular component. We used stoichiometric mixtures of reagent-grade metallic iron or manganese powder, Al_2O_3 and SiO_2 as starting materials for almandine and spessartine components, respectively. We had some difficulties in the synthesis of grossular-almandine solid solution, especially in the almandine-rich side. Thus, synthetic almandine containing a small amount of a spessartine component was used as a crystal seed in the experiments. Ion exchange experiments were conducted using various starting compositions. Anthracene($C_{14}H_{10}$) was used as a reducing agent in order to keep iron and manganese ions in a divalent state during the experiments.

The starting material (10-40 mg) and 2N CaCl$_2$, FeCl$_2$ and/or MnCl$_2$ aqueous solution (15-50 μl) were enclosed into a gold capsule with a few milligrams of anthracene. The charged capsule was kept at 600°C and 1 kb in a standard cold-seal pressure vessel for 4 to 9 days. The temperature was monitored with a chromel-alumel thermocouple attached on the outer wall of the pressure vessel, and the pressure was measured by a Heise gauge. The temperature was controlled within ±5°C and the pressure within ±10 bars.

After the termination of the run, the pressure vessel was quenched with cold water. Gold capsules were opened and the run products were washed away into a beaker with distilled water. Solid phases were separated from a liquid phase with a membrane filter and were identified by the polarizing microscope, the X-

Table 2. Experimental data for the ion exchange in the system $Ca_3Al_2Si_3O_{12}$-$Mn_3Al_2Si_3O_{12}$-$(Ca, Mn)Cl_2$-H_2O at 600°C and 1 kb

Run No.	Duration days	Starting Materials				Run Products					
		Solid	mg	Solution μl		Garnet		Solution			
						Gro	Spe	Σm_{Ca}	Σm_{Mn}	m_{CaCl2}*	m_{MnCl2}*
205	7	Spe	30.6	$CaCl_2$	20	0.088	0.912	0.323	0.677	0.153	0.508
206	7	Spe	20.8	$CaCl_2$	40	0.187	0.813	0.458	0.542	0.257	0.344
207	7	Gro	30.8	$MnCl_2$	30	0.824	0.176	0.864	0.136	0.773	0.054
208	7	Gro	20.3	$MnCl_2$	40	0.715	0.285	0.781	0.219	0.647	0.093
221	7	Gro	29.7	$MnCl_2$	20	0.886	0.114	0.906	0.094	0.839	0.036
222	7	Gro	24.0	$MnCl_2$	25	0.848	0.152	0.884	0.116	0.804	0.045
223	7	Gro	18.7	$MnCl_2$	30	0.757	0.243	0.823	0.177	0.710	0.072
224	7	Gro	15.0	$MnCl_2$	40	0.542	0.458	0.694	0.306	0.525	0.144
225	7	Spe	22.5	$CaCl_2$	20	0.132	0.868	0.381	0.619	0.193	0.434
226	7	Spe	17.5	$CaCl_2$	25	0.158	0.842	0.424	0.576	0.228	0.382
228	7	Spe	15.1	$CaCl_2$	30	0.204	0.776	0.474	0.526	0.272	0.327
247	7	$Spe_{50}Gro_{50}$	25.1	$CaCl_2$	30	0.468	0.532	0.662	0.338	0.482	0.165
248	7	$Spe_{50}Gro_{50}$	27.8	$MnCl_2$	20	0.361	0.639	0.607	0.393	0.414	0.205
249	7	$Spe_{50}Gro_{50}$	15.9	$MnCl_2$	30	0.294	0.706	0.547	0.453	0.345	0.256
250	7	$Spe_{50}Gro_{50}$	13.5	$MnCl_2$	40	0.267	0.733	0.518	0.482	0.315	0.283

* Calculated values.
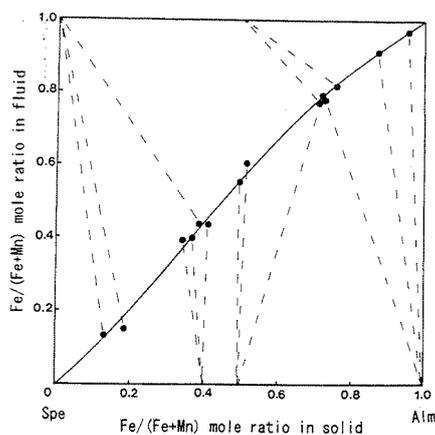
Fig. 1. Ion exchange data in the system $Fe_3Al_2Si_3O_{12}$-$Mn_3Al_2Si_3O_{12}$-$(Fe, Mn)Cl_2$-H_2O at 600°C and 1 kb. The starting and final compositions are connected with dashed lines.

ray diffractometer (Rigaku RAD-IB) and the scanning electron microscope (JEOL JSM-5400). The chemical compositions of the solid phases were determined on the crystal surfaces by the energy dispersive-type microanalyzer

(Link QX-200JI). In some cases, cations in the solid products were analyzed by the atomic absorption spectrophotometer (Shimadzu AA-610S) after dissolution with HF and HCl. The molar ratio of the cations in the liquid phase was also determined by the atomic absorption spectrophotometer.

III. Results

1. Almandine-spessartine-$(Fe^{2+}, Mn^{2+})Cl_2$-H_2O system

The experimental results are summarized in Table 1, and the ion exchange isotherm is shown in Fig. 1. Almandine and spessartine form a complete solid solution with each other.

The ion exchange isotherm suggests that Fe/Mn ratio in the garnet solid solution is nearly equal to that in the coexisting aqueous chloride solution. The grain size of the synthesized garnets reached up to 100 μm. All synthesized garnets have a shape of dodecahedron (Fig. 2-A).
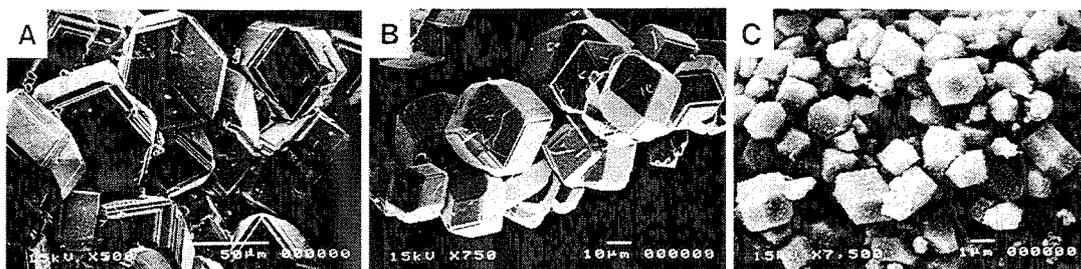
Fig. 2. Secondary electron images of synthesized garnets. A : $Alm_{76}Spe_{24}$ (run no. 215), B : Gro_9Spe_{91} (run no. 205) and C : $Gro_{86}Alm_{14}$ (run no. 315).

2. Grossular-spessartine-$(Ca^{2+}, Mn^{2+})Cl_2$-H_2O system

The experimental results are summarized in Table 2, and the ion exchange isotherm is shown in Fig. 3. Grossular and spessartine also form a continuous solid solution. Manganese ion is slightly preferentially partitioned into the garnet solid solution compared with calcium ion.

The synthesized garnet has a shape of dodecahedron (Fig. 2-B). The grain size decreases with an increase of grossular component from 50 μm to 2 μm.

3. Grossular-almandine-$(Ca^{2+}, Fe^{2+})Cl_2$-H_2O system

The experimental results are compiled in Table 3. Grossular(Gro) and almandine(Alm) form solid solutions in the limited compositional ranges from Gro_0Alm_{100} to Gro_8Alm_{92} and from $Gro_{72}Alm_{28}$ to $Gro_{100}Alm_0$ under the experimental conditions (Fig. 4). The Ca/(Ca+Fe) molar ratio of the coexisting aqueous chloride solution is about 0.21 for the mineral assemblage of garnet(Gro_8Alm_{92})+ fayalite+anorthite, about 0.52 for that of fayalite + hedenbergite + anorthite + wustite, and about 0.80 for that of hedenbergite + anorthite + wustite + garnet($Gro_{72}Alm_{28}$). The bulk chemical compositions of solid products containing the mineral assemblages of fayalite + anorthite and hedenbergite + anorthite + wustite were determined by the atomic
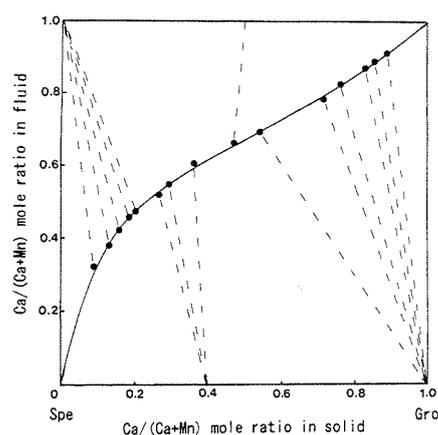
Fig. 3. Ion exchange data in the system $Ca_3Al_2Si_3O_{12}$-$Mn_3Al_2Si_3O_{12}$-(Ca, Mn)Cl_2-H_2O at 600°C and 1 kb. The starting and final compositions are connected with dashed lines.

absorption spectophotometer after dissolution with HF and HCl. Their bulk compositions are plotted in Fig. 4. Mineral assemblages of fayalite + anorthite and hedenbergite + anorthite + wustite appeared in the intermediate compositions. The schematic phase relation in the system CaO-FeO-Al_2O_3-SiO_2 is shown in Fig. 5. This figure is a projection onto the CaO-FeO-SiO_2 plane from Al_2O_3. The anorthite-wustite-hedenbergite plane intersects the grossular-almandine line in the middle point (Gro_{50} Alm_{50}), and the anorthite-fayalite line intersects the grossular-almandine line in the composition of $Gro_{33}Alm_{67}$.

The synthesized garnet in this system has
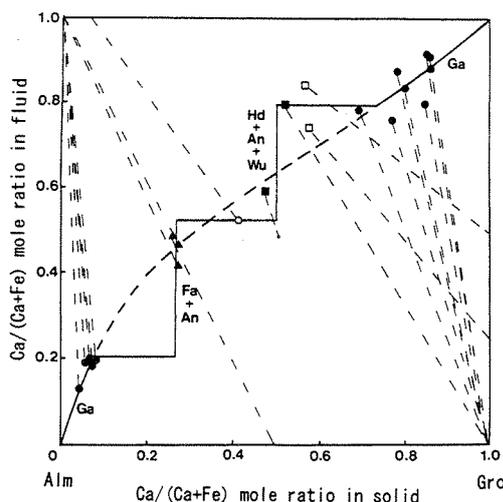
Fig. 4. Ion exchange data in the system $Ca_3Al_2Si_3O_{12}$-$Fe_3Al_2Si_3O_{12}$-$(Ca, Fe)Cl_2$-H_2O at 600°C and 1 kb. The starting and final compositions are connected with thin dashed lines. Bold dashed line is an estimated ion exchange isotherm between garnet solid solution and aqueous chloride solution in the unstable region of garnet solid solution. Symbols : solid circles, Ga ; open squares, Ga+Hd+An+Wu ; solid squares, Hd+An+Wu ; open circle, An+Hd+Fa+Wu ; solid triangles, Fa+An. Abbreviations : Ga, garnet ; Hd, hedenbergite ; An, anorthite ; Fa, fayalite ; Wu, wustite.

Fig. 5. The schematic phase relation in the CaO-FeO-Al_2O_3-SiO_2 at 600°C and 1 kb, projected onto CaO-FeO-SiO_2 plane from Al_2O_3. Abbreviations : Gro, grossular ; Alm, almandine ; Ga, garnet ; Hd, hedenbergite ; An, anorthite ; Fa, fayalite ; Wu, wustite.

also a shape of dodecahedron (Fig. 2-C), and the grain size decreases with an increase of grossular component from 50 μm to 2 μm.

4. Grossular-almandine-spessartine-$(Ca^{2+}, Fe^{2+}, Mn^{2+})Cl_2$-$H_2O$ system

The experimental results are summarized in Table 4. Compositions of garnets synthesized in this system are plotted in Fig. 6. Garnet solid solutions with the compositions corresponding to the semicircular area in Fig. 6 were not stable. The mineral assemblages fayalite+anorthite and hedenbergite+anorthite+wustite appeared in the semicircular area.

Fig. 7 shows concentrations of total Ca, Fe and Mn in the 2N aqueous chloride solution in equilibrium with garnet solid solution, calculated from the experimental results for binary

and ternary systems by the least square method. In the calculation, the aqueous chloride solution was assumed to be an ideal solution (Kubo et al., 1992).

IV. Thermodynamic considerations

Here we define unit formulae of garnet end members as follows :

grossular(Gro) : $1/3(Ca_3Al_2Si_3O_{12})$
almandine(Alm) : $1/3(Fe_3Al_2Si_3O_{12})$
and spessartine(Spe) : $1/3(Mn_3Al_2Si_3O_{12})$.

The ion exchange reactions between garnet solid solution and aqueous chloride solution can be expressed using neutral aqueous species as follows :

$1/3Ca_3Al_2Si_3O_{12}+FeCl_{2aq}$
$\quad = 1/3Fe_3Al_2Si_3O_{12}+CaCl_{2aq}$ (1)
$1/3Mn_3Al_2Si_3O_{12}+CaCl_{2aq}$
$\quad = 1/3Ca_3Al_2Si_3O_{12}+MnCl_{2aq}$ (2)
and $1/3Fe_3Al_2Si_3O_{12}+MnCl_{2aq}$
$\quad = 1/3Mn_3Al_2Si_3O_{12}+FeCl_{2aq}$.   (3)

Uchida et al. (1995) posed a question for the

Table 3. Experimental data for the ion exchange in the system $Ca_3Al_2Si_3O_{12}$-$Fe_3Al_2Si_3O_{12}$-$(Ca, Fe)Cl_2$-H_2O at 600°C and 1 kb

Run No.	Duration days	Starting Materials			Run Products						
		Solid	mg	Solution μl	Garnet		Solution				Phases
					Gro	Alm	Σm_{Ca}	Σm_{Fe}	m_{CaCl2}#	m_{FeCl2}#	
237	8	Gro	20.0	FeCl₂ 30	0.784	0.216	0.878	0.122	0.822	0.075	Ga
315	8	Gro	24.7	FeCl₂ 30	0.862	0.138	0.910	0.090	0.865	0.054	Ga
317	8	Gro	19.9	FeCl₂ 40	0.771	0.229	0.765	0.235	0.676	0.154	Ga
350	4	Alm*	18.7	CaCl₂ 30	0.063	0.937	0.199	0.801	0.127	0.730	Ga
353	4	Gro*	19.1	FeCl₂ 30	0.849	0.151	0.803	0.197	0.724	0.126	Ga
356	4	Alm*	27.0	CaCl₂ 20	0.055	0.945	0.189	0.811	0.120	0.743	Ga
357	4	Alm*	21.5	CaCl₂ 30	0.071	0.929	0.182	0.818	0.115	0.752	Ga
358	4	Alm*	18.9	CaCl₂ 40	0.081	0.919	0.196	0.804	0.124	0.734	Ga
366	4	Alm*	1.9	CaCl₂ 40	0.693	0.307	0.787	0.213	0.704	0.138	Ga
399	7	Alm*	29.9	CaCl₂ 20	0.039	0.961	0.128	0.872	0.078	0.823	Ga
403	7	Gro	30.3	FeCl₂ 30	0.855	0.145	0.919	0.081	0.877	0.049	Ga
404	7	Gro	29.0	FeCl₂ 40	0.862	0.138	0.884	0.116	0.830	0.071	Ga
406	7	Gro	19.5	FeCl₂ 30	0.801	0.199	0.838	0.162	0.770	0.102	Ga
351	4	Alm₅₀Gro₅₀*	15.8	FeCl₂ 30	0.262	0.738**	0.486	0.514	0.384	0.397	An+Fa
360	4	Alm*	11.1	CaCl₂ 40	0.274	0.726**	0.419	0.581	0.302	0.467	An+Fa
361	4	Alm*	7.1	CaCl₂ 30	0.275	0.725**	0.471	0.529	0.350	0.412	An+Fa
395	4	No357	9.6	CaCl₂ 20	0.413	0.587**	0.526	0.474	0.404	0.357	An+Fa+Hd+Wu
A1	10	Gro	10.0	FeCl₂ 40	0.522	0.478**	0.799	0.201	0.719	0.129	An+Hd+Wu
A2	10	Gro	9.9	CaCl₂ 10 / FeCl₂ 30	0.577	0.423**	0.744	0.256	0.650	0.170	Ga+An+Hd+Wu
A3	10	Gro	9.8	CaCl₂ 20 / FeCl₂ 20	0.569	0.431**	0.849	0.151	0.784	0.095	Ga+An+Hd+Wu
A5	10	Alm₅₀Gro₅₀	10.1	CaCl₂ 20 / FeCl₂ 20	0.476	0.524**	0.596	0.404	0.478	0.292	An+Hd+Wu

*, With crystal seed; **, Bulk composition; #, Calculated values.

Abbreviations: Ga,garnet; An,anorthite; Fa,fayalite; Hd,hedenbergite; Wu,wustite.

ideality of 2N $(Ca, Fe, Mn)Cl_2$ aqueous solution under supercritical conditions. The non-ideality is caused by the formation of $FeCl_3^-{}_{aq}$ and $MnCl_3^-{}_{aq}$. Therefore, we calculated the molalities of the neutral aqueous species, $CaCl_{2aq}$, $FeCl_{2aq}$ and $MnCl_{2aq}$, solving the following four mass-balance and four mass-action equations iteratively:

$$\Sigma m_{Ca} = m(Ca^{2+}) + m(CaCl^+) + m(CaCl_2) \quad (4)$$

$$\Sigma m_{Fe} = m(FeCl_2) + m(FeCl_3^-) \quad (5)$$

$$\Sigma m_{Mn} = m(MnCl_2) + m(MnCl_3^-) \quad (6)$$

$$\Sigma m_{Cl} = m(Cl^-) + m(CaCl^+) + 2\{m(CaCl_2) + m(FeCl_2) + m(MnCl_2)\} + 3\{m(FeCl_3^-) + m(MnCl_3^-)\} = 2 \quad (7)$$

$$K(CaCl^+) = \gamma(Ca^{2+})m(Ca^{2+})\gamma(Cl^-)m(Cl^-)/\{\gamma(CaCl^+)m(CaCl^+)\} \quad (8)$$

Ion exchange between garnet solid solution and 2N aqueous chloride solution

Table 4. Experimental data for the ion exchange in the system $Ca_3Al_2Si_3O_{12}$-$Fe_3Al_2Si_3O_{12}$-$Mn_3Al_2Si_3O_{12}$-(Ca, Fe, Mn)Cl_2-H_2O at 600°C and 1 kb

Run No.	Duration days	Starting Materials Solid	mg	Solution μl	Run Products Garnet Gro	Alm	Spe	Solution Σm_{Ca}	Σm_{Fe}	Σm_{Mn}	m_{CaCl2}*	m_{FeCl2}*	m_{MnCl2}*	Phases
280	7	Gro95Spe5	25.1	FeCl2 30	0.749	0.202	0.049	0.767	0.172	0.061	0.665	0.113	0.026	Ga
281	7	Gro95Spe5	19.7	FeCl2 40	0.700	0.250	0.050	0.715	0.224	0.061	0.601	0.151	0.027	Ga+An+Hd+Wu
291	7	Alm75Spe25	32.8	CaCl2 20	0.072	0.826	0.102	0.222	0.711	0.067	0.136	0.643	0.050	Ga
293	7	Alm75Spe25	20.6	CaCl2 30	0.084	0.718	0.198	0.237	0.625	0.138	0.142	0.562	0.108	Ga+An+Fa
295	7	Alm50Spe50	31.4	CaCl2 20	0.174	0.535	0.291	0.416	0.380	0.204	0.269	0.310	0.130	Ga+An+Fa
296	7	Alm50Spe50	25.4	CaCl2 25	0.195	0.465	0.340	0.403	0.358	0.239	0.254	0.295	0.156	Ga+An+Fa
300	7	Alm25Spe75	25.6	CaCl2 25	0.122	0.260	0.618	0.400	0.174	0.426	0.228	0.145	0.285	Ga
311	8	Gro33Alm33Spe33	30.6	FeCl2 30	0.158	0.352	0.490	0.363	0.293	0.344	0.210	0.249	0.239	Ga
313	8	Gro33Alm33Spe33	24.3	CaCl2 30	0.293	0.326	0.381	0.464	0.265	0.271	0.300	0.211	0.165	Ga
314	8	Gro33Alm33Spe33	25.6	MnCl2 30	0.164	0.279	0.559	0.440	0.221	0.339	0.270	0.179	0.214	Ga
319	8	Gro33Alm33Spe33	28.8	FeCl2 15 CaCl2 15	0.261	0.299	0.440	0.476	0.204	0.320	0.303	0.162	0.193	Ga
320	8	Gro33Alm33Spe33	21.1	FeCl2 15 CaCl2 15	0.271	0.323	0.406	0.482	0.226	0.292	0.313	0.178	0.174	Ga
322	8	Gro43Alm43Spe14	29.8	CaCl2 30	0.527	0.284	0.189	0.605	0.233	0.162	0.455	0.169	0.083	Ga+An+Fa
323	8	Gro43Alm43Spe14	22.9	CaCl2 30	0.484	0.324	0.192	0.570	0.274	0.156	0.420	0.202	0.083	Ga+An+Fa
324	8	Gro43Alm43Spe14	16.3	CaCl2 40	0.525	0.318	0.157	0.595	0.258	0.147	0.448	0.188	0.076	Ga+An+Fa
325	8	Gro43Alm43Spe14	30.2	FeCl2 15 CaCl2 15	0.484	0.318	0.197	0.600	0.241	0.159	0.451	0.175	0.082	Ga
331	9	Alm80Spe20	35.3	FeCl2 10 CaCl2 10	0.027	0.607	0.366	0.154	0.520	0.326	0.080	0.490	0.282	Ga
335	9	Gro33Alm33Spe33	19.0	CaCl2 30	0.306	0.318	0.376	0.487	0.249	0.264	0.321	0.195	0.156	Ga
337	9	Gro50Spe50	24.0	FeCl2 24 CaCl2 6	0.433	0.037	0.530	0.632	0.012	0.356	0.447	0.009	0.180	Ga
338	9	Gro50Spe50	16.5	FeCl2 24 CaCl2 6	0.488	0.058	0.454	0.628	0.026	0.346	0.444	0.019	0.176	Ga

* Calculated values.

Abbreviations: Ga,garnet; An,anorthite; Fa,fayalite; Hd,hedenbergite; Wu,wustite.

$$K(CaCl_2) = \gamma(CaCl^+)m(CaCl^+)\gamma(Cl^-)m(Cl^-)/\{\gamma(CaCl_2)m(CaCl_2)\} \tag{9}$$

$$K(FeCl_3^-) = \gamma(Cl^-)m(Cl^-)\gamma(FeCl_2)m(FeCl_2)/\{\gamma(FeCl_3^-)m(FeCl_3^-)\} \tag{10}$$

and

$$K(MnCl_3^-) = \gamma(Cl^-)m(Cl^-)\gamma(MnCl_2)m(MnCl_2)/\{\gamma(MnCl_3^-)m(MnCl_3^-)\} \tag{11}$$

where Σm_i indicates the total molality of i-bearing aqueous species, m(i) the molality of the aqueous species i, γ(i) the activity coefficient of the aqueous species i, and K(i) the

Gro
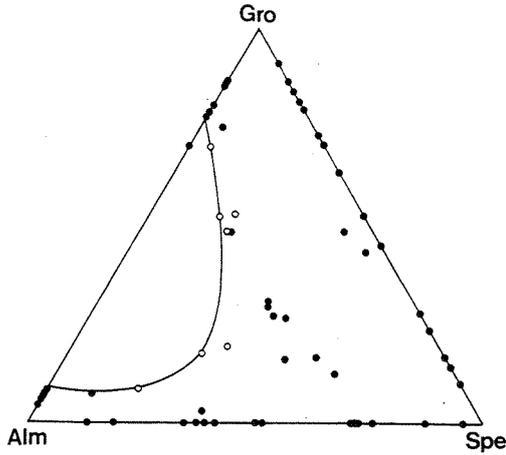
Fig. 6. Chemical compositions of garnets synthesized in the present experiments in the system $Ca_3Al_2Si_3O_{12}$- $Fe_3Al_2Si_3O_{12}$-$Mn_3Al_2Si_3O_{12}$-(Ca, Fe, Mn)Cl_2-H_2O at 600°C and 1 kb. Open circles show the chemical compositions of garnets in equilibrium with the mineral assemblages fayalite+anorthite and hedenbergite+anorthite+wustite, and solid circles show those in equilibrium with no other solid phases.

Fig. 7. Total molality of each cation in the aqueous chloride solution in equilibrium with garnet solid solution, calculated from the binary and ternary experimental data at 600°C and 1 kb by the least-square regression.

dissociation constant of the aqueous species i. The activity coefficients of the charged species were calculated using a Debye-Huckel equation :

$$\log \gamma(i) = -Z_i AI^{1/2}/(1+a_i BI^{1/2}) \qquad (12)$$

where Z_i is the ionic charge and I is the true ionic strength :

$$I = 1/2\Sigma m(i)Z_i^2 \qquad (13)$$

A and B are the Debye-Huckel coefficients and are taken from Helgeson and Kirkham (1974). a_i is the ion-size parameter and is taken from Kharaka and Barnes (1973). In the present study, the activity coefficients of the neutral species are assumed to be unity as done in most previous experimental studies (e.g., Frantz and Popp, 1979). Dissociation constants for $CaCl_{2aq}$ and $CaCl^+_{aq}$ are from Frantz and Marshall (1982) and dissociation constants for $FeCl_3^-_{aq}$ and $MnCl_3^-_{aq}$ from Uchida et al. (1995). In the

calculation, the presence of CO_2 derived from anthracene is neglected.

The calculated molalities of $CaCl_{2aq}$, $FeCl_{2aq}$ and $MnCl_{2aq}$ are included in Tables 1 to 4.

At equilibrium, we have the following relations corresponding to the reactions (1) to (3) :

$$\Delta G_r(1) = \mu(Alm) + \mu(CaCl_{2aq}) - \mu(Gro) - \mu(FeCl_{2aq}) = 0 \qquad (14)$$

$$\Delta G_r(2) = \mu(Gro) + \mu(MnCl_{2aq}) - \mu(Spe) - \mu(CaCl_{2aq}) = 0 \qquad (15)$$

and $\Delta G_r(3) = \mu(Spe) + \mu(FeCl_{2aq}) - \mu(Alm) - \mu(MnCl_{2aq}) = 0,$ $\qquad (16)$

where ΔG_r is the Gibbs energy of reaction, and $\mu(i)$ the chemical potential of the component i. For the components constituting solid phases,

$$\mu(i) = \mu°(i) + RTlnX_i + \mu^{ex}(i) \qquad (17)$$

and for aqueous species,

$$\mu(i) = \mu°(i) + RT\ln m(i) + RT\ln\gamma(i) \qquad (18)$$

where $\mu°(i)$ is the standard chemical potential of the component i, X_i the mole fraction of the component i in the solid solution, and $\mu^{ex}(i)$ the excess chemical potential of the component i.

Kakuda *et al.* (1991, 1994) derived a ternary regular solution model using a Bragg-Williams approximation. The excess Gibbs energy of mixing (G^{ex}) is written as

$$\begin{aligned}
G^{ex} = &X_{Fe}X_{Mn}(X_{Fe}W_{FeFeMn} + X_{Mn}W_{FeMnMn}) \\
&+ X_{Mn}X_{Ca}(X_{Mn}W_{MnMnCa} + X_{Ca}W_{MnCaCa}) \\
&+ X_{Ca}X_{Fe}(X_{Ca}W_{CaCaFe} + X_{Fe}W_{CaFeFe}) \\
&+ 2X_{Ca}X_{Fe}X_{Mn}W_{CaFeMn},
\end{aligned}$$

$$\qquad (19)$$

where W_{ijk} represents the interaction parameter for solid solution.

If we adopt this mixing model for the ternary garnet solid solution, the excess chemical potential of each component can be expressed as follows (Kakuda *et al.*, 1991, 1994):

$$\begin{aligned}
\mu^{ex}(Gro) = &-2X_{Fe}{}^2X_{Mn}W_{FeFeMn} \\
&-2X_{Fe}X_{Mn}{}^2W_{FeMnMn} \\
&+X_{Mn}{}^2(X_{Fe}+X_{Mn}-X_{Ca})W_{MnMnCa} \\
&+2X_{Mn}X_{Ca}(X_{Fe}+X_{Mn})W_{MnCaCa} \\
&+2X_{Ca}X_{Fe}(X_{Fe}+X_{Mn})W_{CaCaFe} \\
&+X_{Fe}{}^2(X_{Fe}+X_{Mn}-X_{Ca})W_{CaFeFe} \\
&+2X_{Fe}X_{Mn}(X_{Fe}+X_{Mn}-X_{Ca}) \\
&\quad W_{CaFeMn}
\end{aligned}$$

$$\qquad (20)$$

$$\begin{aligned}
\mu^{ex}(Spe) = &X_{Fe}{}^2(X_{Ca}+X_{Fe}-X_{Mn})W_{FeFeMn} \\
&+2X_{Fe}X_{Mn}(X_{Ca}+X_{Fe})W_{FeMnMn} \\
&+2X_{Mn}X_{Ca}(X_{Ca}+X_{Fe})W_{MnMnCa} \\
&+X_{Ca}{}^2(X_{Ca}+X_{Fe}-X_{Mn})W_{MnCaCa} \\
&-2X_{Ca}{}^2X_{Fe}W_{CaCaFe} \\
&-2X_{Ca}X_{Fe}{}^2W_{CaFeFe} \\
&+2X_{Ca}X_{Fe}(X_{Ca}+X_{Fe}-X_{Mn}) \\
&\quad W_{CaFeMn}
\end{aligned}$$

$$\qquad (21)$$

and

$$\begin{aligned}
\mu^{ex}(Alm) = \\
&2X_{Fe}X_{Mn}(X_{Mn}+X_{Ca})W_{FeFeMn} \\
&+X_{Mn}{}^2(X_{Mn}+X_{Ca}-X_{Fe})W_{FeMnMn} \\
&-2X_{Mn}{}^2X_{Ca}W_{MnMnCa}-2X_{Mn}X_{Ca}{}^2W_{MnCaCa} \\
&+X_{Ca}{}^2(X_{Mn}+X_{Ca}-X_{Fe})W_{CaCaFe} \\
&+2X_{Ca}X_{Fe}(X_{Mn}+X_{Ca})W_{CaFeFe} \\
&+2X_{Mn}X_{Ca}(X_{Mn}+X_{Ca}-X_{Fe})W_{CaFeMn}.
\end{aligned}$$

$$\qquad (22)$$

Equations (14) to (16) are rewritten using equations (17) to (22) as follows:

$$\begin{aligned}
&\Delta Gr°(1) + RT\ln(m(CaCl_2)X_{Fe}/m(FeCl_2)X_{Ca}) \\
&= -2X_{Fe}X_{Mn}W_{FeFeMn} - X_{Mn}{}^2W_{FeMnMn} \\
&\quad + X_{Mn}{}^2W_{MnMnCa} + 2X_{Mn}X_{Ca}W_{MnCaCa} \\
&\quad + (2X_{Ca}X_{Fe} - X_{Ca}{}^2)W_{CaCaFe} \\
&\quad + (-2X_{Ca}X_{Fe} + X_{Fe}{}^2)W_{CaFeFe} \\
&\quad + (2X_{Fe}X_{Mn} - 2X_{Mn}X_{Ca})W_{CaFeMn}
\end{aligned}$$

$$\qquad (23)$$

$$\begin{aligned}
&\Delta Gr°(2) + RT\ln(m(MnCl_2)X_{Ca}/m(CaCl_2)X_{Mn}) \\
&= X_{Fe}{}^2W_{FeFeMn} + 2X_{Fe}X_{Mn}W_{FeMnMn} \\
&\quad + (2X_{Mn}X_{Ca} - X_{Mn}{}^2)W_{MnMnCa} \\
&\quad + (-2X_{Mn}X_{Ca} + X_{Ca}{}^2)W_{MnCaCa} \\
&\quad - 2X_{Ca}X_{Fe}W_{CaCaFe} - X_{Fe}{}^2W_{CaFeFe} \\
&\quad + (2X_{Ca}X_{Fe} - 2X_{Fe}X_{Mn})W_{CaFeMn}
\end{aligned}$$

$$\qquad (24)$$

and $\Delta Gr°(3) + RT\ln(m(FeCl_2)X_{Mn}/m(MnCl_2)X_{Fe})$

$$\begin{aligned}
&= (2X_{Fe}X_{Mn} - X_{Fe}{}^2)W_{FeFeMn} + (-2X_{Fe}X_{Mn} \\
&\quad + X_{Mn}{}^2)W_{FeMnMn} - 2X_{Mn}X_{Ca}W_{MnMnCa} \\
&\quad - X_{Ca}{}^2W_{MnCaCa} + X_{Ca}{}^2W_{CaCaFe} \\
&\quad + 2X_{Ca}X_{Fe}W_{MnCaCa}W_{CaFeFe} + (2X_{Mn}X_{Ca} - 2X_{Ca} \\
&\quad X_{Fe})W_{CaFeMn},
\end{aligned}$$

$$\qquad (25)$$

where

$$\begin{aligned}
&\Delta Gr°(1) \\
&= \mu°(Alm) + \mu°(CaCl_{2aq}) - \mu°(Gro) - \mu°(FeCl_{2aq})
\end{aligned}$$

$$\qquad (26)$$

$$\begin{aligned}
&\Delta Gr°(2) \\
&= \mu°(Gro) + \mu°(MnCl_{2aq}) - \mu°(Spe) - \mu°(CaCl_{2aq})
\end{aligned}$$

$$\qquad (27)$$

and $\Delta Gr°(3)$

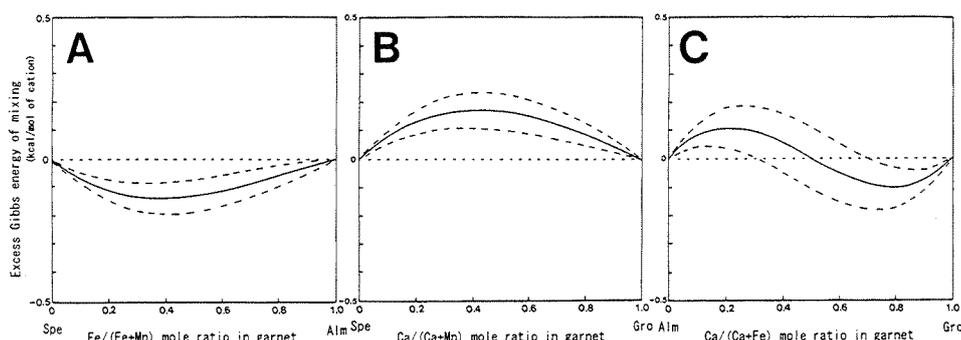$$= \mu°(Spe) + \mu°(FeCl_{2aq}) - \mu°(Alm) - \mu°(MnCl_{2aq}).$$

$$\qquad (28)$$

Fig. 8. Excess Gibbs energies of mixing at 600°C and 1 kb, calculated using interaction parameters listed in Table 5-A. A : Almandine-spessartine solid solution, B : grossular-spessartine solid solution and C : grossular-almandine solid solution. Dashed lines show 1σ deviation.

Interaction parameters W_{ijk} for the garnet solid solution and standard Gibbs energies of the reactions (1) to (3) can be obtained from the equations (23) to (25) by the least-square method using the binary and ternary ion exchange results. The results of the calculation are summarized in Table 5-A. For the comparison, interaction parameters obtained on the assumption that the molality of each neutral species is equal to the total molality of each cation are also listed in Table 5-B. The effect of the formation of $FeCl_3^-{}_{aq}$ and $MnCl_3^-{}_{aq}$ on the interaction parameters is considerable except for the almandine-spessartine system.

Fig. 8 shows excess Gibbs energies of mixing for the three binary garnet solid solutions calculated using interaction parameters in Table 5-A. The excess Gibbs energy of mixing for almandine-spessartine solid solution is slightly negative (Fig. 8-A), but grossular-spessartine solid solution shows positive deviation from ideality (Fig. 8-B). On the other hand, grossular-almandine solid solution shows positive deviation in the almandine side, but negative in the grossular side (Fig. 8-C).

Fig. 9 shows the excess Gibbs energy of mixing for the ternary almandine-spessartine-grossular solid solution calculated using the obtained interaction parameters (Table 5-A).

Table 5. Standard Gibbs energies of the ion exchange reactions and interaction parameters for garnet solutions at 600°C and 1 kb (kcal/mol of cation)

	(A)	(B)
W_{CaCaFe}	-1.091	-0.698
W_{CaFeFe}	1.140	1.852
W_{FeFeMn}	-0.238	-0.321
W_{FeMnMn}	-0.801	-0.841
W_{MnMnCa}	0.913	2.074
W_{MnCaCa}	0.454	1.336
W_{CaFeMn}	0.467	1.221
$\Delta G°_r(Gro-Alm)$	-0.993	-0.851
(s.d.)	(0.433)	(0.400)
$\Delta G°_r(Spe-Gro)$	1.610	1.209
(s.d.)	(0.262)	(0.213)
$\Delta G°_r(Alm-Spe)$	-0.375	-0.243
(s.d.)	(0.233)	(0.220)

(A) The molalities of the neutral aqueous species were calculated using the formation constants for $FeCl_3^-{}_{aq}$ and $MnCl_3^-{}_{aq}$ obtained by Uchida et al. (1995).
(B) Assumed that the total molality of each cation is equal to the molality of each neutral aqueous species.
*s.d. : standard deviation

It can be said that the garnet solid solution shows slight deviation from ideality.

V. Discussions

1. Unstable region of grossular-almandine-spessartine garnet solid solution

The equilibrium curve for the following reaction has been determined experimentally by Bohlen et al. (1983), Grafchikov and Fonarev
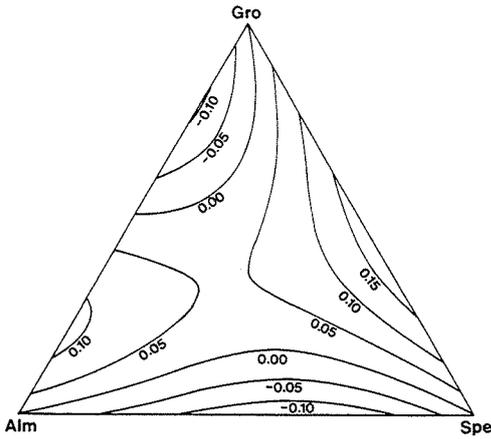
Fig. 9.　Excess Gibbs energy of mixing (kcal/mol of cation) for grossular-almandine-spessartine solid solution at 600°C and 1 kb, calculated using interaction parameters in Table 5-A.
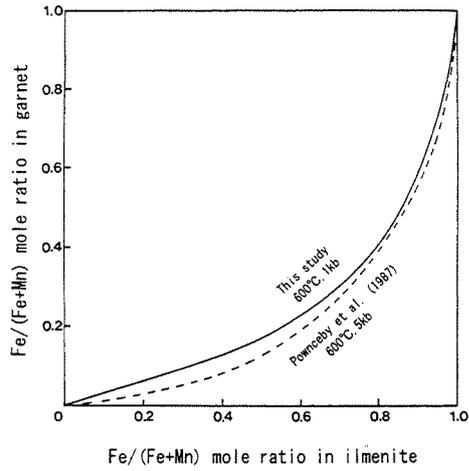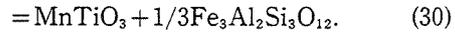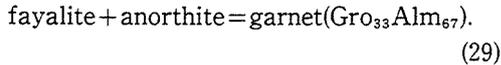

Fe/(Fe+Mn) mole ratio in ilmenite

Fig. 10.　Fe-Mn exchange isotherm between ilmenite and garnet solid solutions.

$$= MnTiO_3 + 1/3Fe_3Al_2Si_3O_{12}. \qquad (30)$$

(1986), Anovitz and Essene (1987) and Berman (1990):

$$fayalite + anorthite = garnet(Gro_{33}Alm_{67}). \qquad (29)$$

Extrapolation of their experimental results to lower pressures suggests that the equilibrium pressure for the reaction (29) is 2.5 to 3.7 kb at 600°C. The mineral assemblage fayalite + anorthite is stable at the lower pressures. The present experimental results at 1 kb are concordant with their experimental results.

No experiments have been carried out for the reaction anorthite + hedenbergite + wustite = garnet(Gro_{50}Alm_{50}).

2.　Mixing properties of garnet solid solutions

The excess Gibbs energy of mixing for almandine-spessartine solid solution was obtained by Ono (1980) and Pownceby et al. (1987, 1991) based on experimental studies of the partitioning of Fe and Mn between ilmenite and garnet. The exchange reaction can be expressed as

$$FeTiO_3 + 1/3Mn_3Al_2Si_3O_{12}$$
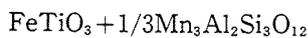
They gave -0.15 to 0.15 kcal/mol of cation as symmetric interaction parameter W_{FeMn} at 600 to 1,000°C and 2 to 10 kb, and concluded that almandine-spessartine solid solution behaves nearly ideally. From ionic size consideration, Ganguly and Kennedy (1974) also considered that spessartine mixes with almandine nearly ideally. The present experimental results show a small negative deviation ($W_{FeFeMn} = -0.24$ and $W_{FeMnMn} = -0.80$ kcal/mol) from ideality for almandine-spessartine solid solution.

Kubo et al. (1992) examined Fe-Mn exchange equilibrium between ilmenite and aqueous chloride solution at 600°C and 1 kb. Therefore, we can deduce the Fe-Mn exchange isotherm between ilmenite and garnet by combining their experimental data with the present results. The resultant isotherm is depicted in Fig. 10. The obtained isotherm is fairly concordant with that of Pownceby et al. (1987) at 600°C and 5 kb. As volume change for the reaction is very small (-0.0067 cm^3/mol calculated from JCPDS card), the pressure effect can be neglected.
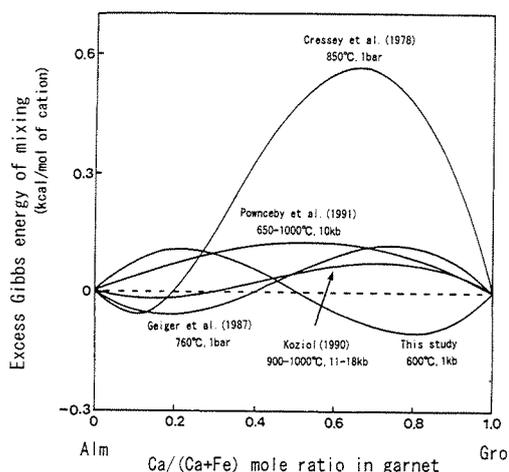
Fig. 11. Comparison of mixing property of grossular-almandine solid solution.

There are few studies on the mixing property of grossular-spessartine solid solution. Ganguly and Kennedy (1974) roughly estimated the mixing property of grossular-spessartine solid solution based on ionic radius, and concluded that grossular-spessartine solid solution has a small positive excess Gibbs energy of mixing $(0 < W_{CaMn} \ll 1.355 \, kcal/mol)$. Based on displaced equilibrium experiments for the reaction anorthite $=$ grossular $+$ 2kyanite $+$ quartz, Koziol (1990) concluded that grossular mixed with spessartine nearly ideally. The results presented here indicate a small positive deviation $(W_{MnMnCa} = 0.91$ and $W_{MnCaCa} = 0.45 \, kcal/mol)$ from ideality.

There are several investigations on the mixing property of grossular-almandine solid solution (Fig. 11). Cressey et al. (1978) and Koziol (1990) obtained excess Gibbs energy of mixing for grossular-almandine solid solution by analyzing chemical compositions of garnet solid solution in equilibrium with anorthite, sillimanite/kyanite and quartz. Geiger et al. (1987) measured enthalpy of mixing for this series garnet using high-temperature solution calorimetry and calculated·the excess Gibbs energy of mixing. Fig. 11 is obtained from

their experimental data on the assumption that interaction parameter for entropy is zero (Ganguly and Saxena, 1984). As a result, grossular-almandine solid solution shows positive deviation from ideality in the grossular side, but negative in the almandine side. This is obviously different from the present result which suggests that grossular-almandine solid solution shows positive deviation from ideality in the almandine side, but negative in the grossular side. Pownceby et al. (1991) gave positive deviation for grossular-almandine solid solution in the entire compositional range based on the experimental study of the Ca effect on Fe-Mn exchange equilibria between ilmenite and garnet. Thus, thermodynamic property for grossular-almandine solid solution obtained in the present study has large uncertainty due to a large unstable region of the garnet solid solution.

3. Summary and conclusions

(1) Grossular and spessartine, and almandine and spessartine form continuous solid solutions at 600°C and 1 kb, respectively.

(2) Mineral assemblages fayalite $+$ anorthite and hedenbergite $+$ anorthite $+$ wustite are stable in the intermediate compositional range of the grossular-almandine join at 600°C and 1 kb.

(3) Calcium ion is slightly preferentially partitioned into aqueous chloride solution against garnet solid solution compared with ferrous and manganese ions.

(4) Almandine-spessartine solid solution shows slightly negative deviation from ideality, whereas grossular-spessartine solid solution shows slightly positive deviation.

(5) Mixing property of grossular-almandine solid solution was not well determined due to the large unstable region.

Otsuka and Prof. S. Tsutsumi of Waseda University for facilities of hydrothermal apparatus.

References

Ackermand, D., Karl, F. and Raase, P. (1972), Granate mit Zusammensetzungen Zwischen Almandine und Grossular aus den westlichen Hohen Tauern, Österreich. *Contrib. Mineral. Petrol.*, **37**, 29-38.

Anovitz, L.M. and Essene, E.J. (1987), Compatibility of geobarometers in the system CaO-FeO-Al_2O_3-SiO_2-TiO_2(CFAST). Implication for garnet mixing models. *J. Geol.*, **95**, 633-645.

Berman, R.G. (1990), Mixing properties of Ca-Mg-Fe-Mn garnets. *Amer. Mineral.*, **75**, 328-344.

Bohlen, S.R., Wall, V.J. and Boettcher, A.L. (1983), Experimental investigation and application of garnet granulite equilibria. *Contrib. Mineral. Petrol.*, **83**, 52-61.

Brown, E.H. (1969), Some zoned garnets from the greenschist facies. *Amer. Mineral.*, **54**, 1662-1677.

Cressey, G., Schmid, R. and Wood, B.J. (1978), Thermodynamic properties of almandine-grossular garnet solid solutions. *Contrib. Mineral. Petrol.*, **67**, 397-404.

Frantz, J.D. and Marshall, W.L. (1982), Electrical conductances and ionization constants of calcium chloride and magnesium chloride in aqueous solutions at temperatures to 600°C and pressures to 4000 bars. *Amer. J. Sci.*, **282**, 1666-1693.

Frantz, J.D. and Popp, R.K. (1979), Mineral-solution equilibria I. An experimental study of complexing and thermodynamic properties of aqueous $MgCl_2$ in the system MgO-SiO_2-H_2O-HCl. *Geochim. Cosmochim. Acta*, **43**, 1223-1239.

Frondel, C. and Ito, J. (1965), Stilpnomelane and spessartine-grossularite from Franklin, New Jersey. *Amer. Mineral.*, **50**, 498-501.

Ganguly, J. and Kennedy, G.C. (1974), The energetics of natural garnet solid solution: Mixing of aluminosilicate end-members. *Contrib. Mineral. Petrol.*, **48**, 137-148.

Ganguly, J. and Saxena, S.K. (1984), Mixing properties of aluminosilicate garnets: constraints from natural and experimental data and application to geothermobarometry. *Amer. Mineral.*, **69**, 88-97.

Geiger, C.A., Newton, R.C. and Kleppa, O.J. (1987), Enthalpy of mixing of synthetic almandine-grossular and almandine-pyrope garnets from high-temperature solution calorimetry. *Geochim. Cosmochim. Acta*, **51**, 1755-1763.

Grafchikov, A.A. and Fonarev, V.I. (1986), Experimental evidence on coexisting garnet, clinopyroxene, and quartz in the FeO-CaO-Al_2O_3-SiO_2-H_2O system. *Geochem. Inter.*, **23**, 158-169.

Hariya, Y. and Nakano, S. (1972), Experimental study of the solid solution between the grossular-almandine series. *J. Fac. Sci. Hokkaido. Univ. Ser. IV*, **15**, 173-178.

Helgeson, H.C. and Kirkham, D.H. (1974), Theoretical prediction of the thermodynamic behavior of aqueous electrolytes at high pressures and temperatures. Debye-Huckel parameters for activity coefficients and relative partial molal properties. *Amer. J. Sci.*, **274**, 1199-1261.

Hsu, L.C. (1980), Hydration and phase relations of grossular-spessartine garnets at $P_{H2O}=2$ Kb. *Contrib. Mineral. Petrol.*, **71**, 407-415.

Ito, J. and Frondel, C. (1968), Synthesis of the grossular-spessartine series. *Amer. Mineral.* **53**, 1036-1038.

Kakuda, Y., Uchida, E. and Imai, N. (1991), A new thermodynamic model for ternary solid solutions. *J. Mineral. Soc. Japan*, **21**, 25-32 (in Japanese).

Kakuda, Y., Uchida, E. and Imai, N. (1994), A new model of the excess Gibbs energy of mixing for a regular solution. *Proc. Japan Acad.*, **70**, Ser. B, 163-168.

Kharaka, Y.K. and Barnes, I. (1973), SOLMNEQ; solution mineral equilibrium computations. *NTIS Technical Rep.*, **PB214-899**, 82 p.

Koziol, A.M. (1990), Activity-composition relationships of binary Ca-Fe and Ca-Mn garnets determined by reversed, displaced equilibrium experiments. *Amer. Mineral.*, **75**, 319-327.

Kubo, T,, Uchida, E., Furukawa, Y. and Imai, N. (1992), Experimental study on ion exchange equilibria between ilmenite solid solution (Fe^{2+}, Mn^{2+}, Mg)TiO_3 and aqueous (Fe^{2+}, Mn^{2+}, Mg)Cl_2 solution. *J. Mineral. Soc. Japan*, **21**, 59-67(in Japanese).

Nemec, D. (1967), The miscibility of the pyralspite and grandite molecules in garnets. *Mineral. Mag.*, **36**, 389-402.

Ono, A. (1980), Partitioning of Fe and Mn between garnet and ilmenite: an experimental study. *J. Japan. Assoc. Min. Petr. Econ. Geol.*, **75**, 160-160.

Pownceby, M.I., Wall, V.J. and O'Neill, H.St.C. (1987), Fe-Mn partitioning between garnet and

ilmenite: experimental calibration and applications. *Contrib. Mineral. Petrol.*, **97**, 116-126.

Pownceby, M.I., Wall, V.J. and O'Neill, H.St.C. (1991), An experimental study of the effect of Ca upon garnet-ilmenite Fe-Mn exchange equilibria. *Amer. Mineral.*, **76**, 1580-1588.

Shimazaki, H. (1977), Grossular-spessartine-almandine garnets from some japanese scheelite skarns. *Can. Mineral.*, **15**, 74-80.

Shoji, T., Tsukada, H. Mariko, T. and Kaneda, H. (1995), Immiscibility of the grossular-spessartine series under a water pressure of 100 MPa. *Mineral. J.*, **17**, 313-321.

Uchida, E., Goryozono, Y., Naito, M. and Yamagami, M. (1995), Aqueous speciation of iron and manganese chlorides in supercritical hydrothermal solutions. *Geochem. J.*, **29**, 175-188.

600°C，1 kb におけるザクロ石と 2N 塩化物水溶液間の Ca^{2+}，Fe^{2+} および Mn^{2+} イオンの交換実験

内田　悦生・儀満　雅隆・今井　直哉

グロシュラー――アルマンディン―スペサルティン系ザクロ石の安定関係と固溶に関する熱力学的性質を調べるために 600°C，1 kb においてザクロ石と 2N 塩化物水溶液間における Ca^{2+}，Fe^{2+} および Mn^{2+} イオンの交換実験を行った。実験結果は Ca^{2+} は Fe^{2+} および Mn^{2+} に比べて塩化物水溶液にやや濃集することを示した。また，グロシュラー――アルマンディン―スペサルティン系ザクロ石ではグロシュラー――アルマンディン系に沿った半円形の領域を除いて固溶体が生成された。この半円形の領域では，ザクロ石固溶体の代わりにファヤライト―灰長石およびヘデン輝石―灰長石―ウスタイトの鉱物組み合わせが出現した。塩化物水溶液中における FeCl$_3^-{}_{aq}$ と MnCl$_3^-{}_{aq}$ の存在を考慮に入れて実験結果からザクロ石固溶体の熱力学的性質を求めた結果，アルマンディン―スペサルティン固溶体は理想固溶体から負のずれを示し，グロシュラー――スペサルティン固溶体は逆に正のずれを示した。グロシュラー――アルマンディン固溶体の混合に関する熱力学的性質はこの系における広い不安定領域のため精度良く求めることができなかった。

論　　文

イルメナイト固溶体－塩化物水溶液間
# イオン交換平衡実験の再解析

内田悦生[*]・山上順民[*]

Re-analysis of Ion Exchange Experiments between
Ilmenite Solid Solution and Aqueous Chloride Solution

Etsuo UCHIDA[*] and Masahito YAMAGAMI[*]

Abstract: The experimental data for ion exchange equilibria between $(Fe,Mn,Mg)TiO_3$ ilmenite solid solution and 2N $(Fe,Mn,Mg)Cl_2$ aqueous chloride solution by Kubo et al. (1992) were re-analyzed taking into consideration the formation of $FeCl_3^-{}_{aq}$ and $MnCl_3^-{}_{aq}$. As a result, the newly obtained excess Gibbs energy of mixing for $(Fe,Mn,Mg)TiO_3$ ilmenite solid solution was slightly smaller than that obtained by Kubo et al. (1992), where 2N $(Fe,Mn,Mg)Cl_2$ aqueous chloride solution was assumed as an ideal solution.

1. まえがき

　鉱物固溶体の熱力学的性質を求めることをその1つの目的として鉱物と塩化物水溶液間におけるイオン交換平衡実験が今までに数多くなされてきた. イオン交換平衡実験結果から鉱物固溶体の熱力学的性質を求めるためには塩化物水溶液の熱力学的性質を予め知っている必要がある. 従来, 超臨界条件下では塩化物はそのほとんどが中性溶存種として水溶液中に溶存していると考えられ, 塩化物水溶液は理想混合溶液として取り扱われてきた. しかしながら, 最近, Uchida et al.[1]は灰重石 $(CaWO_4)$ と鉄重石 $(FeWO_4)$ またはマンガン重石 $(MnWO_4)$ を用いて塩化物水溶液との間におけるイオン交換平衡に及ぼすNaClおよびKClの影響に関する実験を行い, 600℃, 1kbの超臨界条件下では次式で表わされる $FeCl_3^-{}_{aq}$ と $MnCl_3^-{}_{aq}$ の錯体生成反応が無視できないことを明らかにした.

$$FeCl_{2aq} + Cl^-{}_{aq} = FeCl_3^-{}_{aq} \qquad (1)$$
$$MnCl_{2aq} + Cl^-{}_{aq} = MnCl_3^-{}_{aq} \qquad (2)$$
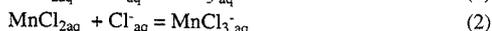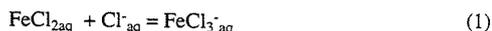
それゆえ, $FeCl_2$-$CaCl_2$ 系および $MnCl_2$-$CaCl_2$ 系の塩化物水溶液は理想混合溶液として取り扱うことができない.

　また, $CaCl_2$ 水溶液と $MgCl_2$ 水溶液の熱力学的挙動は互いに似ていることから[2], 同様に $FeCl_2$-$MgCl_2$ 系および $MnCl_2$-$MgCl_2$ 系の塩化物水溶液も理想混合溶液として取り扱うことができないと推定される.

　そこで, 本論文では久保ら[3]による $(Fe,Mn,Mg)TiO_3$ イルメナイト固溶体と2N $(Fe,Mn,Mg)Cl_2$ 水溶液間の600℃, 1kbにおけるイオン交換平衡実験結果を $FeCl_3^-{}_{aq}$ と $MnCl_3^-{}_{aq}$ の生成を考慮に入れて再解析することを目的として, 600℃, 1kbにおける2N $(Fe,Mn,Mg)Cl_2$ 塩化物水溶液の熱力学的挙動の考察を行う.

2. 水溶液中における $FeCl_2$ および $MnCl_2$ の溶存種

　従来の実験結果に基づき600℃, 1kbの2N $FeCl_2$ および $MnCl_2$ 水溶液中における溶存種について考察する.

　Uchida et al.[1]は $CaWO_4$ と $FeWO_4$, $CaWO_4$ と $MnWO_4$ の各2相と平衡にある塩化物水溶液の Ca/(Ca+Fe) モル分率または Ca/(Ca+Mn) モル分率に及ぼす NaClとKClの影響に関する実験を行い, 1kb, 400℃および600℃における $FeCl_3^-{}_{aq}$ と $MnCl_3^-{}_{aq}$ の生成定数を求めた. $CaWO_4$ と $FeWO_4$ または $CaWO_4$ と $MnWO_4$ の2相と平衡にある塩化物水溶液の Ca/(Ca+Fe) モル分率または Ca/(Ca+Mn) モル分率は NaClおよびKCl濃度が上昇するにつれ急激に減少する. Uchida et al.[1]は, これはNaClとKClの解離により生成さ

れる Cl^-_{aq} が $CaCl^+_{aq}$ および $FeCl_{2aq}$ または $MnCl_{2aq}$ と結合し，それぞれ $CaCl_{2aq}$, $FeCl_3^-_{aq}$, $MnCl_3^-_{aq}$ を生成することにより溶液中の $Ca/(Ca+Fe)$ モル分率または $Ca/(Ca+Mn)$ モル分率が減少すると解釈した．$FeCl_2$ と $MnCl_2$ の水溶液中における挙動は似ており，$FeCl_3^-_{aq}$ と $MnCl_3^-_{aq}$ の生成定数は温度が高くなる程大きくなる傾向がある．600°C, 1kb では $MnCl_3^-_{aq}$ の生成定数の対数値 $logK\ (MnCl_3^-_{aq})$ は 2.3，$FeCl_3^-_{aq}$ の生成定数の対数値 $logK\ (FeCl_3^-_{aq})$ は 1.9 であり，$FeCl_3^-_{aq}$ よりも $MnCl_3^-_{aq}$ の方がやや生成されやすい傾向を示す．いずれにしても $FeCl_3^-_{aq}$ と $MnCl_3^-_{aq}$ の生成定数はかなり大きくこれらの溶存種の存在を無視することができない．このように超臨界条件下で遷移金属イオンが高次のクロロ錯体を生成することはニッケル[4]と亜鉛[5]に対しても実験により確かめられている．

他方，$FeCl_{2aq}$ の解離定数は極めて小さく[6]，600°C, 1kb では Fe^{2+}_{aq} と $FeCl^+_{aq}$ の存在は無視することができる．$MnCl_{2aq}$ に関しては Ag-AgCl バッファー法を用いたバラ輝石の溶解度測定から 400-700°C，1kb および 2kb では $MnCl_{2aq}$ が優勢溶存種であることが分かっており[7]，このことから $MnCl_{2aq}$ は $FeCl_{2aq}$ と同様に極めて小さな解離定数を持つと考えられる．それゆえ，600°C, 1kb では Mn^{2+}_{aq} や $MnCl^+_{aq}$ の存在も無視することができる．

以上のことから，600°C，1kb における 2N 塩化物水溶液中では二価の鉄とマンガンの溶存種として $FeCl_{2aq}$, $FeCl_3^-_{aq}$, $MnCl_{2aq}$, $MnCl_3^-_{aq}$ のみを考慮に入れれば良い．

3. 水溶液中における $MgCl_2$ の溶存種

$MgCl_{2aq}$ の解離定数は，Frantz and Marshall[2] により求められている．また，Luce et al.[8] は CaO-MgO-SiO_2-H_2O-HCl 系における鉱物の溶解度実験から 2kb における $MgCl_{2aq}$ の解離定数を求めており，得られた値は Frantz and Marshall[2] の結果と一致している．$MgCl_{2aq}$ の解離定数は比較的大きく，600°C, 1kb の条件下でも $MgCl^+$ の存在は無視することができない．$MgCl^+_{aq}$ に比べて Mg^{2+}_{aq} の濃度はかなり小さくなると考えられるが，データが揃っていることからここでは Mg^{2+}_{aq} も考慮に入れることにする．

Frantz and Marshall[2] の実験結果から $CaCl_{2aq}$ と $MgCl_{2aq}$ の解離定数はほぼ一致しており，$CaCl_2$ 水溶液と $MgCl_2$ 水溶液は熱力学的に似た挙動を示すことが推測される．ところで，滑石の $NaCl$ 水溶液に対する溶解度実験から Mg^{2+} の高次クロロ錯体がかなりの割合で生成されている可能性が報告されている[9]．しかしながら，Fein and Walther[10] の方解石の溶解度実験からは Ca^{2+} の高次クロロ錯体は生成しないと考えられる．また，$MgCl_2$ も $CaCl_2$ もイオン結合性が強く，Ca^{2+} や Mg^{2+} は高次クロロ錯体を

生成するとは考えにくい．それゆえ，ここでは $MgCl_2$ の溶存種として Mg^{2+}_{aq}, $MgCl^+_{aq}$, $MgCl_{2aq}$ の 3 溶存種のみを考慮に入れ，$MgCl_3^-_{aq}$ 等の Mg^{2+} の高次クロロ錯体は生成されないとする．特に，Fe^{2+} や Mn^{2+} のような高次のクロロ錯体を生成しやすいイオンと共存する場合には Mg^{2+} の高次クロロ錯体は生成されないと推測できる．

4. 塩化物水溶液の過剰混合ギブスエネルギー

超臨界条件下にある塩化物水溶液中では中性溶存種が優勢溶存種であると考えられ[7, 11-13]，超臨界条件下における鉱物と塩化物水溶液間のイオン交換反応は，一般的に中性溶存種を用いて書き表わされる．例えば $(Fe,Mg)TiO_3$ イルメナイトと塩化物水溶液間のイオン交換反応式は

$$FeTiO_3 + MgCl_{2aq} = MgTiO_3 + FeCl_{2aq} \tag{3}$$
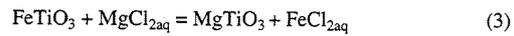
と表わされる．平衡状態においては (3) の反応に対して次の式が成り立つ．

$$\Delta G_r° + RTln\{X(MgTiO_3) \cdot m(FeCl_{2aq})\}/\{X(FeTiO_3) \cdot m(MgCl_{2aq})\} + RTln\{\gamma(MgTiO_3) \cdot \gamma(FeCl_{2aq})\}/\{\gamma(FeTiO_3) \cdot \gamma(MgCl_{2aq})\} = 0 \tag{4}$$

ここで，$\Delta G_r°$ は標準反応ギブスエネルギー，T は絶対温度，R はガス定数，$X(i)$ は鉱物固溶体中の i 成分のモル分率，$m(i)$ は水溶液中の i 溶存種の重量モル濃度，$\gamma(i)$ は鉱物固溶体中の i 成分または水溶液中の i 溶存種の活動度係数である．角田ら[14]の固溶体モデルに基づけば鉱物固溶体中の i 成分に対する活動度係数は

$$RTln\ \gamma(MgTiO_3) = 2X(FeTiO_3)^2 \cdot X(MgTiO_3) \cdot W_{MgMgFe} + X(FeTiO_3)^2 \cdot \{1 - 2X(MgTiO_3)\} \cdot W_{MgFeFe} \tag{5}$$

$$RTln\ \gamma(FeTiO_3) = X(MgTiO_3)^2 \cdot \{1-2X(FeTiO_3)\} \cdot W_{MgMgFe} + 2X(MgTiO_3)^2 \cdot X(FeTiO_3) \cdot W_{MgFeFe} \tag{6}$$

と書き表わされる．ここで，W_{ijk} は固溶体の相互作用パラメータである．(4) ～ (6) 式を用いてイオン交換平衡実験データから最小二乗法により $\Delta G_r°$, W_{MgMgFe}, W_{MgFeFe} を求めることができる[3]が，この時，従来は一般的に次の 2 つの仮定がなされていた．

$$\gamma(FeCl_{2aq}) = \gamma(MgCl_{2aq})(一般的には =1 と仮定される) \tag{7}$$

$$m(FeCl_{2aq}) = \Sigma m_{Fe} および m(MgCl_{2aq}) = \Sigma m_{Mg} \tag{8}$$

ここで，Σm_i は，i 元素を含む全溶存種の重量モル濃度を示す．(7) の仮定は一般的に受け入れられており，ここでは議論しないことにする．(8) の仮定は，Uchida et al.[1] の実験から成り立たないことが明らかとなった．これは水溶液の混合により中性溶存種以外の溶存種が生成されるためであり，これが塩化物水溶液の過剰混合ギブスエネルギーの源である．以下に 600°C, 1kb における各系の 2N 塩化物水溶液の過剰混合ギブスエネルギーについて考察する．

4.1 $FeCl_2$-$MgCl_2$ 系および $MnCl_2$-$MgCl_2$ 系水溶液

2 章および 3 章で述べたように 600°C，1kb における 2N

$FeCl_2$-$MgCl_2$ 系および 2N $MnCl_2$-$MgCl_2$ 系水溶液において
は，溶存種として Mg^{2+}_{aq}, $MgCl^+_{aq}$, $MgCl_{2aq}$, $FeCl_{2aq}$, $FeCl_3^-_{aq}$,
$MnCl_{2aq}$, $MnCl_3^-_{aq}$, Cl^-_{aq} のみを考慮すれば良い．ここで Fe
または Mn を Me で表わすと，これらの溶存種の間には次
の反応式が成り立つ．

$$MgCl_{2aq} = MgCl^+_{aq} + Cl^-_{aq} \tag{9}$$

$$MgCl^+_{aq} = Mg^{2+}_{aq} + Cl^-_{aq} \tag{10}$$

$$MeCl_{2aq} + Cl^-_{aq} = MeCl_3^-_{aq} \tag{11}$$

(9)~(11) の反応に対してそれぞれ次の質量作用式が書
ける．

$$K(MgCl_{2aq}) = a(MgCl^+_{aq}) \cdot a(Cl^-_{aq})/a(MgCl_{2aq}) \tag{12}$$

$$K(MgCl^+_{aq}) = a(Mg^{2+}_{aq}) \cdot a(Cl^-_{aq})/a(MgCl^+_{aq}) \tag{13}$$

$$K(MeCl_3^-_{aq}) = a(MeCl_3^-_{aq})/\{a(MeCl_{2aq}) \cdot a(Cl^-_{aq})\} \tag{14}$$

また，Mg, Me, Cl のそれぞれに対して次の質量保存
式が成り立つ．

$$\Sigma\, m_{Mg} = m(Mg^{2+}_{aq}) + m(MgCl^+_{aq}) + m(MgCl_{2aq}) \tag{15}$$

$$\Sigma\, m_{Me} = m(MeCl_{2aq}) + m(MeCl_3^-_{aq}) \tag{16}$$

$$\Sigma\, m_{Cl} = m(MgCl^+_{aq}) + 2m(MgCl_{2aq}) + 2m(MeCl_{2aq})$$
$$+ 3m(MeCl_3^-_{aq}) + m(Cl^-_{aq}) = 2 \tag{17}$$

各溶存種の濃度は(12)~(17)の質量作用式および質量保
存式を同時に解くことにより求められる．ここで，a(i)は
i溶存種の活動度，K(i)は i溶存種の生成または解離定数
である．計算において $MgCl^+_{aq}$ と $MgCl_{2aq}$ の解離定数とし
ては Frantz and Marshall[2] の値を用いた．電荷を持つ溶存種
の活動度係数の計算には次のDebye-Huckelの式を用いた．

$$\log \gamma_i = -Z_i \cdot A \cdot I^{1/2}/(1 + a_i \cdot B \cdot I^{1/2}) \tag{18}$$

ここで，Z_i は溶存種iの電荷数である．A, Bはデバイ・
ヒュッケル係数で Helgeson and Kirkham[15] の値を用いた．
a_i はイオンサイズパラメータで Kharaka and Barnes[16] の値
を用いた．なお，$MgCl^+_{aq}$ と $MeCl_3^-_{aq}$ のイオンサイズパラ
メータの値は Seward[17] に基づき4とした．また，Iは次
式で表わされるイオン強度である．

$$I = 1/2\, \Sigma\, m(i) \cdot Z_i^2 \tag{19}$$

上式を用いて求められた 2N (Me,Mg)Cl_2 水溶液に対す
る $\Sigma\, m_{Mg}/(\Sigma\, m_{Mg} + \Sigma\, m_{Me})$ と $m(MgCl_{2aq})/(m(MgCl_{2aq}) + m(MeCl_{2aq}))$ の関係を $MeCl_3^-_{aq}$ の生成定数の関数として
Fig. 1 に示した．

ところで，ある元素の中性溶存種濃度とその元素を含む
全溶存種の重量モル濃度との関係は活動度係数 γ_i を用いて
次のように表わすことができる．Mg と Me を例にとると

$$m(MgCl_{2aq}) = \gamma_{Mg} \cdot \Sigma\, m_{Mg} \tag{20}$$

$$m(MeCl_{2aq}) = \gamma_{Me} \cdot \Sigma\, m_{Me} \tag{21}$$

γ_i は塩化物水溶液中の i元素を含む全溶存種の重量モル
濃度に対する i元素の中性溶存種の重量モル濃度の割合
であり，塩化物水溶液の非理想性を示す係数である．先
ほど述べた (8) の仮定は $\gamma_{Mg} = \gamma_{Me} = 1$ とした場合に対応
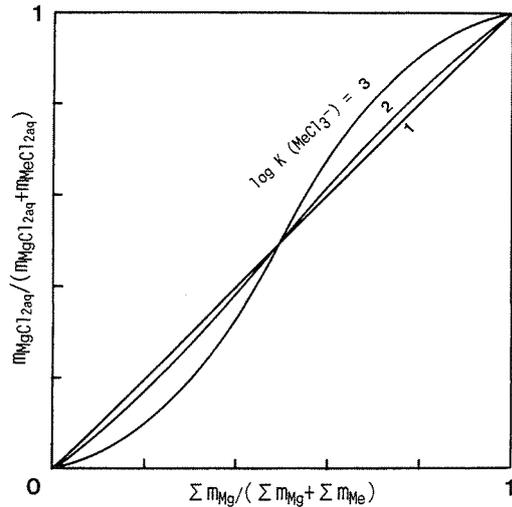
Fig. 1 Relationship between $m(MgCl_{2aq})/(m(MgCl_{2aq}) + m(MeCl_{2aq}))$ and $\Sigma m_{Mg}/(\Sigma m_{Mg} + \Sigma m_{Me})$ of 2N (Me,Mg)Cl_2 aqueous chloride solution at 600°C and 1 kb as a function of the formation constant of $MeCl_3^-_{aq}$ (Me:metal).
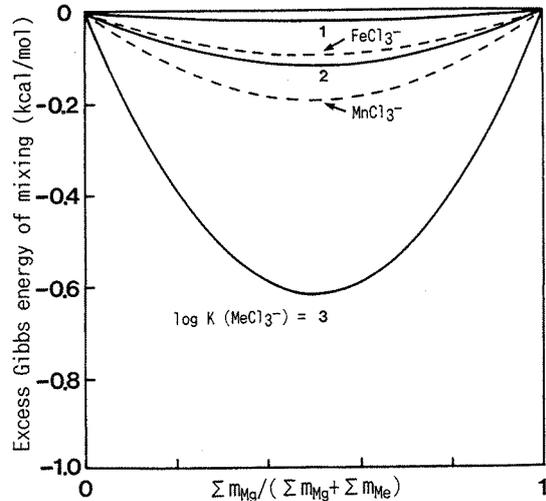

Fig. 2 Excess Gibbs energy of mixing for 2N (Me,Mg)Cl_2 aqueous chloride solution at 600°C and 1 kb as a function of the formation constant of $MeCl_3^-_{aq}$ (Me:metal). Excess Gibbs energy of mixing for the 2N (Mn,Mg)Cl_2 and 2N (Fe,Mg)Cl_2 aqueous chloride solutions at 600°C and 1 kb are shown with dashed lines.

する．Fig. 2は塩化物水溶液の過剰混合ギブスエネルギー
が角田らのモデル[14]で表わせるとして求めた600℃，1kb
における 2N (Me,Mg)Cl_2 水溶液の過剰混合ギブスエネル
ギーである．Fig. 2から明らかなように，この系の塩化物
水溶液は $MeCl_3^-_{aq}$ の生成定数の増加にともない大きな負
の非理想性を示す．600℃，1kb において 2N (Fe,Mg)Cl_2 水
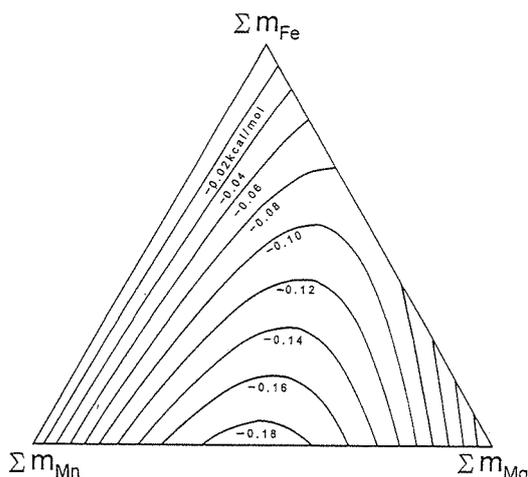
Fig. 3 Excess Gibbs energy of mixing for the 2N (Fe, Mn,Mg)Cl$_2$ aqueous chloride solution at 600°C and 1 kb.

Table 1 Interaction parameters for (Fe,Mn,Mg)TiO$_3$ ilmenite solid solutions and standard Gibbs energies of the ion exchange reactions at 600°C and 1 kb by Kubo et al. (1992).

	(a)	(b)
W_{FeFeMn}	0.035kcal/mol	-0.022kcal/mol
W_{FeMnMn}	-0.214	-0.193
W_{MnMnMg}	0.645	2.985
W_{MnMgMg}	2.829	3.339
W_{MgMgFe}	1.016	1.234
W_{MgFeFe}	0.856	1.034
W_{FeMnMg}	1.024	1.830
$\Delta Gr°(ilm-pyr)$	2.808	2.827
$\Delta Gr°(pyr-gei)$	-1.815	-1.577
$\Delta Gr°(gei-ilm)$	-0.956	-1.027

(a) Non-ideality of aqueous chloride solution is taken into consideraton, and (b) aqueous chloride solution is as-sumed as an ideal solution.

溶液は log K(FeCl$_3^-$$_{aq}$) = 1.9 であるので最大約 -100cal/mol, 2N (Mn,Mg)Cl$_2$ 水溶液は log K(MnCl$_3^-$$_{aq}$) = 2.3 であるので最大約 -200cal/mol の過剰混合ギブスエネルギーを示す (Fig. 2).

4.2 FeCl$_2$-MnCl$_2$ 系水溶液

FeCl$_{2aq}$ および MnCl$_{2aq}$ の解離定数は極めて小さいため $^{6-7)}$ Cl$^-$$_{aq}$ 濃度が低くなり, FeCl$_3^-$$_{aq}$ および MnCl$_3^-$$_{aq}$ はほとんど生成されない. それゆえ, FeCl$_2$-MnCl$_2$ 系水溶液の溶存種としては FeCl$_{2aq}$ および MnCl$_{2aq}$ のみを考えればよい. すなわち, m(FeCl$_{2aq}$) = Σm_{Fe}, m(MnCl$_{2aq}$) = Σm_{Mn} となり, この系の塩化物水溶液は理想混合溶液として取り扱うことができる.

4.3 FeCl$_2$-MnCl$_2$-MgCl$_2$ 系水溶液

4.1 で述べた方法を用いて Mg, Fe, Mn および Cl に対する質量保存式とこれらの元素を含む溶存種に対する質量作用式を同時に解くことにより各溶存種の濃度を求めることができる. このようにして求められた MgCl$_{2aq}$, FeCl$_{2aq}$, MnCl$_{2aq}$ の値を用いて求められた 600℃, 1kb における 2N (Fe,Mn,Mg) Cl$_2$ 水溶液の過剰混合ギブスエネルギーを Fig. 3 に示す.

5. イルメナイト固溶体の過剰混合 ギブスエネルギーの再計算

久保ら $^{3)}$ は (Fe,Mn,Mg)TiO$_3$ イルメナイト固溶体と 2N (Fe,Mn,Mg)Cl$_2$ 塩化物水溶液間におけるイオン交換平衡実験を 600℃, 1kb の条件下で行ない, 塩化物水溶液を理想混合溶液, すなわち, m(FeCl$_{2aq}$)=Σm_{Fe}, m(MnCl$_{2aq}$)=Σm_{Mn}, m(MgCl$_{2aq}$)=Σm_{Mg} と仮定し, イルメナイト固溶体の熱力学的性質を求めた. しかしながら, 先に述べたよ

うに 2N (Fe,Mn,Mg)Cl$_2$ 水溶液は理想混合溶液としては取り扱えない. そこで, 4章で述べた計算方法を用いてイルメナイト固溶体と平衡にある塩化物水溶液中の FeCl$_{2aq}$, MnCl$_{2aq}$, MgCl$_{2aq}$ 濃度を求め, この値を用いて久保ら $^{1)}$ と同じ計算方法を用いて (Fe,Mn,Mg)TiO$_3$ イルメナイト固溶体の過剰混合ギブスエネルギーを求めた. なお, イルメナイト固溶体に対しては角田ら $^{14)}$ の溶液モデルを適用した. 久保ら $^{3)}$ の2成分系および3成分系に対するすべてのイオン交換平衡実験データを用いて計算により求められた (Fe,Mn,Mg)TiO$_3$ イルメナイト固溶体の相互作用パラメータおよびイオン交換反応に対する標準反応ギブスエネルギーを Table 1 に示した. 1つを除くすべての相互作用パラメータに対して塩化物水溶液を理想混合溶液とした場合に比べて小さな値が得られた. 求められた相互作用パラメータを用いて (Fe, Mn, Mg)TiO$_3$ イルメナイト固溶体の過剰混合ギブスエネルギーを計算し, 塩化物水溶液を理想混合溶液とした場合 $^{3)}$ とを Fig. 4 に比較して示した. FeTiO$_3$-MgTiO$_3$ 系においては塩化物水溶液を理想混合溶液とした場合 $^{3)}$ よりも過剰混合ギブスエネルギーは最大約 50cal/mol 小さな値が得られ, また, MnTiO$_3$-MgTiO$_3$ 系においては最大約 110cal/mol 小さな値が得られた.

6. まとめ

(1) 600℃, 1kb において 2N (Fe,Mg)Cl$_2$ および 2N (Mn,Mg)Cl$_2$ 水溶液は負の非理想性を示す.

(2) 600℃, 1kb において 2N (Fe,Mn)Cl$_2$ 水溶液は理想混合溶液として取り扱うことができる.

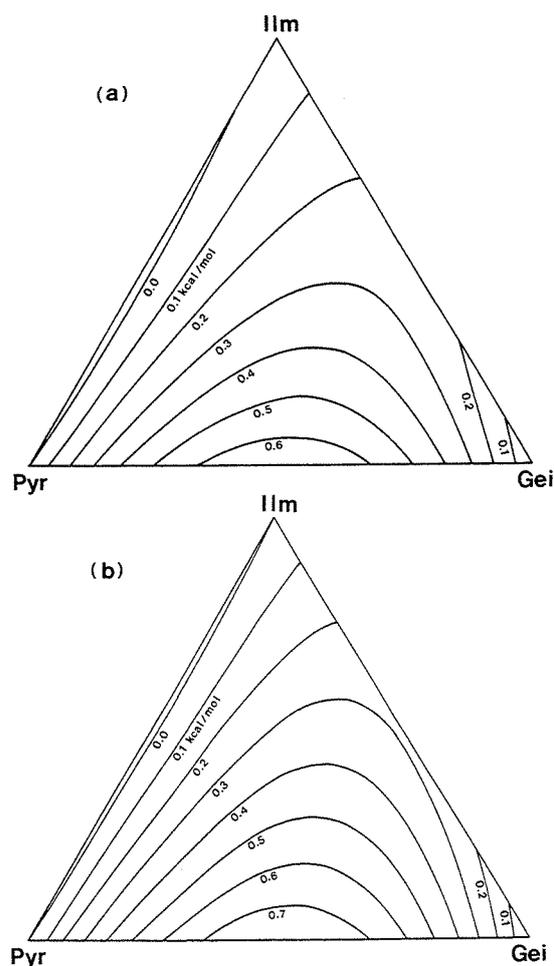(3) 塩化物水溶液の混合における非理想性を考慮することにより久保ら $^{3)}$ によって行われた (Fe,Mn,Mg)TiO$_3$ イルメナイト固溶体と 2N(Fe, Mn, Mg)Cl$_2$ 塩化物水溶液間のイ

Fig. 4 Excess Gibbs energy of mixing for (Fe,Mn,Mg)TiO₃ solid solution at 600°C and 1 kb, calculated from ion exchange experiments between (Fe,Mn,Mg)TiO₃ ilmenite solid solution and 2N (Fe,Mn,Mg)Cl₂ aqueous chloride solution. (a) Non-ideality of aqueous chloride solution is taken into consideration, and (b) aqueous chloride solution is assumed as an ideal solution.

オン交換平衡実験結果を再解析した結果，(Fe,Mn,Mg) TiO₃イルメナイト固溶体に対して久保ら[3]により求められた値より小さな過剰混合ギブスエネルギーが得られた．

文　献

1) UCHIDA, E., GORYOZONO, Y., NAITO, M. and YAMAGAMI, M. (1995): Aqueous speciation of iron and manganese chlorides in supercritical hydrothermal solutions. Geochem. J., **29**, 175-188.

2) FRANTZ, J. D. and MARSHALL, W. L. (1982): Electrical conductances and ionization constants of calcium chloride and magnesium chloride in aqueous solutions at temperatures to 600°C and pressures to 4000 bars. Amer. J. Sci., **282**, 1666-1693.

3) 久保知裕・内田悦生・古川容子・今井直哉 (1992): イルメナイト固溶体 (Fe²⁺, Mn²⁺, Mg)TiO₃ と (Fe²⁺, Mn²⁺, Mg) Cl₂水溶液間におけるイオン交換平衡実験. 鉱物学雑誌, **21**, 59-67.

4) FAHLQUIST, L. S. and POPP, R. K. (1989): The effect of NaCl on bunsenite solubility and Ni-complexing in supercritical aqueous fluids. Geochim. Cosmochim. Acta, **53**, 989-995.

5) CYGAN, G. L., HEMLEY, J. J. and D'ANGELO, W. M. (1994): An experimental study of zinc chloride speciation from 300 to 600°C and 0.5 to 2.0 kbar in buffered hydrothermal solutions. Geochim. Cosmochim. Acta, **58**, 4841-4855.

6) FEIN, J. B., HEMLEY, J. J., D'ANGELO, W. M., KOMNINOU, A. and SVERJENSKY, D. A. (1992): Experimental study of iron-chloride complexing in hydrothermal fluids. Geochim. Cosmochim. Acta, **56**, 3179-3190.

7) BOCTOR, N. Z.(1985) : Rhodonite solubility and thermodynamic properties of aqueous MnCl₂ in the system MnO-SiO₂-HCl-H₂O. Geochim. Cosmochim. Acta, **49**, 565-575.

8) LUCE, R. W., CYGAN, G. L., HEMLEY, J. J. and D'ANGELO, W. M. (1985): Some mineral stability relations in the system CaO-MgO-SiO₂-H₂O-HCl. Geochim. Cosmochim. Acta, **49**, 525-538.

9) GRABMAN, K. B. and POPP, R. K. (1991): Experimental investigation of talc solubility in H₂O-MgCl₂-NaCl-HCl fluids in the range 500-700°C, 2kb. Geochim. Cosmochim. Acta, **55**, 2819-2829.

10) FEIN, J. B. and WALTHER, J. V. (1989): Calcite solubility and speciation in supercritical NaCl-HCl aqueous fluids. Contrib. Mineral. Petrol., **103**, 317-324.

11) Frantz, J. D. and Popp, R. K. (1979): Mineral-solution equilibria I - An experimental study of complexing and thermodynamic properties of aqueous MgCl₂ in the system MgO-SiO₂-H₂O-HCl. Geochim. Cosmochim. Acta, **43**, 1223-1239.

12) POPP, R. K. and FRANTZ, J. D. (1979): Mineral-solution equilibria II. An experimental study of mineral solubilities and the thermodynamic properties of aqueous CaCl₂ in the system CaO-SiO₂-H₂O-HCl. Geochim. Cosmochim. Acta, **43**, 1777-1790.

13) BOCTOr, N. Z., POPP, R. K. and FRANTZ, J. D. (1980): Mineral-solution equilibria IV. Solubilities and the thermodynamic properties of FeCl₂° in the system Fe₂O₃-H₂-H₂O-HCl. Geochim. Cosmochim. Acta, **44**, 1509-1518.

14) 角田康嗣・内田悦生・今井直哉 (1991): 3成分系固溶体に対する新たな熱力学モデル. 鉱物学雑誌, **20**, 25-32.

15) HELGESON, H. C. and KIRKHAM, D. H. (1974): Theoretical prediction of the thermodynamic behavior of aqueous electrolytes at high pressures and temperatures:II. Debye-Huckel parameters for activity coefficients and relative partial molal properties. Amer. J. Sci., **274**, 1199-1261.

16) KHARAKA, Y. K. and BARNES, I. (1973): SOLMNEQ; solution-mineral equilibrium computations. NTIS Tech. Rept. **PB215-899**, 82p.

17) SEWARD, T. M. (1984): The formation of lead (II) chloride complexes to 300°C: Spectrophotometric study. Geochim. Cosmochim. Acta, **48**, 121-134.

Aqueous speciation of zinc chloride in supercritical hydrothermal solutions from 500 to 700°C and 0.5 to 1.0kb

Etsuo UCHIDA, Masahiro NAITO and Shunnosuke UEDA

Department of Mineral Resources Engineering, Waseda University
Ohkubo 3-4-1, Shinjuku, Tokyo 169, Japan

(Abstract)

Aqueous speciation of zinc in 2N chloride solution was determined experimentally at 500 to 700°C and 0.5 to 1.0kb by monitoring the effect of NaCl on ion exchange equilibria in the system $CaTiO_3$ - $ZnTiO_3$ - $CaCl_2$ - $ZnCl_2$ - H_2O. The Ca/(Ca+Zn) value of the 2N aqueous chloride solution in equilibrium with both $CaTiO_3$ and $ZnTiO_3$ decreased with the increase of NaCl under all experimental conditions. This is due to the formation of tri-chloro zinc complex. The formation constant of tri-chloro zinc complex was estimated to be 1.1, 2.1 and 2.7 at 500, 600 and 700°C, 1kb, respectively, and 2.6 at 600°C, 0.5kb in logarithm. The formation constant of tri-chloro zinc complex increases with increasing temperature and with decreasing pressure. This suggests that zinc can be effectively leached from rocks and magmas under higher temperature and lower pressure conditions. This may be the case for Mn^{2+}, Fe^{2+}, Co^{2+} and Ni^{2+}.

INTRODUCTION

In order to elucidate the dissolution state of metal chlorides in supercritical hydrothermal solutions, Uchida et al. (1995, 1996) have investigated the effect of NaCl and KCl on ion exchange equilibria in the system $CaWO_4$-$MeWO_4$-$CaCl_2$-$MeCl_2$-H_2O. The experimental results indicated that first transition metals, Fe, Mn, Ni and Co exist mainly as di-chloro and tri-chloro complexes in 2N chloride solution at 600°C and 1kb, whereas alkali earth elements, Ca, Mg and Sr as di-chloro complex, not as tri-chloro complex. In this study,

47

aqueous speciation of zinc, one of the first transition metals, was investigated using the similar experimental technique. However, our preliminary experiments demonstrated that the $CaWO_4$–$ZnWO_4$–$CaCl_2$–$ZnCl_2$–H_2O system is not suitable because the Ca/(Ca+Zn) value of the aqueous chloride solution in equilibrium with both $CaWO_4$ and $ZnWO_4$ is too low to monitor the effect of NaCl on the ion exchange equilibria. Thus in this study, we adopted the $CaTiO_3$–$ZnTiO_3$–$CaCl_2$–$ZnCl_2$–H_2O system. As similar to $CaWO_4$ and $ZnWO_4$, $CaTiO_3$ (perovskite structure) and $ZnTiO_3$ (ilmenite structure) have different crystal structure from each other and are almost immiscible to each other. As zinc in $ZnTiO_3$ can be replaces by many other elements, the $CaTiO_3$–$MeTiO_3$ system also has a potential to be applied to many other systems.

Zinc chloride speciation was experimentally determined by Ruaya and Seward (1986) from the solubility of AgCl in $ZnCl_2$–HCl–H_2O solution from 100 to 350℃ at the saturated vapour pressure and also by Cygan et al. (1994) from the solubility of sphalerite in KCl–HCl–H_2O solution from 300 to 600℃ at 0.2 to 2.0kb. Cygan et al. (1994) concluded that $ZnCl_2$ and $ZnCl^+$ are dominant aqueous species of zinc under their experimental conditions except for 600℃, 2kb. This study will demonstrate that $ZnCl_{2aq}$ and $ZnCl_3^-{}_{aq}$ are dominant aqueous species of zinc in 2N supercritical hydrothermal solutions from 500 to 700℃ and 0.5 to 1.0kb.

EXPERIMENTAL PROCEDURES

A starting material of $CaTiO_3$ was synthesized from stoichiometric mixtures of CaO and TiO_2 or $CaCO_3$ and TiO_2 by heating at 800℃ during 3 days under the atomospheric condition using an electric furnace. The stoichiometric mixture of ZnO and TiO_2 was used as a starting material of $ZnTiO_3$.

One to 20mg of the starting material was encapsulated into a gold capsule (2.7mm i.d., 3.0mm o.d. and 30 to 40mm in length) with 30 to 40 μ l of 2N aqueous chloride solution. In order to confirm the attainment to equilibrium, $CaTiO_3$ was reacted with 2N $ZnCl_2$–NaCl aqueous solution containing 0, 0.2, 0.4, 0.6, 0.8, 1.2 and 1.6mol/l of NaCl solution, and to the contrary $ZnTiO_3$ with 2N $CaCl_2$–NaCl aqueous solution containing 0, 0.2, 0.4, 0.6, 0.8, 1.2 and 1.6mol/l of NaCl solution. The experiments were conducted using a standard cold–seal pressure vessel settled horizontally in an electric furnace. A stainless steel filler rod was inserted into the pressure vessel in order to minimize the temperature gradient. The experimental conditions were 500, 600 and 700℃ at 1kb and 600℃ at 0.5kb, and the run durations were 6 to 7, 5, 3 to 5 and 5 to 7days, respectively. The temperature was monitored with a chromel–alumel thermocouple inserted into the external well of the pressure vessel and controlled within ±2℃. Water was used as the pressure medium and the pressure was measured with a

Heize gauge.

The pressure vessel was quenched by plunging into cold water. After the gold capsule was checked for a leakage by measuring the weight, the run products were washed away into a beaker with distilled water. The solid run pruducts were separated from the aqueous solution using a millipore filter with a pore size of 0.45μm. The solid products were identified with a X-ray diffractometer (RIGAKU RAD-IR) in order to confirm the coexistence of the two phases $CaTiO_3$ (orthorhombic) and $ZnTiO_3$ (trigonal) and analyzed by an energy dispersive X-ray microanalyzer (JEOL JSM-5400 equipped with LINK QX-200JI). The Ca, Zn and Na concentrations in the separated aqueous solution were determined by an atomic absorption/flame spectrophotometer (SEIKO SAS-727), and normarized to 2N in total concentration.

EXPERIMENTAL RESULTS

Experimental results are listed in Tables 1 to 4.

The all solid products are white in color. The X-ray diffraction revealed that all run products contain both $CaTiO_3$ (orthorhombic) and $ZnTiO_3$ (trigonal). $CaTiO_3$ shows a cubic shape and ranges from 2 to 10μm in the grain size. On the other hand, $ZnTiO_3$ shows a round shape and ranges from 1 to 6μm. $CaTiO_3$ and $ZnTiO_3$ have limited solubilities to each other and dissolved less than 1mol% of $ZnTiO_3$ and $CaTiO_3$ components, respectively.

Figure 1 shows the Ca/(Ca+Zn) molar fraction of the aqueous chloride solutions in equilibrium with both $CaTiO_3$ and $ZnTiO_3$ as a function of NaCl concentration. The direction of approach to equilibrium of the aqueous chloride solutions is shown by the direction of the triangles in the figures which seem to suggest that the experiments reached equilibrium.

In the NaCl-free system, the Ca/(Ca+Zn) molar fraction of the aqueous chloride solution in equilibrium with both $CaTiO_3$ and $ZnTiO_3$ ranges from 0.50 to 0.62 in all experimental conditions. This indicates that the present experimental system is suitable for monitoring the effect of NaCl compared with the system using $CaWO_4$ and $ZnWO_4$. Our preliminary experiments (not published) showed that the Ca/(Ca+Zn) value of the aqueous chloride solution in equilibrium with both $CaWO_4$ and $ZnWO_4$ is 0.10 at 600℃, 1kb in the NaCl-free system. This is too low to monitor the composition of the aqueous chloride solution.

In all experimental conditions, the Ca/(Ca+Zn) value of the aqueous chloride solution in equilibrium with both $CaTiO_3$ and $ZnTiO_3$ decreased considerably with the increase of NaCl. With the increase of NaCl in the aqueous chloride solutions from 0 to 1.6mol/l, the Ca/(Ca+Zn) value decreased from 0.62 to 0.26 at 500℃, 1kb, from 0.50 to 0.08 at 600℃, 1kb, from 0.52 to 0.08 at 700℃, 1kb and from 0.59 to 0.08 at 600℃, 0.5kb.
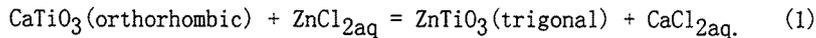
CONSIDERATIONS

Calculation of the formation constant of $ZnCl_3^-{}_{aq}$

As similar to the case for Mn, Fe, Co and Ni in the system $CaWO_4$–$MeWO_4$–$CaCl_2$–$MeCl_2$–H_2O (Uchida et al., 1995, 1996), the decrease in the Ca/(Ca+Zn) molar fraction of the aqueous chloride solution in equilibrium with $CaTiO_3$ and $ZnTiO_3$ with the increase of NaCl concentration can be attributable to the formation of $ZnCl_3^-{}_{aq}$ and/or higher order chloro-complex of zinc.

Uchida et al. (1996) demonstrated experimentally that calcium ion does not form higher-order chloro complex. However, Roselle and Baumgartner (1995) suggested from the experiment of anorthite solubility that $CaCl_3^-{}_{aq}$ can not be neglected at 600 ℃, 2kb. However, this conclusion seems to be supported by only one experimental point of the highest total Cl content in their Fig. 3. Without this experimental point, we can conclude that the existence of $CaCl_3^-{}_{aq}$ is negligible. Thus, we neglect $CaCl_3^-{}_{aq}$ in this study. This is also for the consistency with our previous studies (Uchida et al., 1995, 1996). In this study, we take into account only $ZnCl_3^-{}_{aq}$ as higher-order chloro complex of zinc and calculate the formation constant of $ZnCl_3^-{}_{aq}$ using the same procedure to that of Uchida et al. (1995, 1996). Thus the calculation procedure will be described briefly below.

The ion exchange reaction can be expressed as

$$CaTiO_3(\text{orthorhombic}) + ZnCl_{2aq} = ZnTiO_3(\text{trigonal}) + CaCl_{2aq}. \qquad (1)$$

The equilibrium constant K(1) for the reaction (1) is

$$K(1) = a(ZnTiO_3) \cdot a(CaCl_{2aq})/a(CaTiO_3) \cdot a(ZnCl_{2aq}), \qquad (2)$$

where a(i) is the activity of component i. Because the solid phases, $CaTiO_3$ and $ZnTiO_3$ are almost immiscible to each other,

$$a(CaTiO_3) = a(ZnTiO_3) = 1. \qquad (3)$$

Also the activity coefficient for neutral species is assumed to be 1 as done by almost previous works. Thus the equilibrium constant K(1) can be rewritten as

$$K(1) = m(CaCl_{2aq})/m(ZnCl_{2aq}). \qquad (4)$$

In the calculation, the following eight aqueous species were taken into account: $Na^+{}_{aq}$, $NaCl_{aq}$, $Cl^-{}_{aq}$, $Ca^{2+}{}_{aq}$, $CaCl^+{}_{aq}$, $CaCl_{2aq}$, $ZnCl_{2aq}$ and $ZnCl_3^-{}_{aq}$.

Among the above eight species, the following four mass-balance equations can be written:

$$\Sigma m_{Na} = m(Na^+{}_{aq}) + m(NaCl_{aq}) \qquad (5)$$

$$\Sigma m_{Ca} = m(Ca^{2+}{}_{aq}) + m(CaCl^+{}_{aq}) + m(CaCl_{2aq}) \qquad (6)$$

$$\Sigma m_{Zn} = m(ZnCl_{2aq}) + m(ZnCl_3^-{}_{aq}) \qquad (7)$$

and $\quad \Sigma m_{Cl} = m(Cl^-{}_{aq}) + m(NaCl_{aq}) + m(CaCl^+{}_{aq})$

$$+ 2m(CaCl_{2aq}) + 2m(ZnCl_{2aq}) + 3m(ZnCl_3^-{}_{aq}) = 2 \qquad (8)$$

where Σm_i designates the total molarity of i-bearing species and m(i) the molarity of species i.

The following four reactions can be written among the above eight species:

$$NaCl_{aq} = Na^+{}_{aq} + Cl^-{}_{aq} \qquad (9)$$

$$CaCl_{2aq} = CaCl^+{}_{aq} + Cl^-{}_{aq} \qquad (10)$$

$$CaCl^+{}_{aq} = Ca^{2+}{}_{aq} + Cl^-{}_{aq} \qquad (11)$$

and $\quad ZnCl_{2aq} + Cl^-{}_{aq} = ZnCl_3^-{}_{aq} \qquad (12)$

Corresponding to the above four reactions, the following four mass action equations can be written:

$$K(NaCl_{aq}) = a(Na^+{}_{aq}) \cdot a(Cl^-{}_{aq})/a(NaCl_{aq}) \qquad (13)$$

$$K(CaCl_{2aq}) = a(CaCl^+{}_{aq}) \cdot a(Cl^-{}_{aq})/a(CaCl_{2aq}) \qquad (14)$$

$$K(CaCl^+{}_{aq}) = a(Ca^{2+}{}_{aq}) \cdot a(Cl^-{}_{aq})/a(CaCl^+{}_{aq}) \qquad (15)$$

and $\quad K(ZnCl_3^-{}_{aq}) = a(ZnCl_3^-{}_{aq})/\{a(ZnCl_{2aq}) \cdot a(Cl^-{}_{aq})\} \qquad (16)$

where K(i) denotes the dissociation or formation constant of aqueous species i. The dissociation constant for $NaCl_{aq}$ was taken from Quist and Marshall (1968) and those for $CaCl_{2aq}$ and $CaCl^+{}_{aq}$ were from Frantz and Marshall (1982). The activity coefficient for charged aqueous species was calculated using the Debye-Huckel equation.

The formation constant of $ZnCl_3^-{}_{aq}$ was obtained using equations (4) to (8) and (13) to (16) so as to find the value which fits the experimental results. As a result, the formation constant of $ZnCl_3^-{}_{aq}$ was estimated to be 1.1 at 500℃, 2.1 at 600℃, 2.7 at 700℃, 1kb, and 2.6 at 600℃, 0.5kb in logarithm.

Temperature dependence of the formation constant of $ZnCl_3^-{}_{aq}$

As shown above, the formation constant of $ZnCl_3^-{}_{aq}$ increases significantly with increasing temperature. Fig.2 is the Arrhenius plot of log $K(ZnCl_3^-{}_{aq})$. Linear regression gives the following equation for log $K(ZnCl_3^-{}_{aq})$ as a function of temperature at 1kb:

$$\log K(ZnCl_3^-{}_{aq}) = -6069/T + 8.98 \qquad (T \text{ in Kelvin}) \qquad (17)$$

At constant pressure, there is the following thermodynamic relation:

$$\log K = -\Delta H^\circ /(2.303RT) + \Delta S^\circ /(2.303R) \qquad (18)$$

where ΔH° is the standard enthalpy change for reaction, ΔS° the standard entropy change for reaction and R the gas constant. Fig.2 indicates that ΔH° and ΔS° are nearly constant under the experimental conditions. From the equations (17) and (18), ΔH° and ΔS° for the reaction (12) were estimated to be 27.8kcal/mol and 41.1cal/K·mol, respectively, at 500 to 700℃, 1kb. The positive ΔS° may be attributable to the liberation of H_2O molecules hydrated around the aqueous species through the formation of $ZnCl_3^-{}_{aq}$. Taking into account

the hydration, the formation reaction of $ZnCl_3^-{}_{aq}$ can be written as

$$ZnCl_2 \cdot mH_2O + Cl^- \cdot nH_2O = ZnCl_3^- \cdot 1H_2O + (1-m-n)H_2O. \qquad (19)$$

The positive ΔS° requires $1-m-n > 1$. This is because the total superfices of the aqueous species decreases with the progress of complexing.

Uchida et al. (1995) obtained the formation constant of $FeCl_3^-{}_{aq}$ and $MnCl_3^-{}_{aq}$ at 400 and 600°C, 1kb (Fig. 2). If we ignore the experimental results obtained from the KCl effect on the ion exchange equilibria due to unreliability of the dissociation constant of KCl_{aq}, standard enthalpy changes for the formation of $FeCl_3^-{}_{aq}$ and $MnCl_3^-{}_{aq}$ were calculated to be 22.9 and 25.6kcal/mol, respectively, at 1kb. Thus the temperature dependence of the formation constant of tri-chloro complexes of transition elements is significant. Similarly, the formation constants of other aqueous chloro complexes such as $CaCl_2{}_{aq}$, $CaCl^+{}_{aq}$, $MgCl_2{}_{aq}$, $MgCl^+{}_{aq}$, $NaCl_{aq}$ and KCl_{aq} increase with increasing temperature (e.g., Eugster and Baumgartner, 1987). This is explained by the decrease of the interaction between water molecule and aqueous species due to the decrease of the dielectric constant of water with increasing temperature (e.g., Quist and Marshall, 1965). The standard enthalpy change for $NiCl_3^-{}_{aq}$ is estimated to be 10.8kcal/mol at 550 to 750°C, 2kb from the experiments of Fahlquist and Popp (1989)(Fig. 2), and this value is considerably low compared to those for $ZnCl_3^-{}_{aq}$, $FeCl_3^-{}_{aq}$ and $MnCl_3^-{}_{aq}$ at 1kb.

Pressure dependence of the formation constant of $ZnCl_3^-{}_{aq}$

The present experimental results suggest that the formation constant of $ZnCl_3^-{}_{aq}$ increase with decreasing pressure, that is, $\log K(ZnCl_3^-{}_{aq})$ increases from 2.1 at 1kb to 2.6 at 0.5kb for 600°C (Fig. 3). Cygan et al. (1994) obtained 1.1 as $\log K(ZnCl_3^-{}_{aq})$ value at 600°C, 2kb. Judging from Fig. 3, this value seems to be concordant with the present experimental results. The similar tendency was observed for $NiCl_3^-{}_{aq}$. The $\log K(NiCl_3^-{}_{aq})$ increases from 0.69 at 2kb to 1.5 at 1kb for 600°C (Fahlquist and Popp, 1989; Uchida et al., 1996)(Fig. 3). This is explained by the decrease of dielectric constant of water with decreasing pressure.

At constant temperature, there is the following thermodynamic relation:

$$\log K(P_1) - \log K(P_2) = 1/(2.303RT) \int_{P1}^{P2} \Delta V dP \qquad (20)$$

where P indicates the pressure and ΔV the volume change for reaction. Using average ΔV_{av} in the pressure range from P_1 to P_2, the equation (20) can be rewritten as

$$\log K(P_1) - \log K(P_2) = \Delta V_{av}(P_2-P_1)/(2.303RT). \qquad (21)$$

From the present experimental results at 600°C, ΔV_{av} in the pressure range from 0.5 to 1.0kb was estimated to be 167cc. As water occupies 110cc/mol at 0.5kbar and 48cc/mol at 1kb, 600°C (Burnham et al., 1969), 167cc volume change for the reaction (19) suggests that at

least 2 water molecules are supposed to be released through the reaction (19). The increase of the formation constant of tri-chloro complexes with decreasing pressure can also be ascribed to the positive volume change for the reaction (19).

Thus the formation constant of tri-chloro complexes of first transition metals increases with increasing temperature and with decreasing pressure. This indicates that the first transition metals can be effectively leached from rocks and magmas at higher temperatures and lower pressures. Therefore, granitic rocks solidified near the surface seem to have the potential of metal mineralization.

Comparison with other first transition metals

Uchida et al. (1995, 1996) suggested that the first transition metals tend to form tri-chloro complexes in the order of $Mn^{2+} > Co^{2+} > Fe^{2+} > Ni^{2+}$ at 600℃, 1kb. Based on the ligand field theory, they concluded that the tri-chloro complexes of the first transition metals take tetrahedral coordination with low spin state. The ligand field theory predicts that Zn^{2+} has the lowest formation constant of tri-chloro complex among Mn^{2+}, Fe^{2+}, Co^{2+}, Ni^{2+}, Cu^{2+} and Zn^{2+}. However, the present experiment resulted in the order of $Mn^{2+} > Co^{2+} > Fe^{2+} > Ni^{2+} < Zn^{2+}$. This may suggest that the tri-chloro complex of Zn^{2+} takes the other lower coodination such as trigonal coordination.

As mentionned in Uchida et al. (1996), there is a reverse between Co^{2+} and Fe^{2+} in the sequence of the formation constant of tri-chloro complex. For the first transition metals of octahedral coordination with low spin state, we can find the reverse between Co^{2+}(65nm) and Fe^{2+}(61nm) in the ion size (Shannon, 1976). Though we have no data for the ion size of Co^{2+} and Fe^{2+} in the tetrahedral coordination, the reverse in the ion size for tetrahedral coordination is also expected from the experimental results of Uchida et al. (1996).
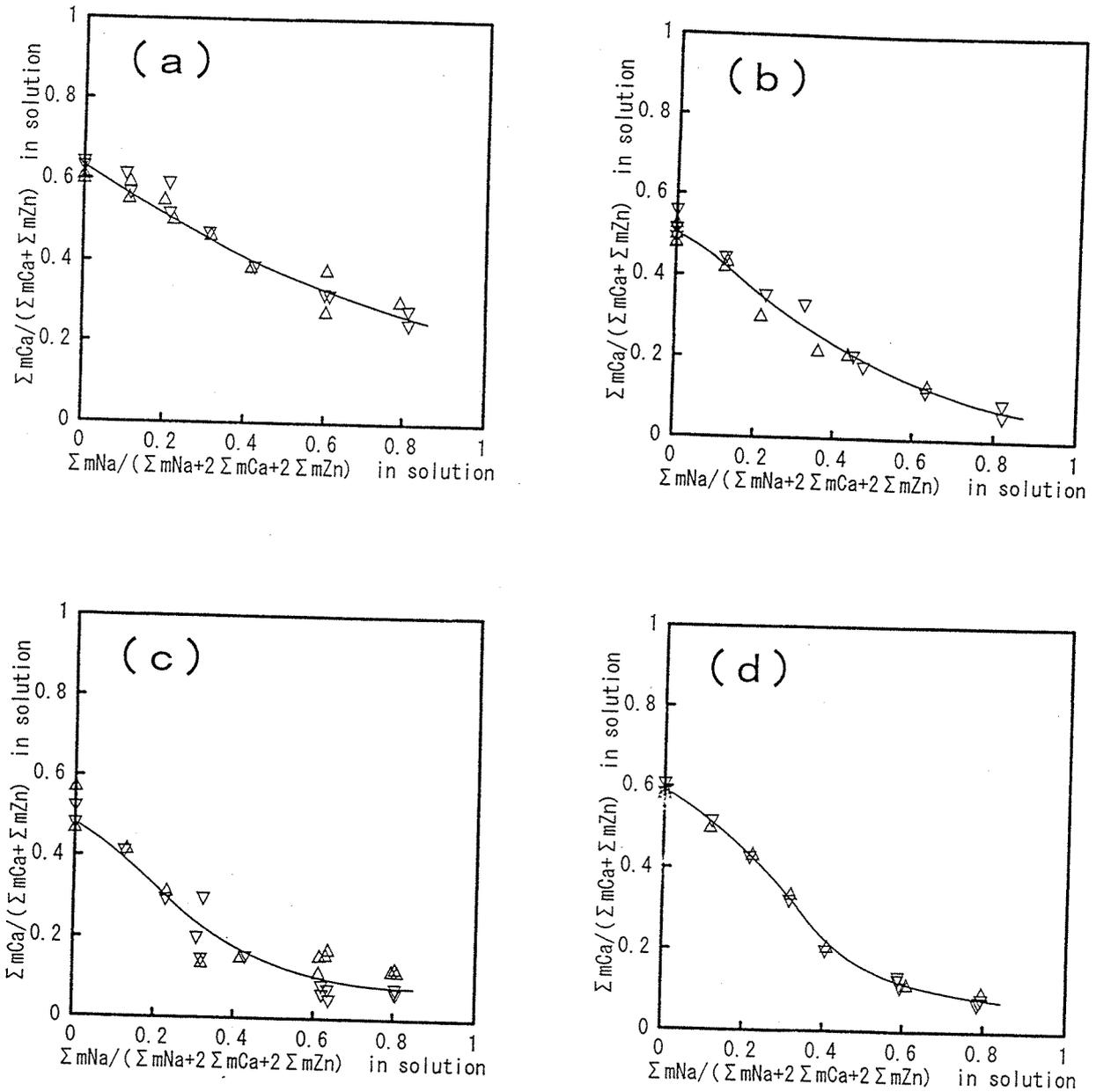
Fig. 1. The effect of NaCl on the chemical composition of the 2N aqueous chloride solution in equilibrium with $CaTiO_3$ and $ZnTiO_3$. The direction of triangles in the figures indicate the direction of change in chemical composition of the aqueous chloride solution from the initial composition. (a) 500°C, 1kb, (b) 600°C, 1kb, (c) 700°C, 1kb and (d) 600°C, 0.5kb.
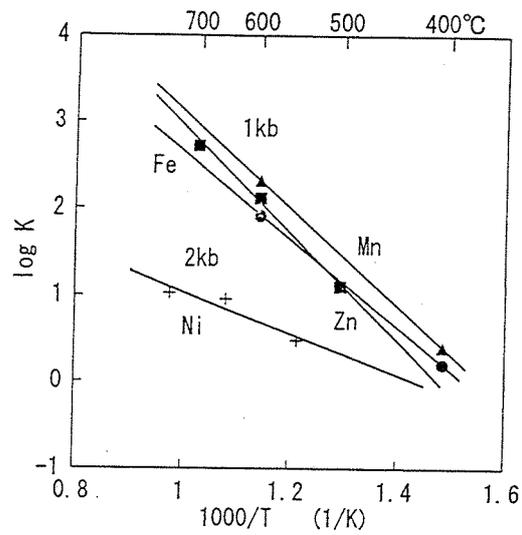
Fig. 2. Arrhenius plot of log K(MeCl$_3^-$aq). Data for ZnCl$_3^-$aq at 1kb are taken from this study, those for MnCl$_3^-$aq and FeCl$_3^-$aq at 1kb from Uchida et al. (1995) and those for NiCl$_3^-$aq at 2kb from Fahlquist and Popp (1989).
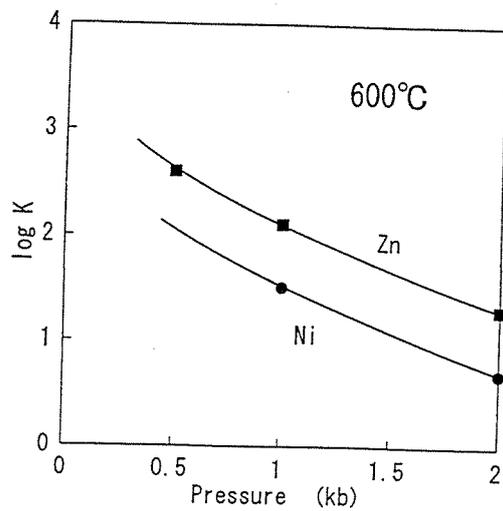
Fig. 3. Pressure dependence of log K(MeCl$_3^-$aq) at 600℃. Data for ZnCl$_3^-$aq at 0.5 and 1kb are taken from this study, those for ZnCl$_3^-$aq at 2kb from Cygan et al. (1994), and those for NiCl$_3^-$aq at 1 and 2kb from Uchida et al. (1996) and Fahlquist and Popp (1989), respectively.

Table 1. Experimental results for ion exchange equlibria in the system
CaTiO$_3$ - ZnTiO$_3$ - CaCl$_2$ - ZnCl$_2$ - NaCl at 500℃ and 1kb.

Run no.	Dur.	Starting materials						Run Products (solution)		
	days	solid		solution		solution		Σ mZn	Σ mCa	Σ mNa
			mg		μ l		μ l			
5Zn01	7	ZnTiO$_3$	12.8	CaCl$_2$	40	NaCl	0	0.364	0.636	0.000
5Zn02	7	CaTiO$_3$	14.0	ZnCl$_2$	40	NaCl	0	0.254	0.600	0.000
5Zn03	7	ZnTiO$_3$	15.7	CaCl$_2$	40	NaCl	0	0.375	0.625	0.000
5Zn04	7	CaTiO$_3$	13.7	ZnCl$_2$	40	NaCl	0	0.390	0.610	0.000
5Zn05	7	ZnTiO$_3$	15.4	CaCl$_2$	36	NaCl	4	0.351	0.545	0.208
5Zn06	7	ZnTiO$_3$	10.6	CaCl$_2$	36	NaCl	4	0.387	0.497	0.231
5Zn07	7	ZnTiO$_3$	16.4	CaCl$_2$	32	NaCl	8	0.328	0.463	0.419
5Zn08	7	ZnTiO$_3$	12.5	CaCl$_2$	32	NaCl	8	0.385	0.404	0.424
5Zn09	7	ZnTiO$_3$	13.3	CaCl$_2$	28	NaCl	12	0.369	0.320	0.622
5Zn10	7	ZnTiO$_3$	15.1	CaCl$_2$	24	NaCl	16	0.356	0.220	0.848
5Zn11	7	ZnTiO$_3$	11.3	CaCl$_2$	16	NaCl	24	0.267	0.121	1.223
5Zn12	7	ZnTiO$_3$	13.1	CaCl$_2$	8	NaCl	32	0.143	0.045	1.624
5Zn13	7	CaTiO$_3$	13.4	ZnCl$_2$	36	NaCl	4	0.397	0.491	0.225
5Zn14	7	CaTiO$_3$	16.6	ZnCl$_2$	36	NaCl	4	0.360	0.526	0.228
5Zn15	7	CaTiO$_3$	12.5	ZnCl$_2$	32	NaCl	8	0.387	0.392	0.443
5Zn16	7	CaTiO$_3$	13.5	ZnCl$_2$	32	NaCl	8	0.361	0.440	0.397
5Zn17	7	CaTiO$_3$	13.2	ZnCl$_2$	28	NaCl	12	0.367	0.319	0.629
5Zn18	7	CaTiO$_3$	18.6	ZnCl$_2$	24	NaCl	16	0.359	0.226	0.832
5Zn25	7	ZnTiO$_3$	12.1	CaCl$_2$	16	NaCl	24	0.274	0.126	1.199
5Zn27	7	ZnTiO$_3$	11.2	CaCl$_2$	8	NaCl	32	0.137	0.052	1.623
5Zn29	6	CaTiO$_3$	7.6	ZnCl$_2$	20	NaCl	30	0.245	0.150	1.208
5Zn31	6	CaTiO$_3$	7.3	ZnCl$_2$	20	NaCl	30	0.288	0.109	1.206
5Zn32	6	CaTiO$_3$	3.4	ZnCl$_2$	10	NaCl	40	0.146	0.064	1.581

Table 2. Experimental results for ion exchange equilibria in the system
CaTiO3 – ZnTiO3 – CaCl2 – ZnCl2 – NaCl – H2O at 600℃ and 1kb.

Run no.	Dur. days	Starting materials						Run Products (solution)		
		solid mg		solution μl		solution μl		Σ mZn	Σ mCa	Σ mNa
6Zn02	5	CaTiO3	5.1	ZnCl2	60	NaCl	0	0.474	0.526	0.000
6Zn03	5	CaTiO3	5.0	ZnCl2	60	NaCl	0	0.522	0.478	0.000
6Zn05	5	ZnTiO3	9.1	CaCl2	40	NaCl	0	0.448	0.552	0.000
6Zn06	5	ZnTiO3	10.9	CaCl2	40	NaCl	0	0.515	0.485	0.000
6Zn07	5	CaTiO3	6.4	ZnCl2	60	NaCl	0	0.518	0.482	0.000
6Zn08	5	CaTiO3	5.3	ZnCl2	60	NaCl	0	0.500	0.500	0.000
6Zn09	5	ZnTiO3	8.7	CaCl2	40	NaCl	0	0.496	0.504	0.000
6Zn10	5	ZnTiO3	9.4	CaCl2	40	NaCl	0	0.493	0.507	0.000
6Zn12	5	CaTiO3	7.7	ZnCl2	36	NaCl	24	0.503	0.140	0.713
6Zn13	5	CaTiO3	5.5	ZnCl2	24	NaCl	36	0.318	0.049	1.268
6Zn15	5	ZnTiO3	9.1	CaCl2	28	NaCl	12	0.458	0.221	0.643
6Zn16	5	ZnTiO3	10.9	CaCl2	24	NaCl	16	0.436	0.091	0.947
6Zn17	5	ZnTiO3	8.5	CaCl2	16	NaCl	24	0.328	0.042	1.261
6Zn19	5	CaTiO3	6.6	ZnCl2	54	NaCl	6	0.493	0.379	0.256
6Zn21	5	CaTiO3	6.3	ZnCl2	48	NaCl	12	0.549	0.238	0.427
6Zn22	5	ZnTiO3	11.7	CaCl2	32	NaCl	8	0.506	0.270	0.448
6Zn31	5	CaTiO3	6.0	ZnCl2	54	NaCl	6	0.507	0.370	0.247
6Zn32	5	ZnTiO3	8.7	CaCl2	36	NaCl	4	0.493	0.384	0.247
6Zn33	5	CaTiO3	5.4	ZnCl2	36	NaCl	24	0.449	0.119	0.865
6Zn34	5	ZnTiO3	9.0	CaCl2	24	NaCl	16	0.442	0.111	0.894
6Zn36	5	ZnTiO3	9.3	CaCl2	8	NaCl	32	0.166	0.016	1.638
6Zn38	5	ZnTiO3	9.2	CaCl2	8	NaCl	32	0.169	0.010	1.640

Table 3. Experimental results for ion exchange equilibria in the system $CaTiO_3$ - $ZnTiO_3$ - $CaCl_2$ - $ZnCl_2$ - $NaCl$ - H_2O at 700°C and 1kb.

Run no.	Dur. days	Starting materials solid mg		Starting materials solution μl		Starting materials solution μl		Run Products(solution) $\Sigma\,mZn$	$\Sigma\,mCa$	$\Sigma\,mNa$
7Zn01	5	CaTiO3	15.1	ZnCl2	40	NaCl	0	0.533	0.467	0.000
7Zn02	5	ZnTiO3	15.2	CaCl2	40	NaCl	0	0.526	0.474	0.000
7Zn13	4	ZnTiO3	12.8	CaCl2	16	NaCl	24	0.348	0.015	1.273
7Zn14	4	CaTiO3	12.1	ZnCl2	16	NaCl	24	0.304	0.064	1.264
7Zn16	4	CaTiO3	10.3	ZnCl2	8	NaCl	32	0.171	0.025	1.608
7Zn17	3	CaTiO3	12.8	ZnCl2	30	NaCl	0	0.430	0.570	0.000
7Zn18	3	ZnTiO3	10.8	CaCl2	30	NaCl	0	0.485	0.515	0.000
7Zn19	3	CaTiO3	10.2	ZnCl2	27	NaCl	3	0.508	0.363	0.259
7Zn20	3.	ZnTiO3	12.3	CaCl2	27	NaCl	3	0.520	0.356	0.248
7Zn21	3	CaTiO3	16.1	ZnCl2	24	NaCl	6	0.531	0.241	0.456
7Zn22	3	ZnTiO3	14.5	CaCl2	24	NaCl	6	0.550	0.224	0.452
7Zn24	3	ZnTiO3	17.0	CaCl2	21	NaCl	9	0.560	0.135	0.610
7Zn27	4	ZnTiO3	16.4	CaCl2	21	NaCl	9	0.481	0.198	0.643
7Zn29	4	ZnTiO3	11.0	CaCl2	18	NaCl	12	0.488	0.085	0.856
7Zn30	4	CaTiO3	11.4	ZnCl2	18	NaCl	12	0.495	0.089	0.832
7Zn31	4	ZnTiO3	11.8	CaCl2	12	NaCl	18	0.885	0.053	0.124
7Zn32	4	CaTiO3	11.9	ZnCl2	12	NaCl	18	0.328	0.061	1.222
7Zn33	4	ZnTiO3	11.5	CaCl2	6	NaCl	24	0.186	0.012	1.604
7Zn37	4	ZnTiO3	7.1	CaCl2	16	NaCl	24	0.342	0.025	1.266
7Zn38	4	CaTiO3	6.4	ZnCl2	16	NaCl	24	0.314	0.060	1.253
7Zn39	4	ZnTiO3	6.6	CaCl2	8	NaCl	32	0.182	0.014	1.609
7Zn40	4	CaTiO3	4.7	ZnCl2	8	NaCl	32	0.168	0.023	1.619
7Zn43	4	ZnTiO3	12.6	CaCl2	28	NaCl	12	0.587	0.097	0.633
7Zn44	4	CaTiO3	10.5	ZnCl2	28	NaCl	12	0.588	0.094	0.635
7Zn45	4	ZnTiO3	7.0	CaCl2	16	NaCl	24	0.353	0.030	1.236
7Zn46	4	CaTiO3	8.2	ZnCl2	16	NaCl	24	0.346	0.045	1.219
7Zn47	4	ZnTiO3	3.5	CaCl2	8	NaCl	32	0.183	0.011	1.612
7Zn48	4	CaTiO3	4.9	ZnCl2	8	NaCl	32	0.181	0.025	1.589

Table 4. Experimental results for ion exchange equilibria in the system
CaTiO$_3$ – ZnTiO$_3$ – CaCl$_2$ – ZnCl$_2$ – NaCl – H$_2$O at 600℃ and 0.5kb.

Run no.	Dur.	Starting materials						Run Products (solution)		
	days	solid		solution		solution		Σ m$_{Zn}$	Σ m$_{Ca}$	Σ m$_{Na}$
			mg		μl		μl			
Zn01p	5	CaTiO$_3$	11.3	ZnCl$_2$	30	NaCl	0	0.420	0.580	0.000
Zn02p	5	ZnTiO$_3$	16.7	CaCl$_2$	30	NaCl	0	0.424	0.576	0.000
Zn03p	5	CaTiO$_3$	11.2	ZnCl$_2$	30	NaCl	0	0.400	0.600	0.000
Zn04p	5	ZnTiO$_3$	11.8	CaCl$_2$	30	NaCl	0	0.490	0.510	0.000
Zn05p	6	ZnTiO$_3$	11.7	CaCl$_2$	27	NaCl	3	0.442	0.440	0.235
Zn06p	6	CaTiO$_3$	15.0	ZnCl$_2$	27	NaCl	3	0.513	0.373	0.229
Zn07p	6	ZnTiO$_3$	10.3	CaCl$_2$	24	NaCl	6	0.447	0.341	0.424
Zn08p	6	CaTiO$_3$	11.8	ZnCl$_2$	24	NaCl	6	0.535	0.246	0.439
Zn09p	7	ZnTiO$_3$	10.9	CaCl$_2$	21	NaCl	9	0.457	0.231	0.623
Zn10p	7	CaTiO$_3$	13.6	ZnCl$_2$	21	NaCl	9	0.553	0.132	0.630
Zn11p	7	ZnTiO$_3$	11.8	CaCl$_2$	18	NaCl	12	0.473	0.123	0.807
Zn12p	7	CaTiO$_3$	12.5	ZnCl$_2$	18	NaCl	12	0.521	0.071	0.815
Zn13p	6	ZnTiO$_3$	11.6	CaCl$_2$	12	NaCl	18	0.337	0.077	1.173
Zn15p	6	ZnTiO$_3$	12.3	CaCl$_2$	6	NaCl	24	0.144	0.072	1.568
Zn17p	5	ZnTiO$_3$	7.2	CaCl$_2$	16	NaCl	24	0.365	0.042	1.186
Zn19p	5	ZnTiO$_3$	3.6	CaCl$_2$	8	NaCl	32	0.197	0.014	1.578
Zn23p	5	ZnTiO$_3$	3.4	CaCl$_2$	16	NaCl	24	0.360	0.053	1.174
Zn24p	5	CaTiO$_3$	1.3	ZnCl$_2$	16	NaCl	24	0.347	0.045	1.217
Zn25p	5	ZnTiO$_3$	1.5	CaCl$_2$	8	NaCl	32	0.191	0.016	1.586
Zn26p	5	CaTiO$_3$	.9	ZnCl$_2$	8	NaCl	32	0.186	0.020	1.588

REFERENCES

Burnham, C. W., Holloway, J. R. and Davis, N. F. (1969) The thermodynamic properties of water to 1000°C and 10,000 bars. *Geol. Soc. Amer. Spec. Paper* 132, 96pp.

Cygan, G. L., Hemley, J. J. and D'Angelo, W. M. (1994) An experimental study of zinc chloride speciation from 300 to 600°C and 0.5 to 2.0 kbar in buffered hydrothermal solutions. *Geochim. Cosmochim. Acta* 58, 367-403.

Eugster, H. P. and Baumgartner, L. (1987) Mineral solubilities and speciation in supercritical metamorphic fluids. *Rev. Mineral.* 17, 367-403.

Fahlquist, L. S. and Popp, R. K. (1989) The effect of NaCl on bunsenite solubility and Ni-complexing in supercritical aqueous fluids. *Geochim. Cosmochim. Acta* 53, 989-995.

Frantz, J. D. and Marshall, W. L. (1982) Electrical conductances and ionization constants of calcium chloride and magnesium chloride in aqueous solutions at temperatures to 600°C and pressures to 4000 bars. *Am. J. Sci.* 282, 1666-1693.

Quist, A. S. and Marshall, W. L. (1965) Estimation of the dielectric constant of water to 800. *J. Phys. Chem.* 69, 3165-3167.

Quist, A. and Marshall, W. L. (1968) Electrical conductances of aqueous sodium chloride solutions from 0 to 800°C and at pressures to 4000 bars. *J. Phys. Chem.* 72, 684-703.

Roselle, G. T. and Baumgartner, L. P. (1995) Experimental determination of anorthite solubility and calcium speciation in supercritical chloride solutions at 2 kb from 400 to 600°C. *Geochim. Cosmochim. Acta* 59, 1539-1549.

Ruaya, J. R. and Seward, T. M. (1986) The stability of chlorozinc(II) complexes in hydrothermal solutions up to 350°C. *Geochim. Cosmochim. Acta* 50, 651-661.

Shannon, R. D. (1976) Revised effective ionic radii and systematic studies of interatomic distances in halides and chalcogenides. *Acta Cryst.* A32, 751-767.

Uchida, E., Goryozono, Y. and Naito, M. (1996) Aqueous speciation of magnesium, strontium, nickel and cobalt chlorides in hydrothermal solutions at 600°C and 1 kbar. *Geochem. J.* 30, 99-109.

Uchida, E., Goryozono, Y., Naito, M. and Yamagami, M. (1995) Aqueous speciation of iron and manganese chlorides in supercritical hydrothermal solutions. *Geochem. J.* 29, 175-188.